



**Codes And Methods Improvements
for VVER comprehensive safety assessment**

Grant Agreement Number: 945081

Start date: 01/09/2020 - Duration: 36 Months

WP7 - Task 7.4

**D7.4 Results of Transient 2 Benchmark: Main Steam
Line Break Analysis**

V. H. Sanchez, G. Huaccho, K. Zhang (KIT), B. Calgaro, B. Vezzoni, A. Mas, T. Quenouille, O. Bernard (Framatome), A. Stefanova, P. Vryashkova, N. Zaharieva, P. Groudev (INRNE), A. Hashymov, Y. Onyshchuk (ENERGORISK)




Version 1 – 01/09/2023



CAMIVVER – Grant Agreement Number: 945081

Document title	Results of Transient 2 Benchmark: Main Steam Line Break Analysis
Author(s)	V. H. Sanchez, G. Huaccho, K. Zhang, B. Calgaro, B. Vezzoni, A. Mas, T. Quenouille, O. Bernard, A. Stefanova, P.Vryashkova, N. Zaharieva, P. Groudev, A. Hashymov, Y. Onyshchuk
Document type	Deliverable
Work Package	WP7
Document number	D7.4 - version 1
Issued by	KIT
Date of completion	01.09.2023
Dissemination level	Public

Approval

Version	First Author	WP leader	Project Coordinator
1	V. Sanchez (KIT) 01/09/2023	A Hashymov (Energorisk) 01/09/2023	D. Verrier (Framatome) 01/09/2023
	 Dr. V. Sanchez		

Summary

This deliverable describes the analysis performed by four partners in the frame of Task7.4 devoted to the benchmark-2 analysis focuses on the Main Steam Line Break (MSLB) transient analysis of the Kozloduy 6 Nuclear Power Plant (KNPP), a VVER-1000 reactor located in Bulgaria at the Kozloduy site.

The MSLB transient is analyzed using both system thermal hydraulic codes with the point kinetics approach using RELAP5 (INRNE, ENERGORISK) and the coupled codes TRACE/PARCS (KIT) and CATHARE3/APOLLO3 (FRAMATOME). Eventhough the MSLB is evaluated at EOC conditions, it was decided to perform the analysis for the BOC conditions in order to facilitate the cross section generation work and avoid other source of discrepancies using Serpent2 and APOLLO3® lattice physics part (via NEMESI prototype at WP4) to be used by the core simulators PARCS and APOLLO3®. In addition, the point kinetics parameters needed by the system thermal hydraulic codes were generated by KIT and provided to the partners.

This deliverables starts with the description of the accidental scenario, which is followed by a bried description of the applied tools. In the next chapter the KNPP models developed by the involved partners is described including the assumptions. Then, the main results obtained by the partners is presented and discussed. Finally, a chapter is dedicated to compare the different simulations obtained by the codes RELAP5, and TRACE/PARCS. Final conclusions and recommendations are included at the end of the report.

Table of contents

1	DESCRIPTION MSLB TRANSIENT SCENARIO	11
1.1	INTRODUCTION.....	11
1.2	INITIAL STEADY STATE CONDITIONS	12
1.3	TRANSIENT SCENARIO	13
1.4	BOUNDARY CONDITIONS FOR THE TRANSIENT PHASE	15
2	SHORT DESCRIPTION OF THE TOOLS	19
2.1	SHORT DESCRIPTION OF RELAP5 (ENREGORISK).....	19
2.2	SHORT DESCRIPTION OF TRACE/PARCS (KIT)	19
2.2.1	<i>The system thermal hydraulic code TRACE.....</i>	19
2.2.2	<i>The nodal diffusion code PARCS</i>	20
2.2.3	<i>Description of the nodal cross sections needed by PARCS</i>	20
2.3	SHORT DESCRIPTION OF CATHARE3/APOLLO3®	20
2.3.1	<i>The system thermal hydraulic code CATHARE3</i>	21
2.3.2	<i>The nodal diffusion code APOLLO3®.....</i>	21
2.3.3	<i>Short description of the nodal cross sections needed by APOLLO3® core solver.....</i>	23
2.3.3.1	<i>Coupling engine</i>	23
3	MODELS DESCRIPTION	24
3.1	RELAP5 MODEL OF THE KNPP (ENERGORISK)	24
3.1.1	<i>General description of the integral plant model for RELAP5</i>	24
3.1.2	<i>Extension of the plant model for the transient simulation</i>	30
3.2	RELAP5 MODEL OF THE KNPP (INRNE).....	31
3.2.1	<i>General description of the integral plant model for RELAP5</i>	31
3.2.2	<i>Extension of the plant model for the transient simulation</i>	32
3.3	TRACE/PARCS MODEL OF THE KNPP (KIT).....	33
3.3.1	<i>General description of the integral plant model for TRACE</i>	33
3.3.2	<i>Extension of the plant model for the transient simulation</i>	36
3.3.3	<i>Description of the core model in PARCS.....</i>	36
3.4	CATHARE3 MODEL.....	41
3.4.1	<i>General description of the integral plant model for CATHARE3</i>	41
3.4.1.1	<i>Primary loops.....</i>	41
3.4.1.2	<i>Steam generators</i>	41
3.4.1.3	<i>Secondary side.....</i>	42
3.4.1.4	<i>Main controllers</i>	43
3.4.2	<i>Initial conditions.....</i>	44
3.4.3	<i>Extension of the plant model for the transient simulation</i>	44
3.4.4	<i>Description of the core model for APOLLO3®.....</i>	44
3.4.4.1	<i>Core neutronic model.....</i>	45
4	SELECTED RESULTS FOR THE STATIONARY FULL POWER CONDITIONS	47
4.1	RELAP5 RESULTS FOR THE STATIONARY PLANT CONDITIONS (ENERGORISK).....	47
4.2	RELAP5 RESULTS FOR THE STATIONARY PLANT CONDITIONS (INRNE)	47
4.3	TRACE RESULTS FOR THE STATIONARY PLANT CONDITIONS (KIT)	48
4.4	CATHARE3/APOLLO3® RESULTS FOR THE STEADY STATE PLANT CONDITIONS	50
4.4.1	<i>Core modeling issues for Kozloduy core.....</i>	50
4.4.2	<i>Boundary conditions and steady-state conditions before transient</i>	50
4.4.3	<i>Comparison of main thermal hydraulic parameters predicted by CATHARE3 with the reference data</i>	52

4.4.4	<i>First test with the coupling core 3D neutronics and full system thermal-hydraulics</i>	53
4.4.5	<i>CATHARE3 results for the stationary plant conditions</i>	53
5	SELECTED RESULTS OF TRANSIENT SIMULATIONS OF EACH PARTNER	58
5.1	RELAP5 (ENERGORISK)	58
5.2	RELAP5 (INRNE)	67
5.3	TRACE/PARCS (KIT)	73
5.3.1	<i>Core behavior during the transient</i>	73
5.3.2	<i>Plant behavior during the transient</i>	75
5.4	CATHARE3/APOLLO3® (FRAMATOME)	78
6	COMPARATIVE ANALYSIS	84
6.1	THERMAL HYDRAULIC PARAMETERS	84
6.2	TRANSIENT PHASE	85
6.2.1	<i>Sequence of main events</i>	85
6.2.2	<i>Selected global thermal hydraulic parameters (all partners)</i>	85
7	CONCLUSIONS AND RECOMMENDATIONS	90
8	REFERENCES	92
9	APPENDIX I: REACTIVITY COEFFICIENTS & KINETIC PARAMETERS	94
9.1	REACTIVITY COEFFICIENTS	94
9.2	KINETIC PARAMETERS	94

List of figures

Figure 1: Break location with simplified steam system.....	14
Figure 2: Scheme of the main steam system with the location of the break.....	15
Figure 3: Feedwater flow as boundary condition for both the intact and affects SG-secondary side.....	17
Figure 4. Chain tools to generate macroscopic XS for PARCS.	20
Figure 5: APOLLO3® solvers available.....	22
Figure 6: C3PO data management [11].....	23
Figure 7: Nodalisation of the Konloduy NPP.....	25
Figure 8: Nodalisation scheme of the MCL loops.....	26
Figure 9: Nodalisation scheme of «hot» and «cold» SG reservoirs.....	27
Figure 10: Nodalisation diagram of the tube bundle for layers 1 - 5.....	28
Figure 11: Nodalisation diagram of the second circuit of the PGV – 1000M model.....	29
Figure 12: Nodalisation scheme of the steam pipelines.....	30
Figure 13: Nodalisation scheme of the steam pipelines break model.....	31
Figure 14: Kozloduy Reactor and Pressurizer RELAP5 Four Loops.....	32
Figure 15: <i>The Reactor Pressure Vessel and its radial, axial and azimuthal discretization (R, Z, Theta) for the analysis of the MSLB transient</i>	34
Figure 16: Integral model of the Kozloduy Nuclear Power Plant (KNPP) developed for TRACE (primary/secondary circuits, safety systems).....	35
Figure 17. Core model developed in PARCS.....	36
Figure 18. Control rod banks layout.	36
Figure 19. Cell model in SERPENT2 for FA1. Without control rods.	37
Figure 20. Cell model in SERPENT2 for FA2. Without control rods.	37
Figure 21. Cell model in SERPENT2 for FA3.....	37
Figure 22. Cell model in SERPENT2 for FA4.....	37
Figure 23. PARCS and Serpent2 difference in power per FA distribution in ARO condition without reflector DFs.....	38
Figure 24. PARCS and Serpent2 difference in power per FA distribution in ARO condition with reflector DFs.	38
Figure 25. PARCS and Serpent2 difference in power per FA distribution in ARI condition without reflector DFs.....	39
Figure 26. PARCS and Serpent2 difference in power per FA distribution in ARI condition with reflector DFs.	39
Figure 27: VVER-1000 UNIT geometry of one primary loop CATHARE3.....	41
Figure 28: VVER-1000 UNIT 6 Steam generator CATHARE3.....	42
Figure 29: VVER-1000 UNIT 6 Steam lines CATHARE3.....	43
Figure 30: VVER-1000 UNIT 6 Steam headers and BRUKs.....	43
Figure 31: Kozloduy-6 NPP CORE.....	45
Figure 32: a) CORE LAYOUT CYCLE 1 and b) CR LOCATION.....	46
Figure 33: Axially averaged relative radial power distribution of the core as predicted by TRACE/PARCS... ..	49
Figure 34: Radially averaged relative axial power distribution of the core as predicted by TRACE/PARCS.. ..	49
Figure 35: MCP start-up simulation CATHARE3 deck (Task 7.2) core + system thermal hydraulic simulation – Feasibility of the full system plus 3D neutronics coupling.....	53
Figure 36: Stationary plant conditions – Primary pressure.....	54

Figure 37: Stationary plant conditions – Pressurizer level	54
Figure 38: Stationary plant conditions – Core inlet (red) and outlet (green) temperatures	55
Figure 39: Stationary plant conditions – Mass flow in the cold legs	55
Figure 40: Stationary plant conditions – Pressure in the steam generators.....	56
Figure 41: Stationary plant conditions – Inlet mass flow in the Main Steam Lines	56
Figure 42: Stationary plant conditions – Water level in the steam generators	57
Figure 43: Stationary plant conditions – Water mass in the steam generators.....	57
Figure 44: Total Reactor Power.....	59
Figure 45: Primary pressure (at core exit)	59
Figure 46: Secondary pressure at MSH	60
Figure 47: Core exit coolant liquid temperature	60
Figure 48: Core exit cladding temperature	61
Figure 49: Core exit coolant (gas) temperature.....	61
Figure 50: Pressurizer water level	62
Figure 51: MSLB - differential break flow rate	62
Figure 52: MSLB - differential break flow rate (on both sides)	63
Figure 53: Integral MSLB flow rate from secondary circuit.....	63
Figure 54: Cold leg liquid temperature	64
Figure 55: Hot leg liquid temperature	64
Figure 56: Steam generators water level.....	65
Figure 57: Coolant flow rates in cold legs.....	65
Figure 58: Coolant flow rates in in hot legs	66
Figure 59: Total reactivity	66
Figure 60: Heat transfer from primary to SGs (initial -750 MWx4)	67
Figure 61: Evolution of the break mass flow rate	67
Figure 62: Evolution of the integrated mass of the coolant leaving the break.....	68
Figure 63: Evolution of the pressure at the core outlet.....	68
Figure 64: Evolution of the core exit temperature	69
Figure 65: Evolution of the PZR-water level.....	69
Figure 66: Evolution of the mass flow rate of the intact loop-1	70
Figure 67: Evolution of the mass flow rate of the Loop-4 primary.....	70
Figure 68: Evolution of the pressure of the intact SG-1	71
Figure 69: Evolution of the pressure of the broken SG-4 dome.....	71
Figure 70: Evolution of the mass inventory of the intact SG-1	72
Figure 71: Evolution of the mass inventory in the fault SG-4	72
Figure 72: Evolution of the total reactivity predicted by RELAP5.....	73
Figure 73: 3D coolant temperature at the fuel assembly outlet at 36 s transient time (lowest value of the coolant temperature at core inlet)	73
Figure 74: 3D fuel assembly power distribution at 36 s transient time (lowest value of the coolant temperature at core inlet).....	74
Figure 75: 3D coolant temperature at the fuel assembly outlet at 323 s transient time (lowest value of the coolant temperature at core inlet)	74
Figure 76: 3D fuel assembly power distribution at 323 s transient time (lowest value PZR water level)	75
Figure 77: Evolution of the break-outflow as predicted by TRACE/PARCS.....	76

Figure 78: Evolution of the pressure in the SG-dome part of loop-4 (broken Steam line) and the adjacent loop-1 as predicted by the coupled code 76

Figure 79: Coolant temperature evolution of the cold leg 1 and 4 during the transient progression as predicted by TRACE/PARCS..... 77

Figure 80: Evolution of the total reactivity after the SCRAM as predicted by TRACE/PARCS..... 77

Figure 81: Evolution of the total power after the SCRAM as predicted by TRACE/PARCS 78

Figure 82: CATHARE3 transient – Core power..... 79

Figure 83: CATHARE3 transient – Pressure in the pressurizer 79

Figure 84: CATHARE3 transient – Level in the pressurizer 80

Figure 85: CATHARE3 transient – Core temperature 80

Figure 86: CATHARE3 transient – Cold legs mass flow 81

Figure 87: CATHARE3 transient – Pressure in the steam generators..... 81

Figure 88: CATHARE3 transient – Water mass in the steam generators 82

Figure 89: CATHARE3 transient – Steam mass flow in the main steam line..... 82

Figure 90: CATHARE3 transient – Feed water mass flow 83

Figure 91: Evolution of the break-outflow as predicted by the partners (right: zoom of the first 50 s)..... 86

Figure 92: Evolution of the pressure at the main steam header of the secondary side and of the pressure at the core outlet as predicted by the partners 86

Figure 93: Evolution of the break-outflow as predicted by the partners 87

Figure 94: Evolution of the total power as predicted by the different codes (right: zoom of 50 s) 87

Figure 95: Evolution of the total reactivity as predicted by the different codes (right: zoom of first 50 s) 88

Figure 96: Evolution of the water level in the pressurizer..... 88

Figure 97: Evolution of the water level of the SG4 (left) and SG-1 (right) during the MSLB..... 89

Figure 98. Kinf as a function of DC for different boron concentration in FA type 1..... 94

Figure 99. Kinf as a function of DC for the different FA types, with fixed 1200 ppm boron concentration..... 94

List of tables

Table 1: Main thermal hydraulic parameters of the plant at nominal conditions 12

Table 2. PARCS and SERPENT2 keff comparisons at HFP state..... 38

Table 3. Variation points considered for the macroscopic cross section generation [15]. 39

Table 4. Selected branches for the XS generation..... 39

Table 5. Critical boron search fat HFP state. 40

Table 6: Cycle 1 type of ASSEMBLIES 45

Table 7: Cycle 1 CR POSITION 46

Table 8: Initial parameters 47

Table 9: Initial parameters 47

Table 10: Comparison of reference plant data for the nominal conditions compared to the predictions of TRACE/PARCS 48

Table 11: Comparisons at assembly level (Kinf at BOL without Xenon) for the 4 KZL6 FAs composing cycle 1 51

Table 12: comparisons at core level - KZL6..... 51

Table 13: Relationship between Safety banks position and boron concentration..... 52

Table 14: Initial parameters 52

Table 15: Chronological sequence of events for the “MSLB”	58
Table 16: Comparison of selected thermal hydraulic parameters for the nominal plant conditions just before the MSLB transient	84
Table 19: Comparison of sequence of main events predicted by partners	85
Table 20. Reactivity coefficients for nominal and critical boron concentration.....	94
Table 21. Kinetic data	95
Table 22. Delayed neutron fraction and decay constant data.....	95
Table 23. SCRAM worth with stuck control rod.....	95

Abbreviations

AC/DC	Alternating current / Direct current
AFW	Auxiliary Feed Water
ARO	All Rods Out
ARI	All Rods In
BDBA	Beyond Design Basis Accident
DBA	Design basis accident
DG	Diesel Generator
BOL	Beginning of Life
BOC	Beginning of cycle
BRU - A	Steam Dump to Atmosphere
BRU - K	Steam Dump to Condenser
BRU - SN	Steam Dump Facility for House Load
BZOK	Fast Acting Cut-off Valve
CAMP	Code Applications and Maintenance Program
ECCS	Emergency Core Cooling Systems
EOL	End of Life
EOC	End of fuel cycle
FA	Fuel Assemblies
FW	Feed Water
HA	Hydro Accumulator
HE	Hydrodynamic Element
HPI	High Pressure Injection
HFP	Hot Full Power
ICAP	International Code Assessment and Applications Program
KZL6	Kozloduy Nuclear Power Plant Unit 6
LOFT	Loss-of-fluid Test
MCP	Main Coolant Pump
MSLB	Main Steam Line Break
MIV	Main Isolating Valve

MSH	Main Steam Header
MSIV	Main Steam Isolation Valve
NPP	Nuclear Power Plant
NRC	Nuclear Regulatory Commission
NRU	National Research Universal
PBF	Power Burst Facility
PRZ	Pressurizer
PWR	Pressurizer Water Reactor
SBO	Total Station Blackout
SG	Steam Generator
SCRAM	Emergency shutdown of the reactor (Safety control rod assembly moving)
SVs	Safety Valves
UVC	Control and Computing System
VVER	Water-Water Cooled Reactor
XS	Cross Sections

1 DESCRIPTION MSLB TRANSIENT SCENARIO

1.1 Introduction

An important goal of the CAMIVVER-project is the development of reliable both neutron physical core models and system thermal hydraulic models of VVER-1000 reactors for the analysis of transients, where distortions of the core behavior are expected to occur as may be the case in the main steam line break (MSLB) in a loop, the boron dilution transients, or control rod ejection accidents, etc. This kind of transients are traditionally analyzed with system thermal hydraulic codes using the Point Kinetics models, which are characterized by large conservatism since e.g. the axial power distributions put in the codes does not change during the transient and it use global core parameters e.g. the Doppler and moderator reactivity coefficients to take into account the feedbacks between the neutronic and thermal hydraulic core parameters.

Especially in case of a MSLB transient there is a concern of re-criticality and return to power despite the reactor is shut-down by SCRAM due to the strong undercooling of a portion of the core linked with the defect loop, where the break of the respective steam line is assumed to occur.

Since decades, 3D neutron diffusion solvers for both square and hexagonal fuel assemblies are being developed world wide and these solvers are coupled with different system thermal hydraulic codes resulting in powerful coupled codes such RELAP5/PARCS, TRACE/PARCS, ATHLET/DYN3D, ATHLET/CUBBOX-QUABOX, CATHARE2/CRONOS2, etc.

These codes are being validated using plant data in the frame of different international OECD/NEA Benchmarks e.g. the TMI-1 MSLB Benchmark, the Peach Bottom Turbine Trip 2, the VVER-1000-Coolant transient, the VVER-1000 Main Coolant Pump Restart, the VVER-1000 MSLB, the Rostov2 Boron Dilution, etc.

In recent years, the CEA/EDF/FRAMATOME have developed new advanced code versions such as APOLLO3 and CATHARE3, which are being coupled and extensively applied to the analysis of French PWR nuclear power plants. In addition, new initiatives are devoted to extend the application of such coupled tools i.e. CATHARE3/APOLLO3 for the transient analysis of different type of VVER-reactors. This is one goal of the CAMIVVER-project.

An academic MSLB-transient scenario was defined in CAMIVVER to assess the prediction capability of coupled codes (CATHARE3/APOLLO3, TRACE/PARCS) and also system thermal hydraulic codes (RELAP5, TRACE using Point Kinetics) for the analysis of a MSLB transient that may happen at BOC-conditions (fresh core, opposite to the OECD VVER-1000 MSLB transient that is defined for Cycle 6) with specific assumptions intended to simplified the analysis and be more focus on the analysis of code capabilities as a first step.

For this purpose, KIT and FRAMATOME developed a core loading specifications in order to generate own two-group nodal cross sections for PARCS and APOLLO3 core solvers using different lattice physics codes e.g. Serpent2 (KIT) and APOLLO3 lattice solver (FRAMATOME). In addition, KIT also performed static core analysis with PARCS in order to generate the reactivity coefficients, the kinetic parameters such as effective fraction of delay neutrons, prompt neutron lifetime, and the shut-down reactivity needed by the RELAP5 (ENERGORISK) and TRACE (INRNE) Point Kinetics models. Doing so, a consistent approach is assured for the comparison of the 3D core analysis and the one performed with Point Kinetics.

In this report, the initial conditions of the MSLB-transient as well as the transient scenario will be described, which deviates from the one of the OECD/NEA VVER-1000 MSLB benchmark. Then, the different computer codes are shortly described. It is followed by the characterization of the respective models performed by each institution.

In addition, the main thermal hydraulic and neutronic results obtained by the partners using the different computational tools are presented and discussed, also in comparison with the main reference plant data.

Finally, each partner present selected results of the transient phase and discuss them.

A last chapter is focused on the comparative analysis –where it is possible- of the main transient results obtained by the partners. Conclusions and further work are given at the end of the report.

1.2 Initial Steady State Conditions

In [1] the MSLB transient initial conditions and scenario description is described in detail, which was developed based in the Final Specifications of the OECD/NEA V1000-MSLB Benchmark [2]. Contrary to the official benchmark, in [1] it is assumed that the MSLB occurs at BOC conditions i.e. a fresh core loading when the plant is operated at nominal power i.e. 3000 MWth.

All the needed details about the geometry, materials, dimensions, operational conditions are collected in [1] so that each partner can develop their own plant models for the analysis of the MSLB-transient.

The reactivity coefficients obtained by KIT for the fresh core are described in the PARCS Subchapter. In Table 1, the main parameters of the Kozloduy NPP at nominal conditions just before the transient are given.

Table 1: Main thermal hydraulic parameters of the plant at nominal conditions

Parameter	Reference Data
Reactor thermal power, MW	3000
Primary pressure, MPa	15.7
Pressurizer Level, m	8.77
Coolant temperature at reactor inlet, K	560.15
Coolant temperature at reactor outlet, K	592.05
Mass flow rate through one loop, kg/s	4400
Reactor mass flow rate, kg/s	17600
RPV bypass, %	0.1
Total bypass of reactor core, %	3-5
Pressure in SG, MPa	6.27
Feedwater temperature, K	493.15
Pressure in the main steam header (MSH), MPa	6.08
Steam mass flow rate through SG steam line, kg/s	408
SG Water Levels, m	2.40
Liquid mass in the SG secondary side, t (assumed)	48

For the point kinetics models in TRACE and RELAP5, the following parameters needs to be used:

- Critical control rod position:
 - Critical boron concentration: 1630 ppm
 - Position of CR-Banks 1-9: 100 % ARO
 - Position of CR-Bank 10: 80 % ARO
- Reactivity coefficients:

State, boron	$\$/\Delta$ Coolant density	$\$/\Delta$ Boron in coolant	$\$/\Delta$ Fuel temperature	$\$/\Delta$ Coolant temperature
	$\$/\text{kgm}^3$	$\$/\text{ppm}$	$\$/\text{K}$	$\$/\text{K}$
HFP,	2.23E-03	-1.53E-02	-3.37E-03	-1.03E-03

1200 ppm				
HFP, 1630 ppm	-4.54E-03	-1.43E-02	-3.36E-03	-3.40E-03

- Shutdown reactivity: 10.9 \$
- Kinetic parameters of the BOC conditions:
 - Effective fraction of delay neutrons: 0.00705
 - Neutron generation time: 0.0000257 s
 - Fraction of delay neutrons and decay constants:

Group	Beta fraction	Lambda (1/s)
1	2.085E-04	1.2467E-02
2	1.023E-03	2.8292E-02
3	5.940E-04	4.2524E-02
4	1.334E-03	1.3304E-01
5	2.264E-03	2.9247E-01
6	7.558E-04	6.6649E-01
7	6.261E-04	1.6348E+00
8	2.474E-04	3.5546E+00

1.3 Transient scenario

The transient scenario is characterized as follows [1], [2]:

(1) Initiating event

- Break: A large break of the steam line of loop-4 is assumed to occur at time 0 sec. The break is located between the steam generator (SG) and the steam isolation valve (SIV), see Figure 1.
- The break size is of 580 mm diameter

(2) Assumptions

- The break happens when the plant is operated at nominal plant conditions,
- Core is loaded with fresh fuel at begin of cycle (BOC) conditions,
- SCRAM is assumed just after the break initiation for simplifications (normally SCRAM is caused either by low secondary side pressure, low primary circuit pressure or high thermal power);
 - Most reactive peripheral control assemblies remain stuck out in case of scram,
 - Location of stuck rod is close to the core sector with the highest overcooling,
 - The time for the full control rod insertion is 4 sec

- Turbine stop valves (MSIV) closes for 10 s after the reactor scram. Time for fully open/close MSIV – 0.2 s;
- Turbine bypass to condenser (BRU-Ks) starts to open and switches to MSH pressure control mode after closing MSIV.
- The Opening of all 4 BRU-Ks at $P_{MSH} > 6.67\text{MPa}$ and supporting $P_{MSH} = 6.2807\text{ MPa}$. BRU-Ks closes at 5.79 MPa and will be re-open again only if $P_{MSH} > 6.67\text{MPa}$;
- BZOK #4 (FAIV) is closing after reaching the signals. The signals applied in the scenario are: Signal for close SIV-4 (BZOK) is $P_2 < 4.9\text{ MPa}$ and $T_{s1} - T_{s2} > 75\text{°C}$;
- Make up and Let down systems are used only during the steady state. During the transient these systems are not used. It is assumed that they are isolated within 2 sec after transient start;
- PRZ heaters are switched on after primary depressurization for some period until primary pressure is back after dry-out of SG#4 and due to decay power. In our case they are switched off after PZR water level became below 4.2m which happen in first 50 s.
- The main coolant pump (MCP) of the affected loop-4 is shutdown with a coast down time of 55 s,
- Feed water valve fails and remains open (additional FW into SG)
- No credit is taken for the negative reactivity effect from the addition of borated water into the primary system by the high pressure injection pumps (HPI),

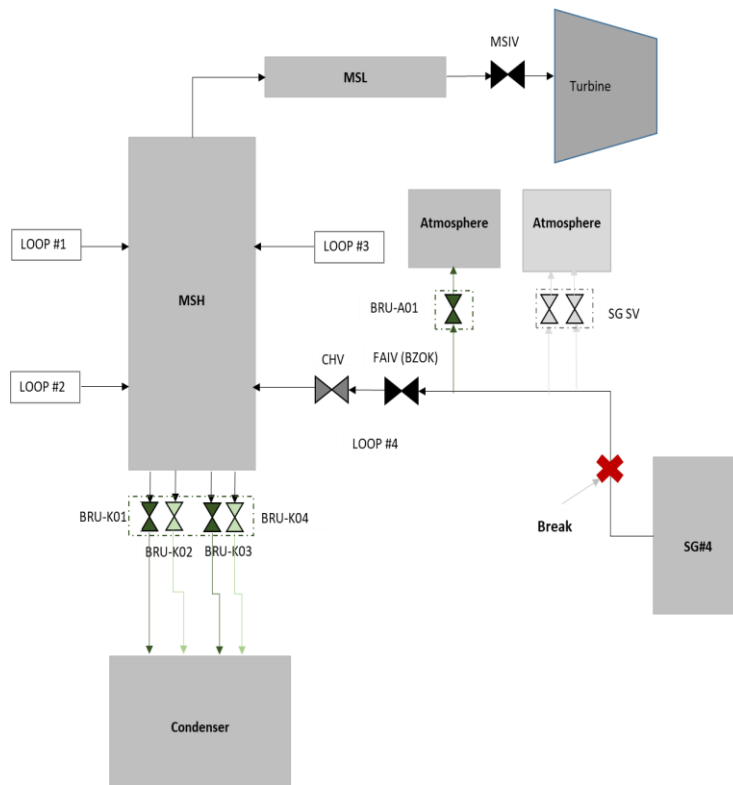


Figure 1: Break location with simplified steam system

Summarizing, the MSLB-scenario can be described as follows: After break initiation, the SIV-4 starts to close and the “check valve” of affected loop-4 closes to isolate the main steam header (MSH) from the break. The turbine stop valves close 10 s after scram due to protection signal while the turbine bypass valve (to condenser) starts to open and it switches to MSH pressure control mode. Due the break the primary-to-secondary heat transfer over the affected SG increases considerably by the flashing and two-phase flow heat transfer conditions on the SG-secondary side. The loop-1, which is close to affected loop-4, experiences a maximum overcooling of around 50 K relative to the conditions before break initiation.

Due to the overcooling, the primary system pressure decreases continuously. Once the level of 10.75 MPa is reached, the HPI-pumps (TQ3 and TQ4) start to inject borated water. But not credit it taken to it.

The main concern here is the possibility of re-criticality and power increase even though reactor scram has happened. The local power distribution within the core will strongly depends of the multidimensional coolant mixing taking place in the downcomer and lower plenum. Since the MCP-4 is switched off, reverse flow establishes in loop-4 leading to complex mixing process in the upper plenum. In Figure 2, a schematic view of the main steam supply system with the location of the break is shown. It can be seen that this system is complex compared to the one of Western type PWR.

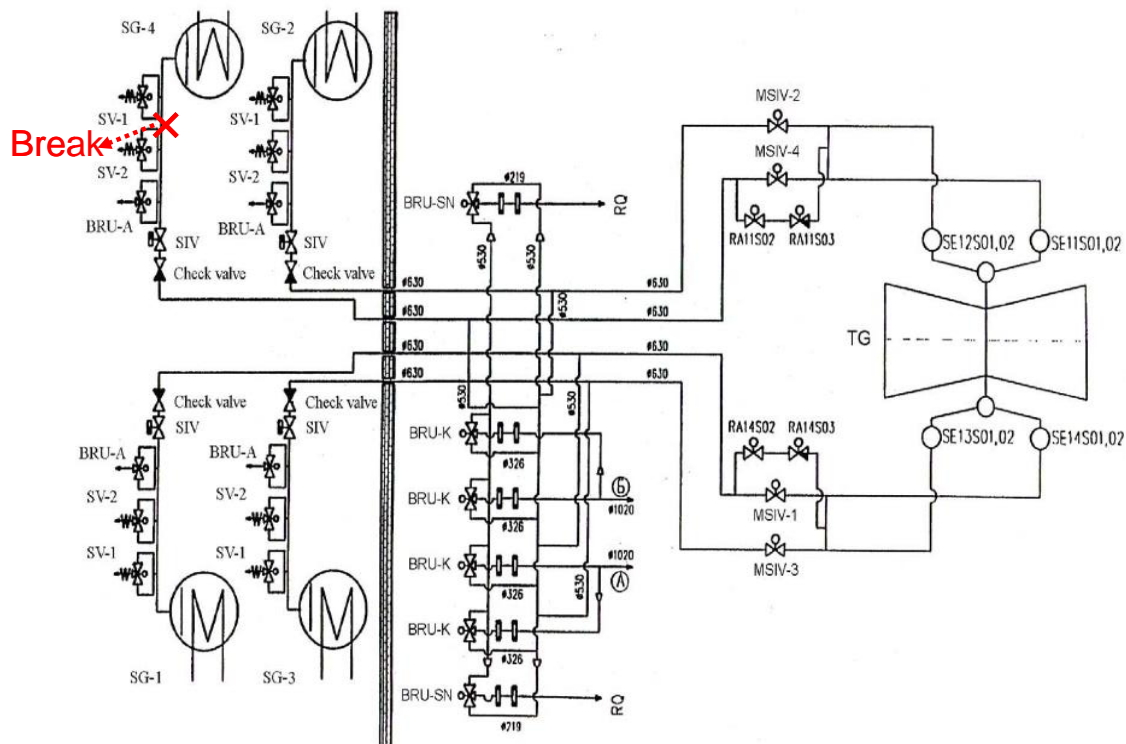


Figure 2: Scheme of the main steam system with the location of the break

1.4 Boundary conditions for the transient phase

For the transient phase, the following boundary conditions needs to be considered according to [1]:

- Feed water boundary condition to SG #4 (Scenario 1)

Time (s)	Flow (kg/s)	Feed water temperature	Time (s)	Flow (kg/s)	Feed water temperature
0	410.32	220	125	28.34	160
5	587.92	220	130	34.74	160
10	646.93	220	135	24.39	160
15	608.65	220	140	26.08	160
20	426.22	220	145	25.40	160
25	370.68	220	150	11.40	160
30	335.13	220	155	20.83	160
35	332.32	220	160	21.37	160
40	251.78	160	165	9.47	160
45	217.05	160	170	16.02	160
50	155.94	160	175	17.16	160
55	106.67	160	180	15.27	160
60	66.90	160	185	10.73	160
65	25.36	160	190	3.66	160
70	0.00	160	195	1.37	160
75	0.00	160	200	0.49	160
80	0.00	160	205	2.36	160
85	0.00	160	210	4.22	160
90	9.46	160	215	13.10	160
95	8.78	160	220	12.23	160
100	7.95	160	225	5.78	160
105	9.78	160	230	0.42	160
110	39.71	160	235	0.90	160
115	34.41	160	236	0.0	
120	43.21	160	600	0.0	

* Based on OECD benchmark 2 the feed water temperature in broken SG#4 is conservatively fixed to 160°

- Feed water flow boundary conditions to intact SGs

Time (s)	Flow (kg/s)	Feed water temperature
0	410	220
10	366	220
11	362	170
40	237.0	170
41	232.0	170
95	0.0	170
96	0.0	
600	0.0	

* Based on OECD benchmark 2 the feed water temperature in SG#1, 2 and 3 is conservatively fixed to 170°C

The evolution of the feedwater flow during the transient is for the SG-secondary side are shown in Figure 3.

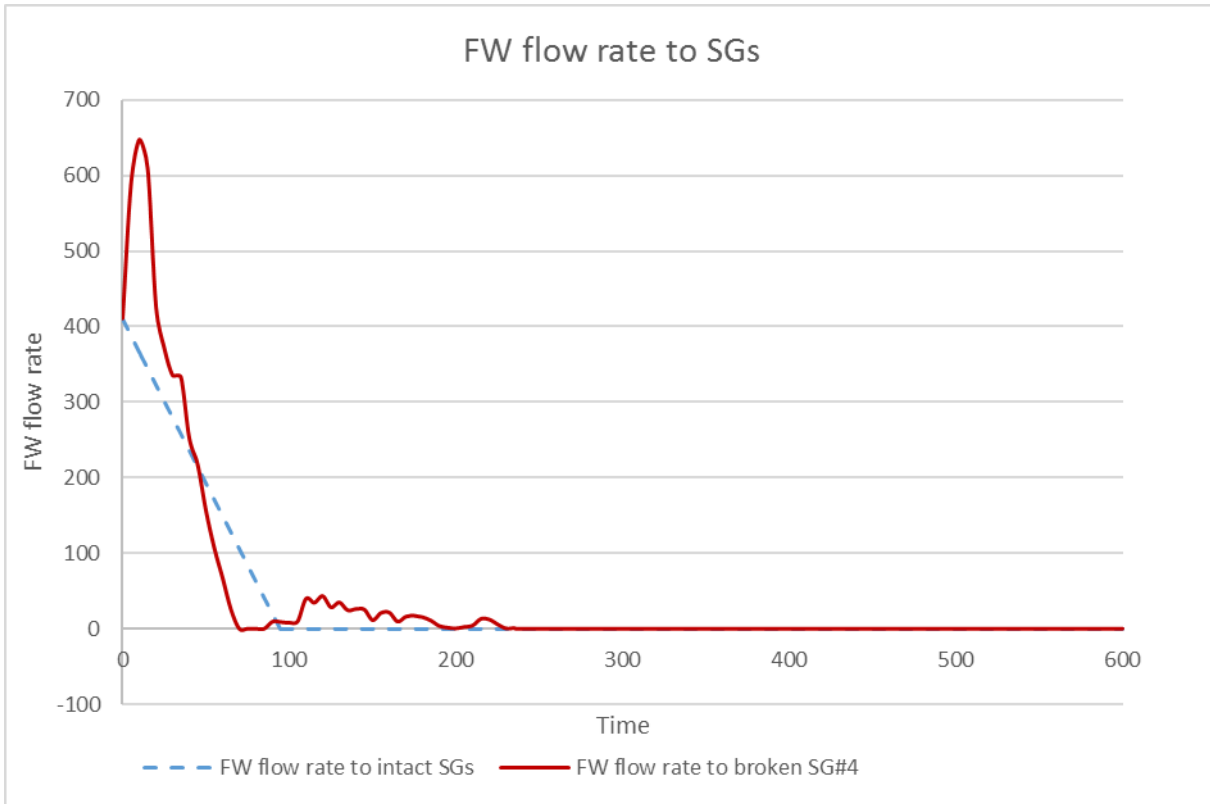


Figure 3: Feedwater flow as boundary condition for both the intact and affects SG-secondary side

- Pressurizer heaters status during steady state:

Heater 1 On	P<159.5	[kgf/cm ²]	YP10W01
Heater 2 On	P<159,5	[kgf/cm ²]	YP10W02
Heater 3 On	P<157	[kgf/cm ²]	YP10W03
Heater 4 On	P<157	[kgf/cm ²]	YP10W04
Heater 1 Off	P>161	[kgf/cm ²]	
Heater 2 Off	P>160	[kgf/cm ²]	
Heater 3 Off	P>158	[kgf/cm ²]	
Heater 4 Off	P>158	[kgf/cm ²]	

The power of each heater is given in the following table:

<i>N^o</i>	<i>Parameter</i>	<i>Units</i>	<i>Value</i>
1.	Power of single heater	kW	10
2.	Power of single blocks	kW	90
3.	Power of groups:	kW	2520
	• YP10W01 (3 blocks)		270

<i>N^o</i>	<i>Parameter</i>	<i>Units</i>	<i>Value</i>
	<ul style="list-style-type: none">YP10W02 (3 blocks);YP10W03 (8 blocks);YP10W04 (14 blocks)		270 720 1260
4.	Elevation of first row of heaters from the bottom of pressurizer	mm	1310

It is worth to mention that all heaters must be switch off as long the water level is below 4.20 m.

2 SHORT DESCRIPTION OF THE TOOLS

2.1 Short description of RELAP5 (ENREGORISK)

The RELAP5 code has been developed for best-estimate transient simulation of light water reactor coolant systems during postulated accidents. The code models the coupled behavior of the reactor coolant system and the core for loss-of-coolant accidents and operational transients such as anticipated transient without scram, loss of offsite power, loss of feedwater, and loss of flow. A generic modelling approach is used that permits simulating a variety of thermal hydraulic systems. Control system and secondary system components are included to permit modelling of plant controls, turbines, condensers, and secondary feedwater systems.

The MOD3 version of RELAP5 has been developed jointly by the NRC and a consortium consisting of several countries and domestic organizations that were members of the International Code Assessment and Applications Program (ICAP) and its successor organization, Code Applications and Maintenance Program (CAMP) [3].

The RELAP5/MOD3 code is based on a nonhomogeneous and non-equilibrium model for the two-phase system that is solved by a fast, partially implicit numerical scheme to permit economical calculation of system transients. The objective of the RELAP5 development effort from the outset was to produce a code that included important first-order effects necessary for accurate prediction of system transients but that was sufficiently simple and cost effective so that parametric or sensitivity studies were possible.

The code includes many generic component models from which general systems can be simulated. The component models include pumps, valves, and pipes, heat releasing or absorbing structures, reactor point kinetics, electric heaters, jet pumps, turbines, separators, accumulators, and control system components. In addition, special process models are included for effects such as form loss, flow at an abrupt area change, branching, choked flow, boron tracking, and no condensable gas transport.

The system mathematical models are coupled into an efficient code structure. The code includes extensive input checking capability to help the user discover input errors and inconsistencies. Also included are free-format input, restart, re-nodalisation, and variable output edit features. These user conveniences were developed in recognition that generally the major cost associated with the use of a system transient code is in the engineering labor and time involved in accumulating system data and developing system models, while the computer cost associated with generation of the final result is usually small.

RELAP5 represents the aggregate accumulation of experience in modelling reactor core behavior during accidents, two-phase flow processes, and LWR systems. The code development has benefitted from extensive application and comparison to experimental data in the LOFT, PBF, SEMISCALE, ACRR, NRU, and other experimental programs [4].

2.2 Short description of TRACE/PARCS (KIT)

Hereafter the coupled code TRACE/PARCS used by KIT will be described shortly.

2.2.1 The system thermal hydraulic code TRACE

The system thermal-hydraulic code TRACE is a best-estimate system code of the U.S. NRC for the analysis of Light Water Reactor (LWR) and more recently extended for liquid metal cooled fast reactors. TRACE solves the static or time-dependent system of six conservation equations of a two-fluid mixture in 1D and 3D (Cartesian and Cylindrical coordinates) computational domain using the finite volume and donor-cell approach. Additional equations are formulated to describe the transport of boron in the liquid phase and of

non-condensable gases in the gas phase. Due to its versatility, not only NPPs but also different experimental test sections or loops can be simulated with TRACE.

A complete set of constitutive equations are formulated to close the balance equations describing the interphase and wall-to-fluid mass and heat transfer in all flow regimes of the boiling curve (i.e. pre- and post-CHF) for both horizontal and vertical flow conditions. In this approach, mechanical and thermal non-equilibrium situations are considered. Various models for components of an NPP e.g. pumps, valves, pipes, heat structures, as well as dedicated models for trips and control systems are also implemented in TRACE.

Two numerical methods, a semi-implicit method, and the SETS method are implemented in TRACE to solve any kind of slow and fast transients [5]. Dedicated models describe specific physical phenomena such as thermal stratification, point kinetics, critical flow, etc. TRACE is recently equipped with an Exterior Communication Interface (ECI) for the coupling with any kind of solvers [ECI]. Typically, system codes such as TRACE are coupled 3D nodal diffusion solvers for the enhanced simulation of non-symmetrical transients in NPPs. At KIT, multi-scale coupling approaches for TRACE with CFD and subchannel codes are being developed [6] based on the ICoCo-Method [7].

2.2.2 The nodal diffusion code PARCS

The PARCS (Purdue Advanced Reactor Core Simulator) neutronic code is a widely used reactor physics code developed by Purdue University for simulating the behavior of nuclear reactor cores. PARCS is a three-dimensional (3D) reactor core simulator which solves the steady-state and time-dependent, multi-group neutron diffusion and SP3 transport equations in orthogonal and non-orthogonal geometries. PARCS is coupled directly to the thermal-hydraulic system code TRACE which provide the temperature and flow field information to PARCS during the transient calculations via the few group cross sections. A separate code module, GENPMAXS, is used to process the cross sections generated by a lattice physics code into the PMAXS format that can be read by PARCS [8].

2.2.3 Description of the nodal cross sections needed by PARCS

Macroscopic cross sections (XS) are generated using SERPENT2 version 2.1.32. GENPMAXS version 6.2 is used to process the XS generated by SERPENT2 into the PMAXS format that PARCS can read, as illustrated in Figure 4. Details of the XS generation process are described in section 3.3.3.

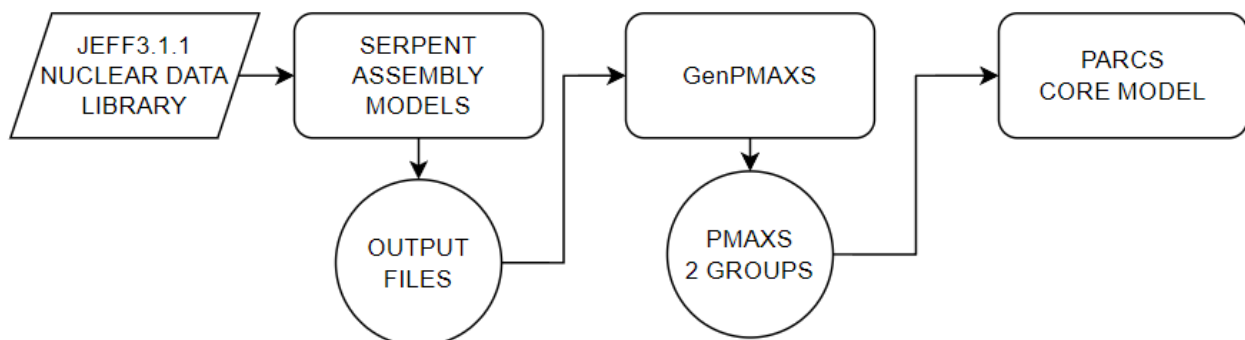


Figure 4. Chain tools to generate macroscopic XS for PARCS.

2.3 Short description of CATHARE3/APOLLO3®

One of the H2020 CAMIVVER purpose is the development and validation of best estimate calculation tools for VVER and PWR reactors. The development of a first prototype of APOLLO3® core code and CATHARE3 core 3D multi-physics coupling with its first testing on a Cartesian small PWR core is the result of several

months and interactions among different R&D Projects, in collaboration with CEA developers of both APOLLO3® and CATHARE3 codes.

The development of this coupling is achieved in collaboration among French partners (mainly FRAMATOME and CEA) and is one of the first feasibility assessments of 3D coupling between the thermal-hydraulic code CATHARE3 [9] with a neutronic core code, such as APOLLO3® [10], at core level.

Both codes are coupled through the C3PO Python coupling library [11].

APOLLO3® code sources are shared with FRAMATOME in the framework of the CAMIVVER project as presented in reference [9]. CATHARE3 was already provided to French partners and C3PO has an Open-source access [11].

The CATHARE3 3D functionalities used in the framework of the past 3 years of CAMIVVER project mainly support cartesian geometry.

For VVER small and full core calculations, the PoC APOLLO3®/CATHARE3 coupling prototype was extended to hexagonal FAs core geometry too. For this first tentative application, a simplified representation of hexagonal FAs through equivalent thermal-hydraulic and geometrical properties (surface area, hydraulic diameter, etc.), while paying a small error in representation, has been realized, too, in the framework of the project.

This approach has been judged sufficient, for the purpose of providing thermal-hydraulic feedbacks to APOLLO3® neutronic core code, as complementary contribution in comparison with the APOLLO3®/THEDI option in Task 5.3, and for supporting the task 7.4. Some results will be proposed in next chapters.

The CATHARE3 code enables the simulation of both core and system thermal-hydraulics and a first feasibility analysis was also oriented to extend the calculation domain from the core to the vessel and then to the primary system with a multiscale approach. Thanks to the functionalities of CATHARE3 code, enabling 3D junctions, the 3D core may be associated to vessel and primary circuit modeling in Cartesian geometry. This activity has been identified as a possible contribution, feeding the discussion about improvements in MSLB accident simulation. For this purpose, full core Kozloduy NPP Unit 6 3D neutronics core modeling at steady-state calculations have been realized in collaboration between WP5 and WP7. The last part of the project is dedicated to the integration of such a core into a Kozloduy NPP Unit 6 full primary and secondary CATHARE3 model, based initially on a MCP start-up test case. The same functionalities will be injected into a deck of first attempt modeling an MSLB scenario as asked in Task 7.4.

Further improvements are expected during the follow-up of the project.

2.3.1 The system thermal hydraulic code CATHARE3

CATHARE-3, as mentioned in [10], is the new version of the French thermal-hydraulic code for the safety analysis of nuclear reactors. The main new features of this CATHARE3 code are: the 3-fields modelling capabilities, the predictive pump model; the multi-fluid and multi-reactor modelling tools and the improved 3D modelling capabilities.

Concerning major development evolutions the following point is of major importance:

- A new architecture for 3D simulations, that is still under development and that will be implemented in a CEA's open-source software development platform;
- An Application Programming Interface (API) for software coupling, called ICoCo, that makes it possible to use each software as a callable library through C function calls: these calls allow a small C++ or Python program, known as the "supervisor" to perform and control a calculation.

2.3.2 The nodal diffusion code APOLLO3®

In the activities carried out at WP5 and WP7 Task 7.4, APOLLO3® core solver has been used. It has been the occasion of testing Python API for PWR and VVER configurations. APOLLO3® is the new generation

French deterministic code for lattice and core calculations, developed since 2007 at the CEA with support of EDF and FRAMATOME [9].

A synthetic description of the solvers available for APOLLO3® lattice and core calculations is shown in Figure 5.

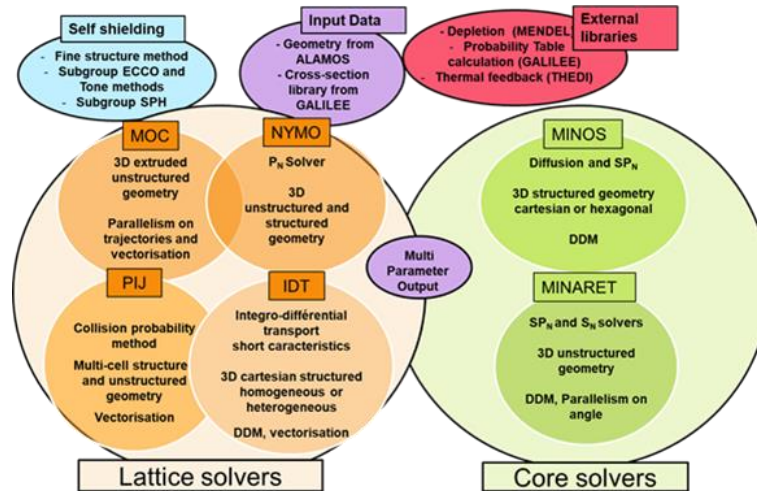


Figure 5: APOLLO3® solvers available.

For the activities carried out in Task 7.4, for core calculations the following options have been used:

- MINOS solver: SP_N equation on Cartesian and Hexagonal 3D structured geometries using Raviart-Thomas space finite elements,
- Diffusion approximation adopted,
- 2 energy groups calculations,
- Homogeneous assembly XS.

In WP7 both THEDI, multi-1D, two-phase flow solver [9], and CATHARE3 have been used for providing thermal and thermal-hydraulic feedbacks to the APOLLO3® code.

The THEDI coupling option has been mostly used to run sensitivities on full core steady-state configurations in order to test MPO provided by WP4 for the KNPP cycle 1 case.

Cycle1 KNPP keff calculation, critical boron concentration and control rod position preliminary calculations have been run with these tools.

In WP7 both THEDI, multi-1D, two-phase flow solver [9], and CATHARE3 have been used for providing thermal and thermal-hydraulic feedbacks to the APOLLO3® code.

The THEDI coupling option has been mostly used to run sensitivities on full core steady-state configurations in order to test MPO provided by WP4 for the KNPP cycle 1 case.

Cycle1 KNPP keff calculation, critical boron concentration and control rod position preliminary calculations have been run with these tools.

The coupling between APOLLO3® and THEDI can be achieved by either using THEDI as an internal library of the APOLLO3® code (approach used in CAMIVVER) or externally using C3PO coupling kernel as it has been the choice for CATHARE3.

The coupling APOLLO3®/CATHARE3 proof of concept application to VVER was successfully developed to be addressed to:

- Small and full core configurations,
- Full plant core plus system calculations.

In both cases the radial discretization available for the time being has un homogeneous assembly mesh approach. Several tests have been realized towards small core configurations in task 5.2 (D53). A calculation of first attempt has been realized for testing the POC on a full plant model, coupled with neutronics, too.

2.3.3 Short description of the nodal cross sections needed by APOLLO3® core solver

In the framework of the CAMIVVER project, the APOLLO3®/CATHARE3 coupling first prototype has been managed under GitLab platform for participative development purposes and it has been installed on the FRAMATOME/EDF HPC computing cluster.

The components and different modules directly called and supervised by the C3PO [11] coupling engine are the following:

- ICoCo [10]
- APOLLO3®-2.2 (following version 2.3 has been tested too on a limited number of cases and new versions should be easily compatible too) [9]
- CATHARE3 (dynamically driven by a specially conceived python API) [10].

Input options are provided by a short ASCII input deck for both core and system, specifying the scenario data and the python preprocessor options for PWR or VVER geometries. Calculations are then possible in steady-state and transient conditions.

A limited number of optional features and procedures for post-processing are available but further improvements will be necessary with developments oriented to consolidate and automatize the approaches.

2.3.3.1 Coupling engine

In the framework of the CAMIVVER project the standard approach for code interfaces follows the ICoCo norm [10] defined by CEA. This is the case for both APOLLO3® and CATHARE3 codes. Any new code API already compatible with ICoCo norm may be easily coupled to the others thanks to a derived class implemented at the interface between the code and the coupling engine C3PO.

Figure 6 presents the information management offered by C3PO.

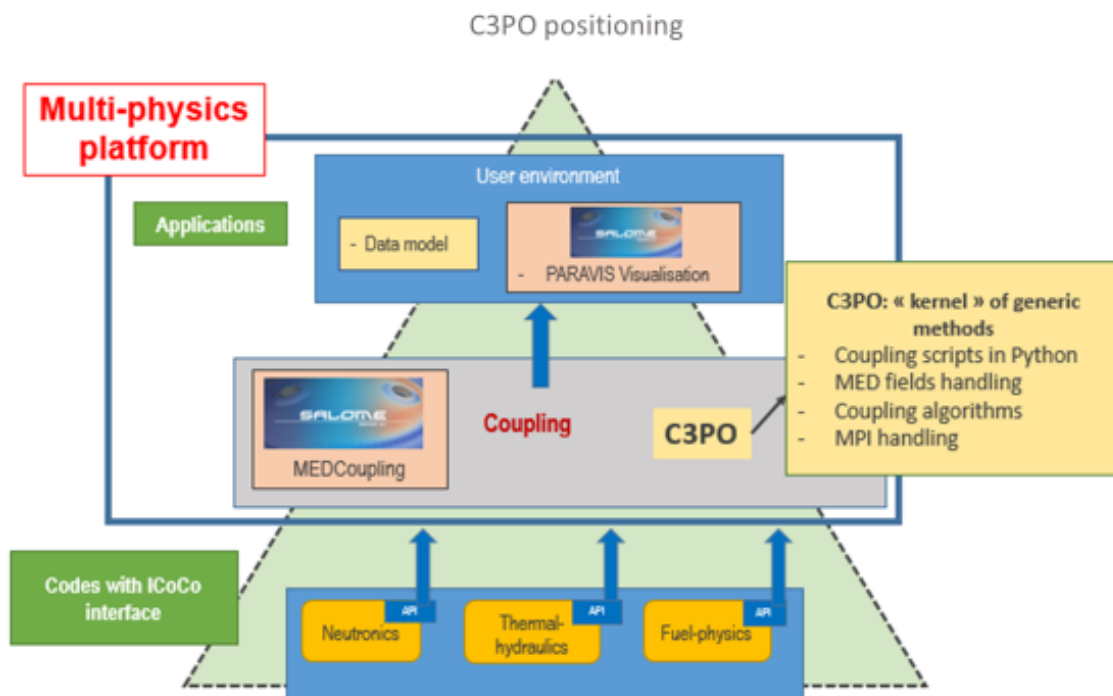


Figure 6: C3PO data management [11]

3 MODELS DESCRIPTION

3.1 RELAP5 model of the KNPP (ENERGORISK)

3.1.1 General description of the integral plant model for RELAP5

The developed model of the reactor is a 4-sector one with cross-links to simulate flows between sectors, Figure 7 . This layout allows simulating the independent movement of the coolant within one loop. The area of the inlet and outlet pipes is divided into 8 equal parts, simulating annular gaps between the shaft and the reactor vessel. This allows you to properly separate flows during partial MCP operations, [12] .

The disturbance introduced by the ECCS branch pipes in the lowering section on the connections 67-1 and 69-1 has a turning effect on the flow of the coolant down the lowering section and causes the coolant to mix with the neighbouring sector counter clockwise. The user can turn off the additional resistance of the ECCS pipes and get the so-called «symmetric» model, where the loop coolant enters the corresponding core sector almost unmixed. By default, the model is left «asymmetric», which is important for modelling asymmetric processes in the active zone.

The core is divided into 4 sectors, preserving the symmetry of the connected loops. No radial separation is provided. There are 3 channels allocated in each sector – medium fuel element, medium fuel element in hot fuel element and hot fuel element in hot fuel element. Bypasses are simply represented as common to all sectors.

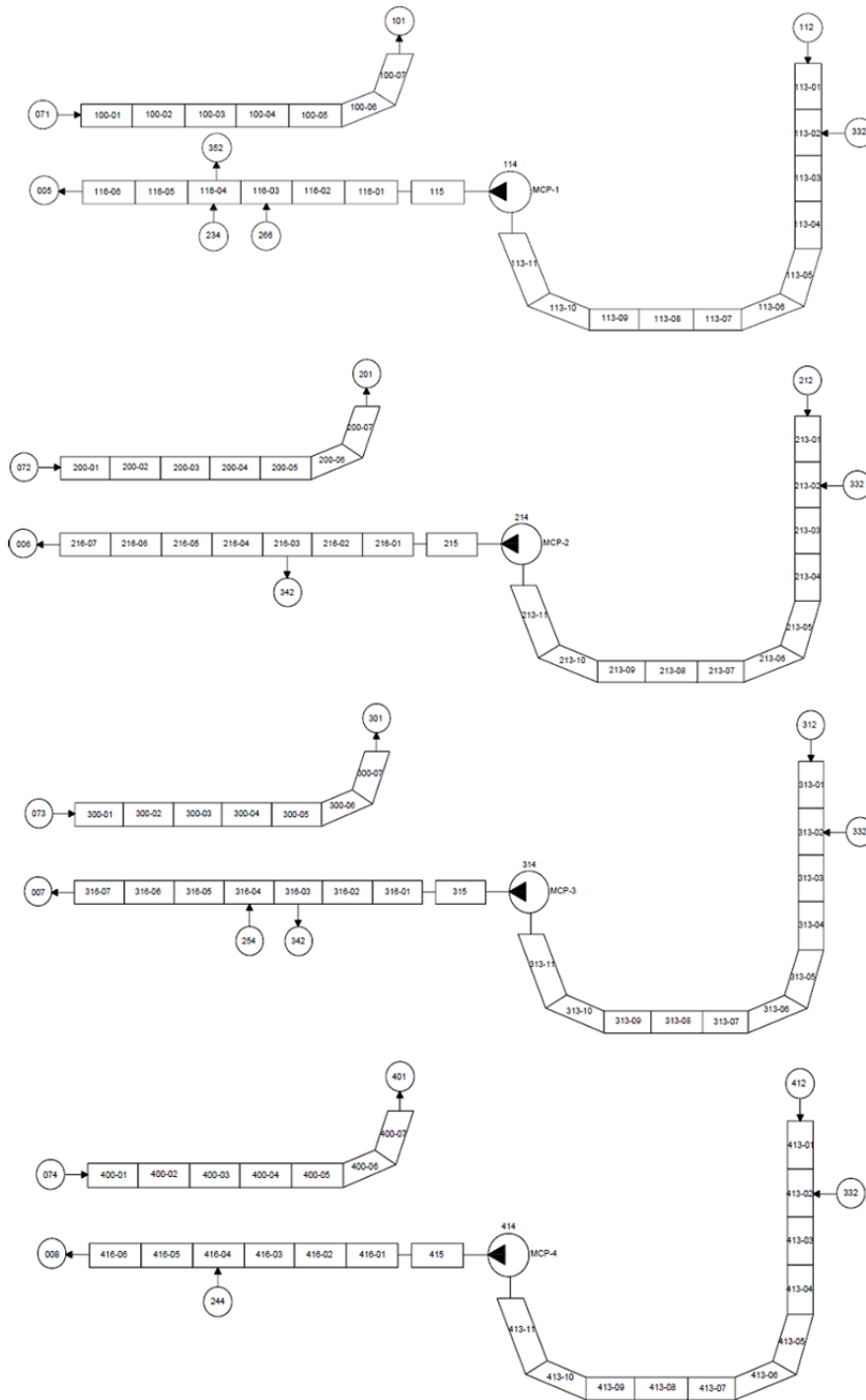


Figure 1: Nodalization scheme of the MCL loops

Figure 8: Nodalisation scheme of the MCL loops

The nodalisation scheme of the «hot» and «cold» SG reservoirs is shown in Figure 9. The first SG circuit consists of «hot» and «cold» collectors and pipes. HE 101 – «hot» SG collector, HE 112 – «cold» SG collector, HE 102,103,104,105,106,107,108,109,110,111-describe the SG tube.

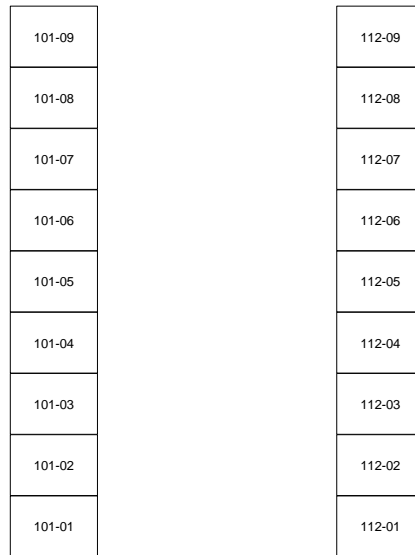


Figure 9: Nodalisation scheme of «hot» and «cold» SG reservoirs

Hydrodynamic element of the tube bundle are located in the first five layers of the second circuit of the computational model. The nodalisation diagram of the tube bundle for layers 1 - 5 is shown in Figure **10**.

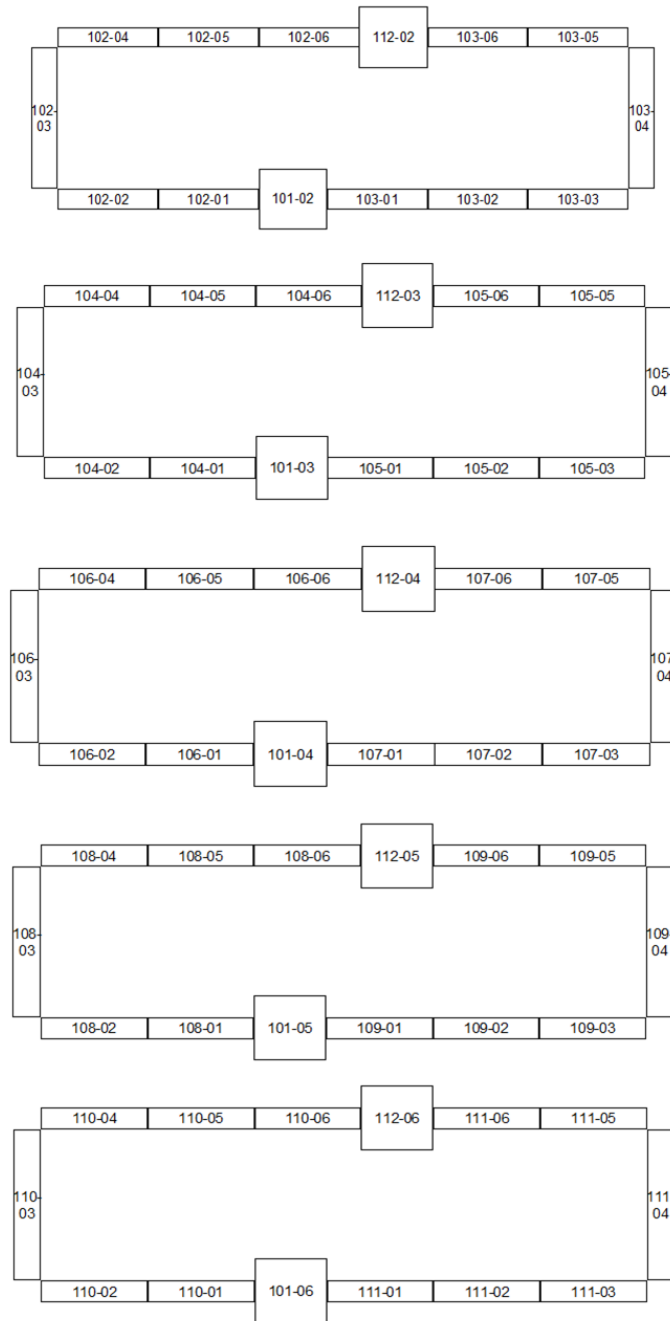


Figure 10: Nodalisation diagram of the tube bundle for layers 1 - 5

Figure **11** shows the nodalisation scheme of the second circuit of the PGV-1000M steam generator, [12]. All 4 steam generators (SG) in the model are similar.

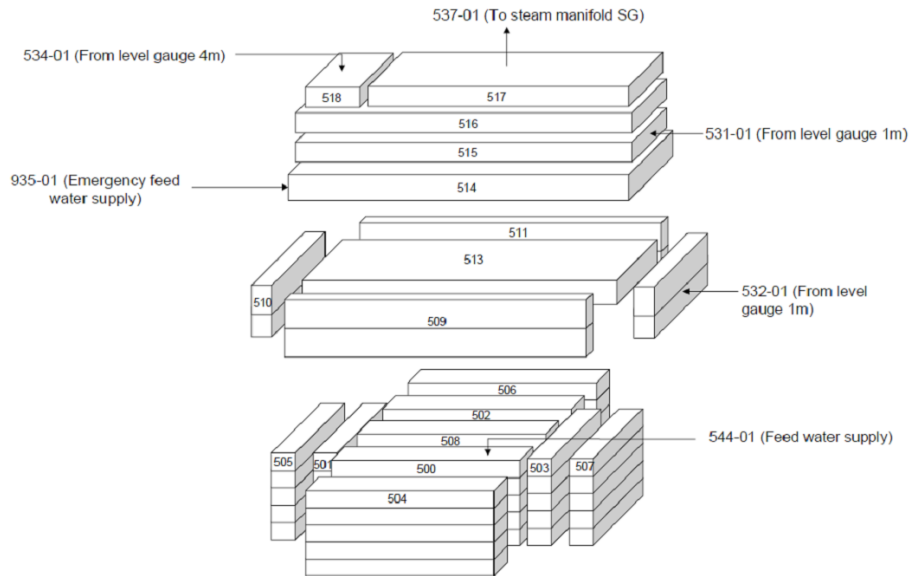


Figure 11: Nodalisation diagram of the second circuit of the PGV – 1000M model

The calculated model of the PGV-1000M is made in the 3D approximation of the RELAP5/Mod3 code.2. The three-dimensional approximation was chosen to correctly distribute the heat load over the volumes of the second SG circuit. HE 500,502 – side packages that describe the volume of the second circuit enclosed in the pipe bundle, HE 501,503-end packages that describe the volume of the second circuit enclosed in the pipe bundle. HE 504, 506-side bypasses, which up to the 4th element describe the volume of the second circuit between the external pipe bundle and the SG body and between the external and main pipe bundles. The 5th element of these HE includes the volume of the second SG circuit between the outer and main pipe bundles, as well as between the outer pipe bundle and the SHS SG rim. HE 505, 507-end bypasses. Distribution of the second circuit volume by the height distribution in HE 505, 507 is similar to that in HE 504, 506. HE 508 is the central bypass, which describes the volume in the center of the SG surrounded by a tube. HE 509,510,511,512 – volume of the second circuit of the SG between the edge of the SHS SG and the body of the SG. HE 513 – volume of the second circuit of the SG between the SHS SG and the upper row of the tube. HE 514,515,516,517,518-describe the vapor space of SG. The steam collector is represented by HE 537,538.

HE of the first circuit are connected to HE of the second circuit by thermal structures.

Steam generated in the steam generators of the reactor plant is transported through steam lines to the high-pressure cylinder of the turbine with a total steam flow rate of 6154.2 t/h.

This section provides some basic assumptions and assumptions for modelling the entire steam pipeline system. When modelling, we will use some assumptions and simplifications.

The change in the volume of the steam line due to its finite diameter at the bends will be ignored. We assume that the volume of the element is its length along the centreline of the steam pipeline multiplied by the cross-sectional area (we consider this to be true for any steam pipelines, including those leading to steam-throwing valves). That is, the lengths of bends, if they are not given in the data, will be calculated along the centreline of the pipeline, taking into account its diameter and radius of the bend.

MSV are not modelled separately. Their functions are performed by the turbine stop and control valves. The hydraulic resistance of the MSV is taken into account in the corresponding connection of the steam line.

The roughness of steam pipes is assumed to be 10^{-4} m for seamless steel pipes.

Heat losses from the surface of steam pipes are not taken into account (thermal structures are not modelled).

The turbine is modelled by the boundary condition as a relation to a constant pressure volume.

The nodalisation diagram of the steam pipeline system is shown in Figure 12.

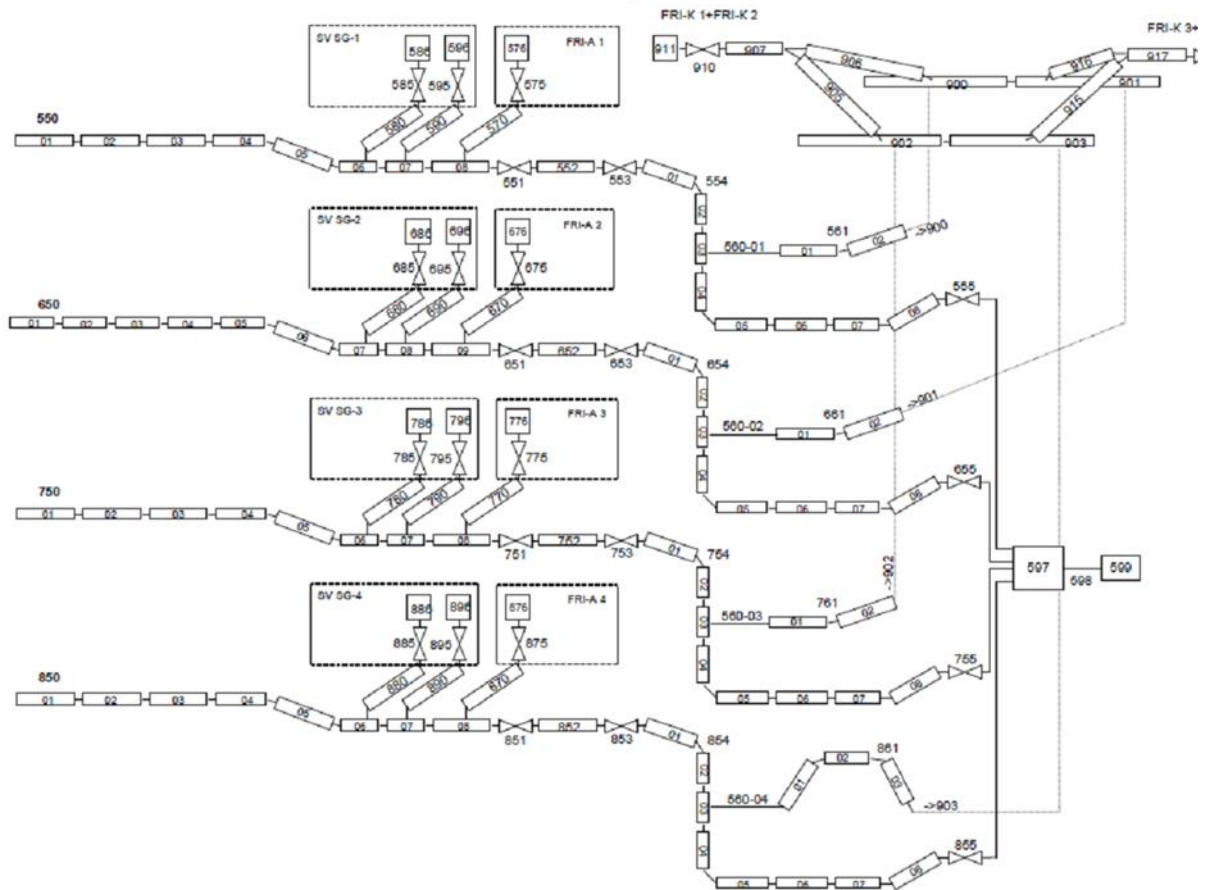


Figure 12: Nodalisation scheme of the steam pipelines

3.1.2 Extension of the plant model for the transient simulation

To model the Main Steam Line Break transient, the following assumptions have been introduced to the RELAP5 input deck:

- the leak is modeled on main steam line #4 with internal diameter 580 mm between the steam generator (SG) and the steam isolation valve (SIV) (element 850-08), outside the containment (Figure 13);
- the free flow of two breaks is assumed without mutual influence between them: two leaks are modeled with equivalent diameters and hydraulic flow diameters equal to the inner diameter of the pipeline;
- the formation of the leak occurs in one time step of the calculation (0.01 s);
- turbine stop valves (MSIV) closes for 10 s after the reactor scram.

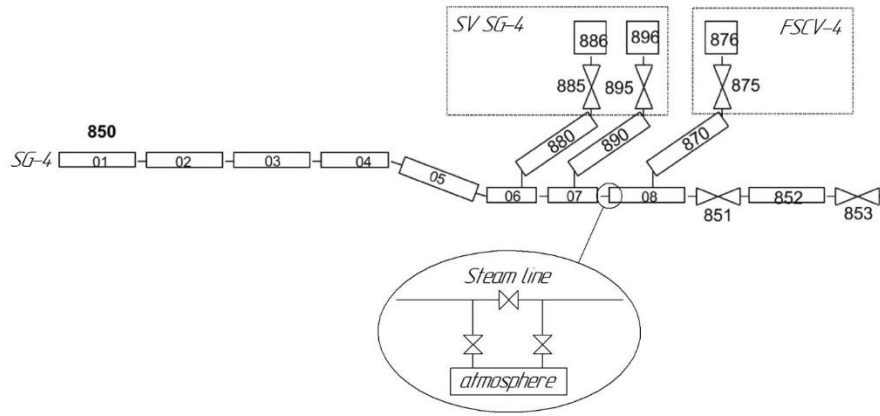


Figure 13: Nodalisation scheme of the steam pipelines break model

3.2 RELAP5 model of the KNPP (INRNE)

3.2.1 General description of the integral plant model for RELAP5

The Baseline input deck for VVER-1000/V320 Kozloduy Nuclear Power Plant, Unit 6 was developed by the INRNE-BAS. The VVER1000 RELAP5 model was developed for analysis of operational occurrences, abnormal events, and design basis scenarios. The model provides a significant analytical capability for the specialists working in the field of the NPP safety. Data and information for the modelling of all main systems and components were obtained from the Kozloduy documentation and from the power plant staff. The reactor and the pressurizer model nodalisation are shown schematically in Figure 14. The Kozloduy VVER-1000 RELAP5 model was defined to include all major systems of Kozloduy NPP, Unit 6, namely: reactor core, reactor vessel, Main Coolant Pumps (MCPs), SGs, steam lines and Main Steam Header (MSH), emergency protection system, pressure control system of the primary circuit, makeup system, safety injection system, steam dumping devices (BRU-K, BRU-A, SG and pressurizer safety valves), and main feedwater system.

In the RELAP5 model of VVER-1000, the primary system has been modelled using four coolant loops each one including one MCP and horizontal SG. The RELAP5 model configuration provides a detailed representation of the primary, secondary, and safety systems. A hot and average heated flow paths and a core bypass channel represent the reactor core region. The reactor vessel model includes a downcomer, lower plenum, and outlet plenum. The Pressurizer (PRZ) system includes heaters, spray and pressurizer relief valves. The safety system representation includes accumulators, high and low pressure injection systems, and reactor scram system. The model of the make-up and let-down systems includes associated control systems.

RELAP5 heat structure components are used to represent fuel rods, vessel structural internals (core barrel, core baffle, lower and upper plates, protective tube block and etc.) and the reactor vessel. Heat transfer from the primary to the secondary side is modelled by heat structure components. The Henry-Fauske critical flow model is accepted for modelling of break flow.

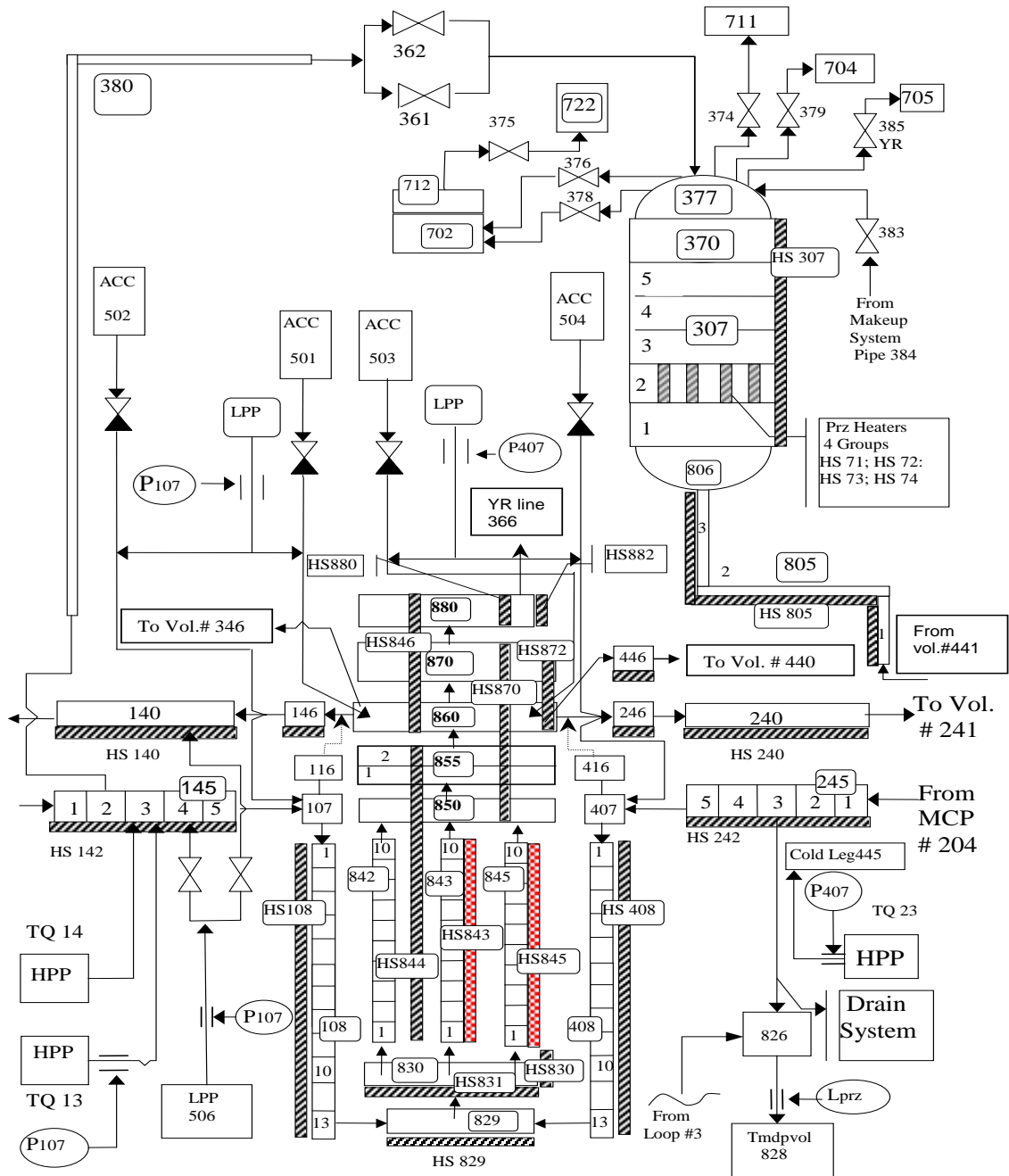


Figure 14: Kozloduy Reactor and Pressurizer RELAP5 Four Loops

3.2.2 Extension of the plant model for the transient simulation

All the components e.g. break, trips to open it, trip to initiate the SCRAM and open valves on the secondary side are included in the main input deck developed for the steady state simulation. Hence, here no description is provided.

3.3 TRACE/PARCS model of the KNPP (KIT)

For the simulation of the Main Steam Line Break (MSLB) using TRACE/PARCS, the respective models i.e. the integral plant model for TRACE comprising the whole plant primary/secondary circuits, the core and the reactor pressure vessel including safety systems, etc. and the 3D neutronic core model need to be developed.

The PARCS nodal diffusion solver needs a set of cross sections for the core loading of interest (BOC conditions) to be generated for two energy groups and homogenized at Fuel Assembly level using a lattice physics code and considering the whole range of variation of thermal hydraulic parameters e.g. fuel temperature, coolant density, boron concentration and control rod positions. At KIT, the Monte Carlo Serpent2 code is used for this purpose. A short description of each of these modelling issues will be presented hereafter.

3.3.1 General description of the integral plant model for TRACE

For the analysis of the Main Steam Line Break (MBLOCA) coincident with the Steam Generator Tube Rupture (SGTR), where it is assumed that one tube located in the upper group of tubes is broken, an integral plant model of the VVER-1000/V320 plant (Kozloduy Unit 6) is developed, based on a previous VVER-1000/V320 RELAP5 model [14].

The four loops are represented separately with 1D thermal hydraulic components of TRACE (PIPE, VALVE) consisting of the hot legs, the steam generator, the cold legs, and the main coolant pump. In addition, the Pressurizer is also modelled by different 1D-volumes, HTSTR-component to represent the heater together with the POWER-component. It is connected to the cold leg 1 with the surge line and to the hot leg 4 with the spray lines. On the secondary side, each loop consists of the steam lines, the different valves to control the pressure in the secondary side, the common header, the turbine stop valve and the turbine represented by a BREAK-component, where the secondary pressure as boundary condition is fixed. Following valves are considered in the steam lines: one steam dump valve to the containment (BRU-A), two safety valves (SV), one main isolation valve (BZOK), and a check valve (CHV). The steam header is connected with the condenser via the steam dump valves (BRU-K), with the atmosphere by the steam dump valves (BRU-SN) and with the turbine by the main steam isolation valve (MSIV). The Feedwater lines are represented in a very simplified manner by a short PIPE-component and by the FILL-component, where the mass flow rate and temperature of the feedwater are defined as boundary conditions.

The flow conditions of the steam Generator on the primary side is modelled representing the flow through the tubes modelled, where the around 11000 tubes lying horizontally are grouped in three groups at different elevations represented by a PIPE-component. There hot and cold collectors are also represented by different PIPE-components. On the secondary side, the large water volumes are also represented by three PIPE-components at different levels. The tubes itself are represented by HTSTR-components by cylindrical tubes, where the inner wall is connected with the PIPES representing the primary coolant flow and the outer wall is connected with the secondary side volumes (PIPES). In this way, the heated-up primary coolant is cooled down along the SG-tubes and the heat is used to heat-up the secondary circuit until evaporation. At the upper part of the SG, a separator is considered and represented by SEPARATR-component of TRACE. There, the steam is separated from the entrained droplets and the liquid fraction flows back to the downcomer part of the SG.

The Reactor Pressure Vessel (RPV) of the VVER-1000 plant is represented by a three-dimensional component: the VESSEL-component. It allows to discretize the RPV in three directions: axial, radial and azimuthal. In this case, the RPV was subdivided in 26 axial nodes, 6 azimuthal sectors and 4 radial sectors. The core is represented by three rings, the next ones represent the bypass, core barrel and downcomer. The VESSEL-component allows to consider the location of the lower and the upper grid plate as well as the upper head. The core itself is represented by 18 HTSTR-components to represent the 50856 fuel rods contained in the 163 hexagonal fuel assemblies. One six of the fuel rods are represented in each radial and azimuthal sector. The number of fuel rods represented in each HTSTR-component is described by the RDX-parameter (in this study RDX amounts 1924, 2808 and 3744). Each HTSTR must be axially and radially

discretized so that the heat conduction equation can be solved for this discretization considering the heat source in the pellet material in Figure 15.

A power component is also needed to represent the reactor power using different options e.g. as a table, or using the point kinetics model of TRACE and considering the provided reactivity coefficients. Also, the reactor SCRAM and the external reactivity to shut-down the reactor can be included in the POWER-component.

In this investigation, the core neutronics will be described by the PARCS diffusion solver. Hence, the core representation of the core coolant channels and the fuel assemblies in TRACE is done using the 3D Cylindrical VESSEL (Ring 1 to 3, axial nodes: 6 to 17, azimuthal: 1 to 6) as indicated in Figure 15. For the coupling of TRACE Thermal hydraulics with the PARCS core model, in order to exchange feedbacks during the simulation, the core in TRACE needs also to consider a node below and above the core, which will provide the coolant temperature for the radial reflector cross-sections.

All additional and needed safety systems e.g. the Emergency Boron Injection System (EBIS), the Control Volume and Chemical System (CVCS) that consists of the Make-up and the Let-down system, the Emergency Core cooling systems (EECCS) including the passive accumulators (HA) the high-pressure injection system (HPIS) and the low pressure injection system (LPIS), as well as the emergency feed water system (EFW) are included in the basic model.

The integral steady state model includes all necessary Trip variables, and Control blocks to facilitate the initiation of actions of the reactor protection and control system (RPCS) during the accident progression e.g. shutdown of the MCP#4, the opening of the break, etc. Also the break modelling is already included in the main steady state TRACE plant model.

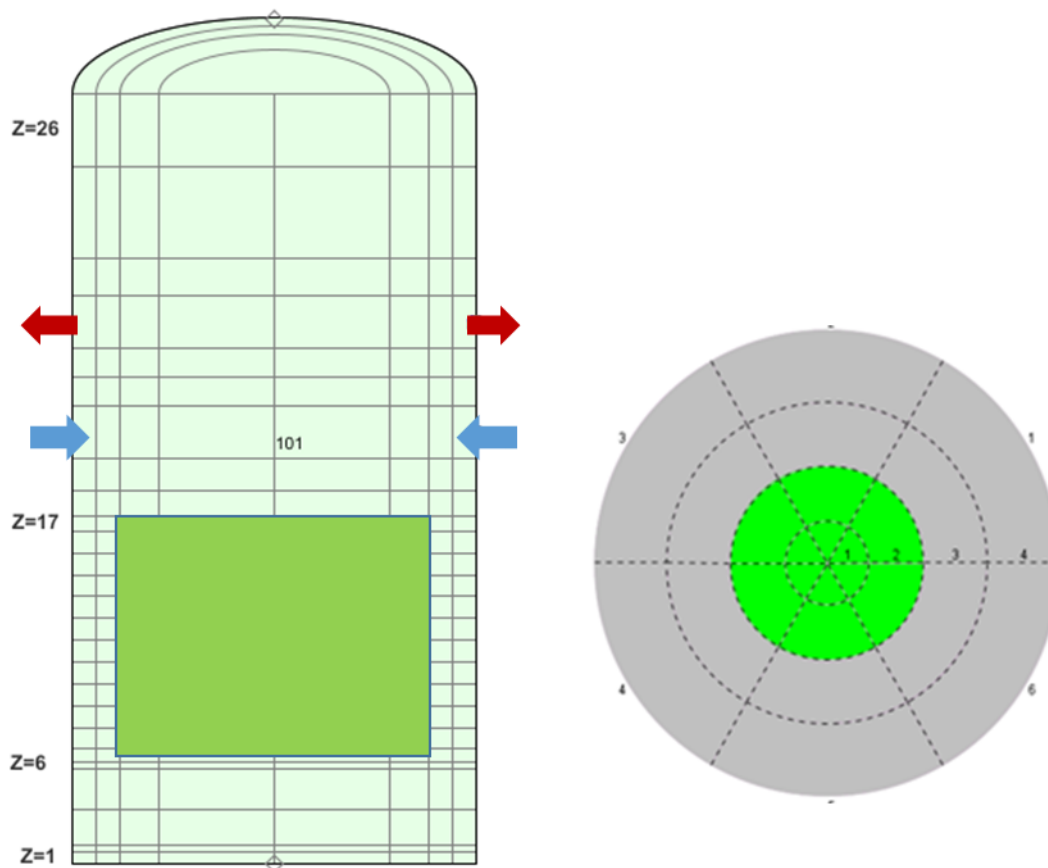


Figure 15: *The Reactor Pressure Vessel and its radial, axial and azimuthal discretization (R, Z, Theta) for the analysis of the MSLB transient*

The geometrical and thermal hydraulic data as well as neutron kinetic information of the core were taken from the CAMIVVER-deliverables describing the transient scenario [1] and the NPP-details [15].

In the first step, a reference plant model is developed to describe the steady state plant conditions at full power just before the transient takes place. In Figure 16 the integral TRACE plant model developed for the study of the MSLB transient is shown. There, you can find the main components of the NPP such as the RPV, the pressurizer (PZR), the steam generators (SG1 to SG4), the break modelling, the main steam header (MSH) on the secondary side, the turbine, etc.

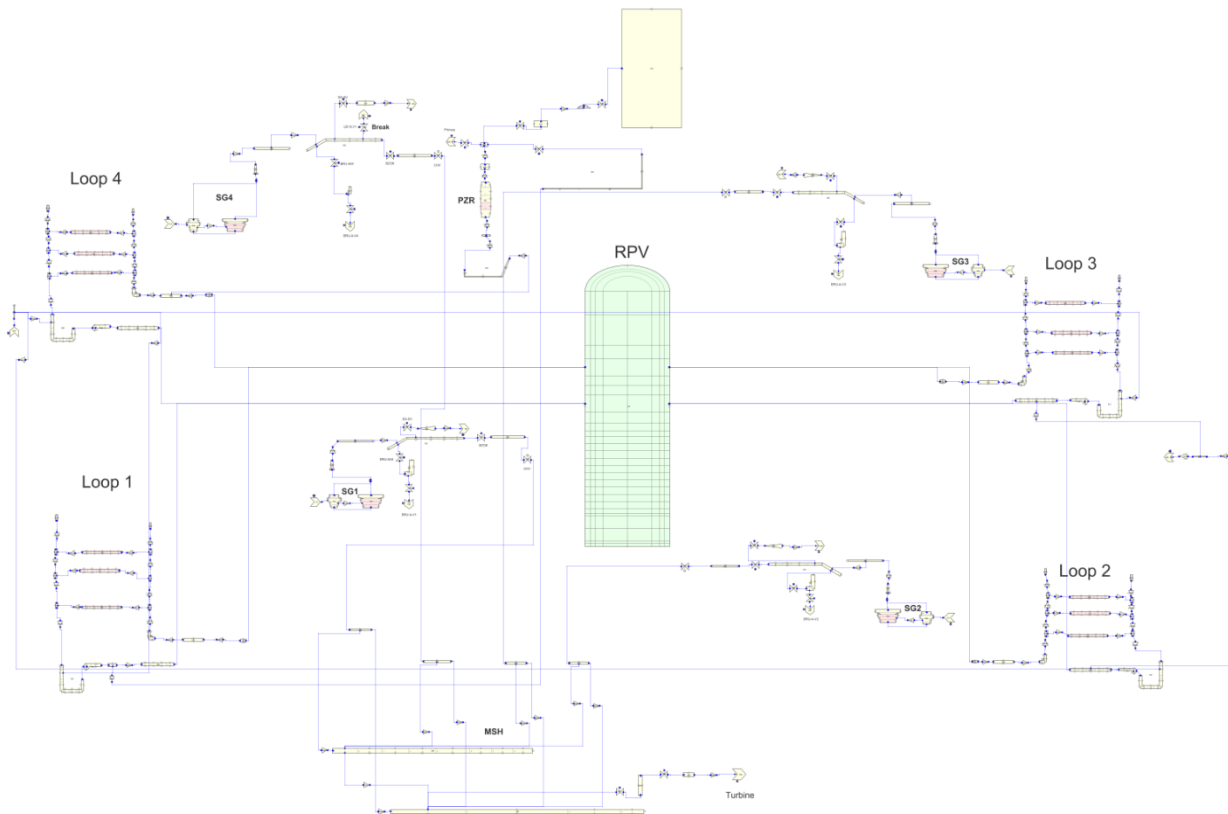


Figure 16: Integral model of the Kozloduy Nuclear Power Plant (KNPP) developed for TRACE (primary/secondary circuits, safety systems)

In a second step, a coupled steady state TRACE/PARCS simulation is performed as starting point for the transient simulation with the coupled code. For this purpose, a small TRACE restart steady state input is developed. This input is used with the steady-state PARCS core model for the coupled steady state simulation.

Then, after a converged solution is obtained, a transient coupled simulation with TRACE/PARCS is performed, for which a transient TRACE model and a PARCS transient input model must be developed. The TRACE transient model is also quite small; it only includes the components, trips, control variables that have changed compared to the steady state simulations. It means only the trips related to with the actions during the transient are included here e.g. break opening time, cost-down time of the MCP#4, isolation of the turbine, etc.

A comparison of the stationary plant conditions with the one of the reference plant data was done and after acceptable values were predicted by TRACE [16] for the full power conditions to assure that the model is able to predict the reference plant data at nominal conditions.

3.3.2 Extension of the plant model for the transient simulation

The full plant model included all the safety systems, the break modelling, and all trips needed to activate e.g. the break opening, to insert the shutdown rods, for turbine isolation, to cost-down the main coolant pumps, for stopping the feedwater injection and so on.

Merely, a restart file is generated with the transient option to run the 600 seconds problem time, where settings of the trips and signals to control the accident sequence are changed.

3.3.3 Description of the core model in PARCS

The KZLD6 core model developed in PARCS v3.3.1 consists of four different hexagonal fuel assembly types, as described in D5.2 [17]. FA type 1 (FA1) and 2 (FA2) with enrichments of 2% and 3%, respectively, fill almost 75% of the centre part of the core. FA type 3 (FA3) of enrichment of 3%wt U235 is distributed in the peripheral part of the core. Finally, FA type 4 (FA4) of combined enrichments of 3% and 3.3%, complete the peripheral corners of the core, as illustrated in Figure 17. Additionally, the core is surrounded by 48 reflectors with the same hexagonal FA shape. The distinction between each reflector is considered to evaluate the influence of surface discontinuity factors. For the reactivity control of the core, ten control rod banks are distributed in the core, as illustrated in Figure 18. Control rod banks are only associated with FAs types 1 and 2. Axially the active core is 355 cm long and divided into 30 axial slices, and extra widths of 23.6 cm each are considered for the bottom and top axial reflectors.

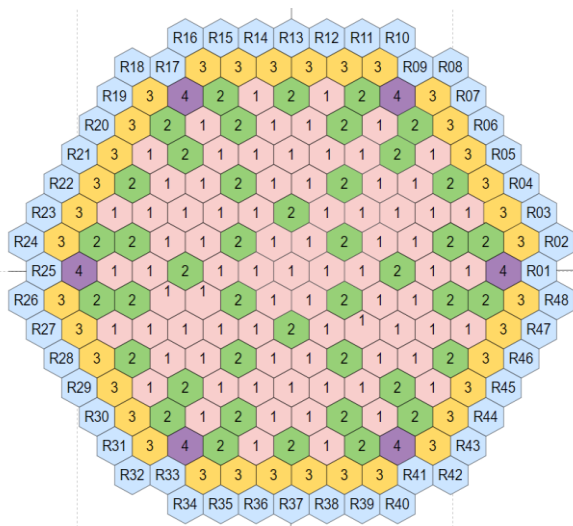


Figure 17. Core model developed in PARCS.

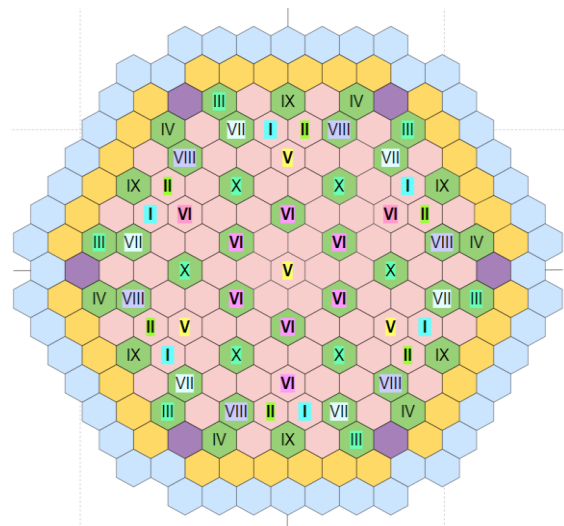


Figure 18. Control rod banks layout.

The Triangular Polynomial Expansion Nodal (TPEN) method, available in PARCS only for hexagonal geometry, is used to solve the neutron diffusion equation with 2 energy group macroscopic XS. The TPEN kernel solves two transverse-integrated neutron diffusion equations for a single hexagonal node. One is the radial equation defined for a hexagon and the other is the axial equation defined for the z-direction. The radial problem is solved by splitting the hexagon into six triangles and employing a polynomial expansion of the flux within each triangle. The axial problem is then solved using the nodal expansion method (NEM) [8].

For the 2-energy macroscopic XS generation, assembly models are developed in SERPENT v2.1.32. Special attention was paid to the core configuration (e.g. fuel assemblies in the surroundings) to generate more precise assembly models. For FA1, a single assembly with reflective boundary conditions is considered, as illustrated in Figure 19. For FA2, see Figure 20, six extra FA1 surrounds the FA2, as is considered to be more representative according to the core layout, in this case the homogenization and condensation of XS is carried out only in the centre where FA2 remains. Similar approaches are considered for FA3 and FA4 as illustrated in Figure 21 and Figure 22.

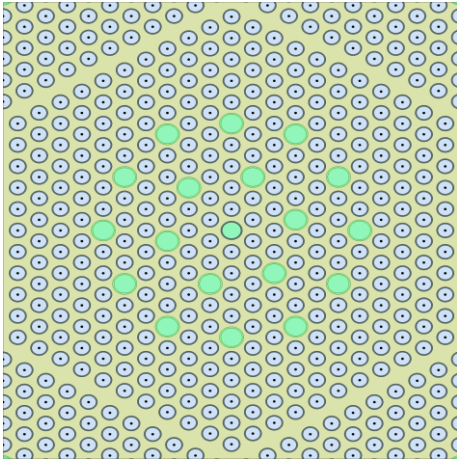


Figure 19. Cell model in SERPENT2 for FA1.
Without control rods.

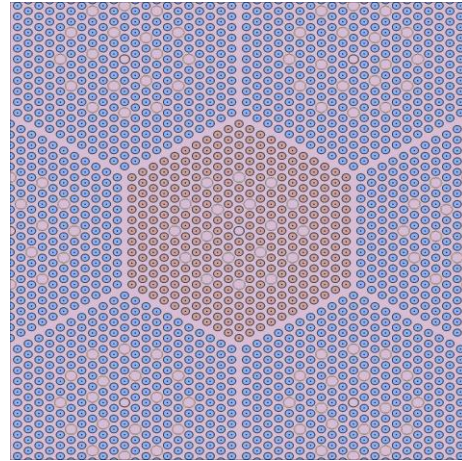


Figure 20. Cell model in SERPENT2 for FA2.
Without control rods.

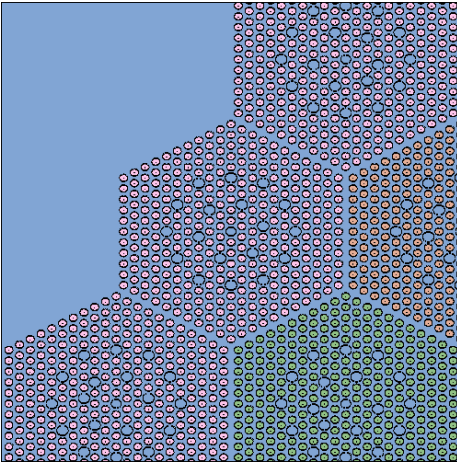


Figure 21. Cell model in SERPENT2 for FA3.

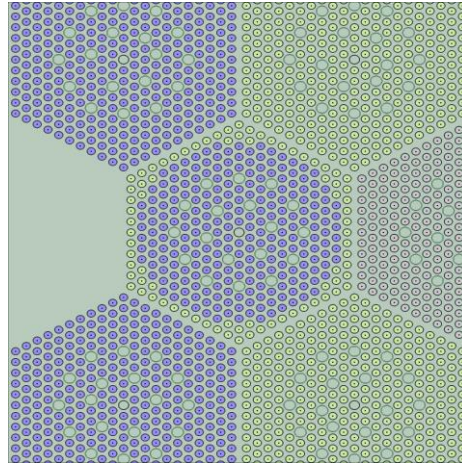


Figure 22. Cell model in SERPENT2 for FA4.

Two-energy group¹ homogenized constants are generated in a leakage-corrected spectrum. Fundamental mode (FM) with Cumulative Migration Method (CMM) diffusion coefficients are considered. An intermediate 70-group structure is considered for the calculation of the leakage-corrected critical spectrum. No discontinuity factors are considered for the fuel assemblies. Radial reflectors XS are extracted considering a full 2D core model in SERPENT2. As mentioned, each of the 48 radial reflectors is homogenized independently, and discontinuity factors are considered only in the surfaces in contact with the fuel assemblies. For the bottom and top axial reflectors, a 3D FA type 1 infinite reflected in the X and Y directions, and black conditions in the Z direction, is considered. A first set of macroscopic XS at a Hot Full Power (HFP) state [17] was generated using GENPMAXS v6.2 and provided to PARCS. In parallel, a full 3D core model in SERPENT2 is developed to evaluate and verify the consistency of the XS generation process. Table 2 presents the comparisons between the codes at different control rod positions. As DF was considered and included in the PMAXS files, it can be switched on or off using the control block in PARCS. Therefore, two solutions for PARCS are presented. In terms of reactivity, a very good agreement can be observed even when no DFs are considered. Radial reflector DFs improve the differences more.

¹ Typical 0.625eV is the cutting energy between the two groups.

Table 2. PARCS and SERPENT2 keff comparisons at HFP state.

Control rod configuration ² (% extraction)				KEFF		DIFFERENCE PARCS/SERPENT2 (pcm)	
SB 1-8	SB 9	RB 10	SERPENT2 ³	PARCS without DFs	PARCS with DFs	PARCS without ADF	PARCS with ADF
100%	100%	100%	1.04800	1.04730	1.04781	-64	-17
100%	100%	0	1.04012	1.03897	1.03974	-106	-35
100%	0	100%	1.04223	1.04155	1.04195	-63	-26
100%	0	0	1.03227	1.03104	1.03171	-116	-53
0	0	0	0.954806	0.952003	0.952864	-308	-213

In terms of power comparisons, Figure 23 shows the difference in FA power between PARCS and SERPENT2 in ARO (All Rods Out) condition without DFs. It can be observed that PARCS predicts around 3% more power in the center of the core and 6% less power in the peripheral compared to SERPENT2. Taking into account the DFs improves the power in the center, getting differences close to ~0%, which may explain a better agreement also in reactivity differences, but differences in the peripheral increase up to 6%, as illustrated in Figure 24.

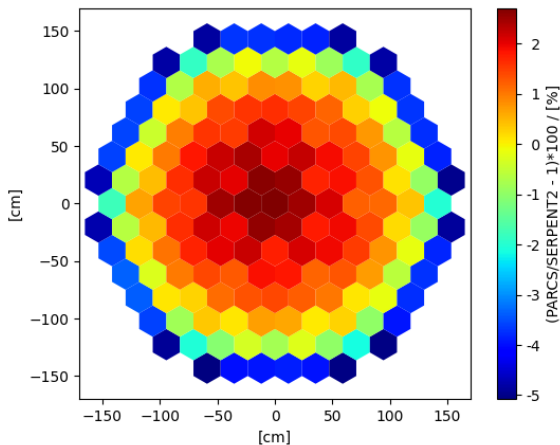


Figure 23. PARCS and Serpent2 difference in power per FA distribution in ARO condition without reflector DFs.

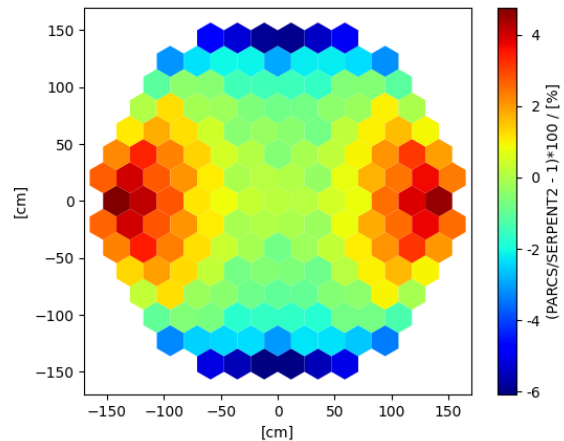


Figure 24. PARCS and Serpent2 difference in power per FA distribution in ARO condition with reflector DFs.

In ARI (All Rods In) condition, differences increase up to 10% without considering DFs, mainly in FAs where control rods are inserted, see Figure 25. Differences in those positions improve when DFs are considered. Nevertheless, it gets worst in other positions as illustrated in Figure 26. It is worth mentioning that radial reflector XSs and DFs were generated with the 2D full core model in SERPENT2 in the ARO condition only, so it is expected that DFs are not correcting very well in the ARI condition.

² SB *i*: stands for Safety Bank *i*, and RB *j*: for Regulation Bank *j*.

³ 1σ standard deviation of the Monte Carlo results are less than 2 pcm.

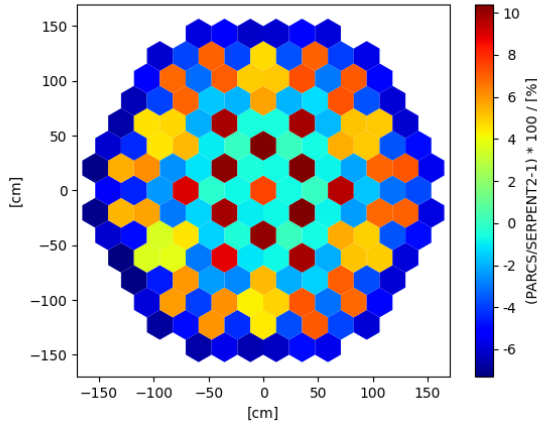


Figure 25. PARCS and Serpent2 difference in power per FA distribution in ARI condition without reflector DFs.

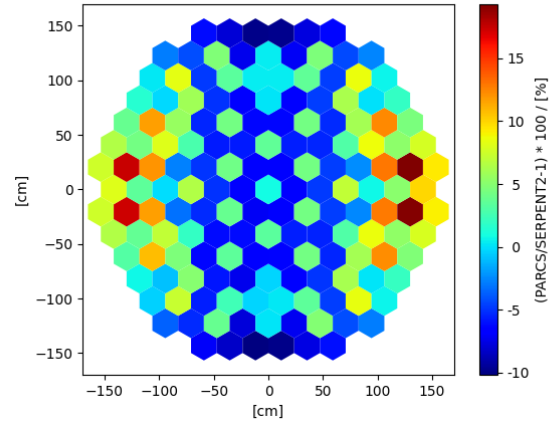


Figure 26. PARCS and Serpent2 difference in power per FA distribution in ARI condition with reflector DFs.

Finally, for the MSLB transient problem, XS dependent of thermal hydraulic parameters are needed. Table 3 shows the variations points took into account during the XS generation.

Table 3. Variation points considered for the macroscopic cross section generation [17].

Parameter	HFP	Variations
	Nominal condition	Points
Coolant density (DC) [g/cm3]	0.725	0.1, 0.2, 0.3, 0.4, 0.5, 0.6, 0.8, 0.9
Boron concentration (PC) [ppm]	1200	1, 2000
Fuel temperature (TF) [K]	900	470, 1500
Coolant temperature (TC) [K]	574	470, 620

Table 4 shows the 45 branches selected according to the variation points presented in Table 3. For each PC concentration, all the DC points are evaluated as it was observed that PC influence in reactivity depends strongly on the DC value. Some assembly level results are presented in Appendix 9. For TF and TC variations, more priority is taken in the higher density points, as is expected to happen during the MSLB transient problem. As a summary, each FA type includes 45 unrodded branches, and only for FA1 and FA2 additional 45 rodded branches (control rods inserted) are considered.

Table 4. Selected branches for the XS generation.

Branch Name	DC [g/cm3]	PC [ppm]	TF [K]	TC [K]	Branch Name	DC [g/cm3]	PC [ppm]	TF [K]	TC [K]	Branch Name	DC [g/cm3]	PC [ppm]	TF [K]	TC [K]
BASE	0.725	1200	900	574	DCPC7	0.725	1	900	574	TF4	0.725	2000	1500	574
DC1	0.1	1200	900	574	DCPC8	0.8	1	900	574	TF5	0.6	2000	470	574
DC2	0.2	1200	900	574	DCPC9	0.9	1	900	574	TF6	0.6	2000	1500	574
DC3	0.3	1200	900	574	DCPC10	0.1	2000	900	574	TF7	0.8	2000	470	574
DC4	0.4	1200	900	574	DCPC11	0.2	2000	900	574	TF8	0.8	2000	1500	574
DC5	0.5	1200	900	574	DCPC12	0.3	2000	900	574	TF9	0.9	2000	470	574
DC6	0.6	1200	900	574	DCPC13	0.4	2000	900	574	TF10	0.9	2000	1500	574

DC7	0.8	1200	900	574	DCPC14	0.5	2000	900	574	TC1	0.725	1200	900	470
DC8	0.9	1200	900	574	DCPC15	0.6	2000	900	574	TC2	0.725	1200	900	620
DCPC1	0.1	1	900	574	DCPC16	0.725	2000	900	574	TC3	0.8	1200	900	470
DCPC2	0.2	1	900	574	DCPC17	0.8	2000	900	574	TC4	0.8	2000	900	470
DCPC3	0.3	1	900	574	DCPC18	0.9	2000	900	574	TC5	0.9	1200	900	470
DCPC4	0.4	1	900	574	TF1	0.725	1200	470	574	TC6	0.9	2000	900	470
DCPC5	0.5	1	900	574	TF2	0.725	1200	1500	574	TC7	0.6	1200	900	620
DCPC6	0.6	1	900	574	TF3	0.725	2000	470	574	TC8	0.6	2000	900	620

For the initial state before the MSLB transient analysis, a critical state in the core is desirable. Due to the simplifications made in the neutronic model, such as omitting spacer grids and Xe/Sm poison absorbers, more boron concentration is needed. From Table 2, an excess reactivity of 4436 pcm is observed when all control rods are extracted. Therefore, a boron search is conducted taking the following consideration:

With all the safety banks 1-9 at 100% extraction and regulation bank 10 at 80% extraction, a boron search is performed in order to get a critical core configuration ($k_{eff}=1$).

Table 5. Critical boron search fat HFP state.

TH Feedback	Control rods configuration		BORON [ppm]	PARCS KEFF
	SB 1-9	RB 10		
NO	100 %	80 %	1200	1.04579
NO	100 %	80 %	1625	1.00000
YES ⁴	100 %	80 %	1630	1.00000

⁴ For the TH feedback, internal PARCS TH module was used.

- Secondary side, including SG vessel.

The nodalization scheme of the steam generator model is presented on the following figure. On the primary side (left on the figure below), the tubes in the steam generator are represented as 3 bundles, each at a different altitude.

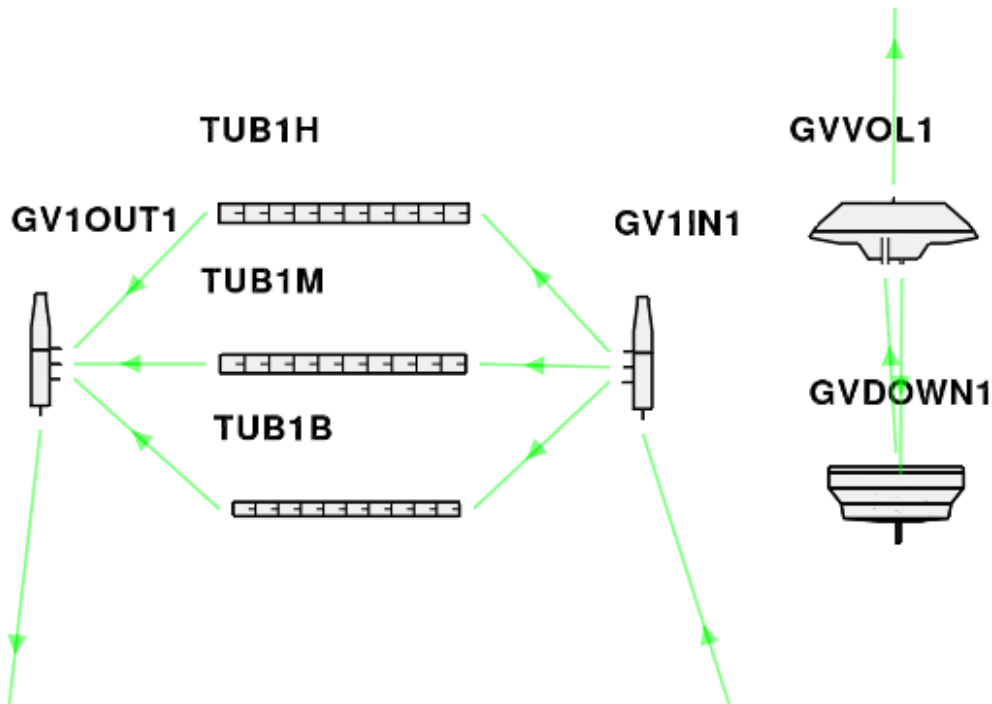


Figure 28: VVER-1000 UNIT 6 Steam generator CATHARE3

The heat structures, modelled in SGs, include the hot and cold collectors, the horizontal tubing arranged into three levels and the pressure vessel.

3.4.1.3 Secondary side

The four steam lines are modelled. The double ended break is modelled on the Main Steam Line (MSL) 4 with a RUPTURE element. The mesh is refined at the break location.

The four MSL are feeding two steam headers, which feed the BRU-K lines. The BRU-K valves are modelled with the PIQVANNE element. The BRU-K open if the pressure in the steam lines rises above 66.7 bar and support a pressure of 62.8 bar. The BRU-K close if the pressure drops below 57.9 bar.

Check valves are also present before the lines leading to the main steam header. They ensure no steam goes from one SG to another via the main header.

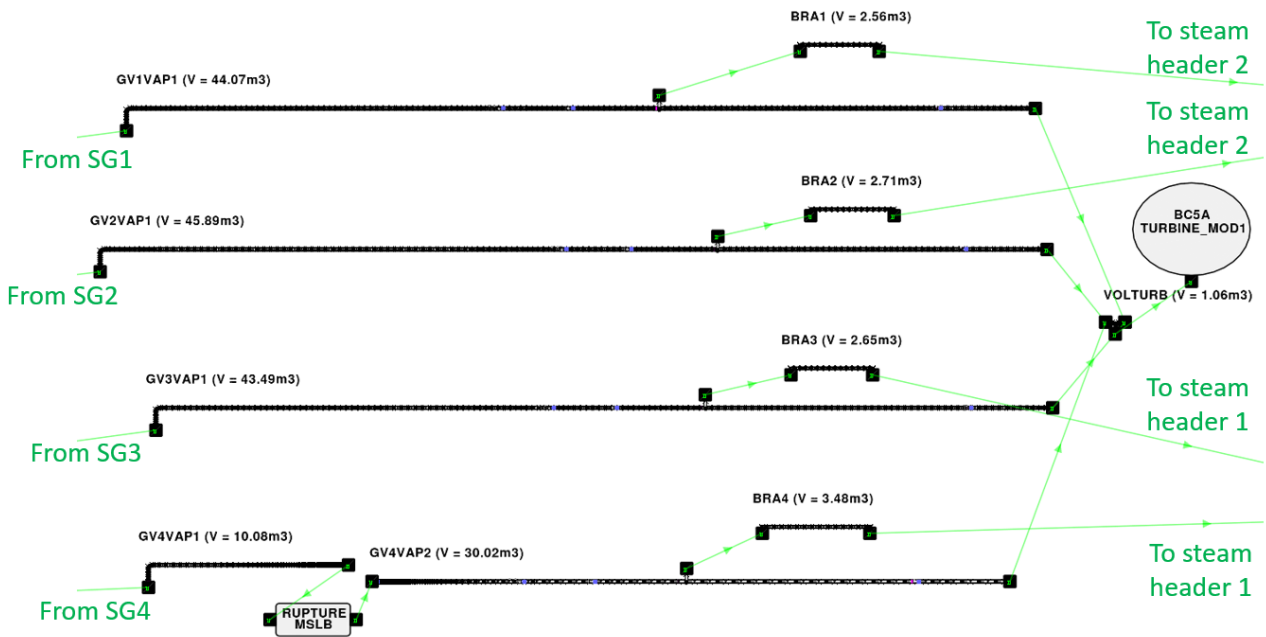


Figure 29: VVER-1000 UNIT 6 Steam lines CATHARE3

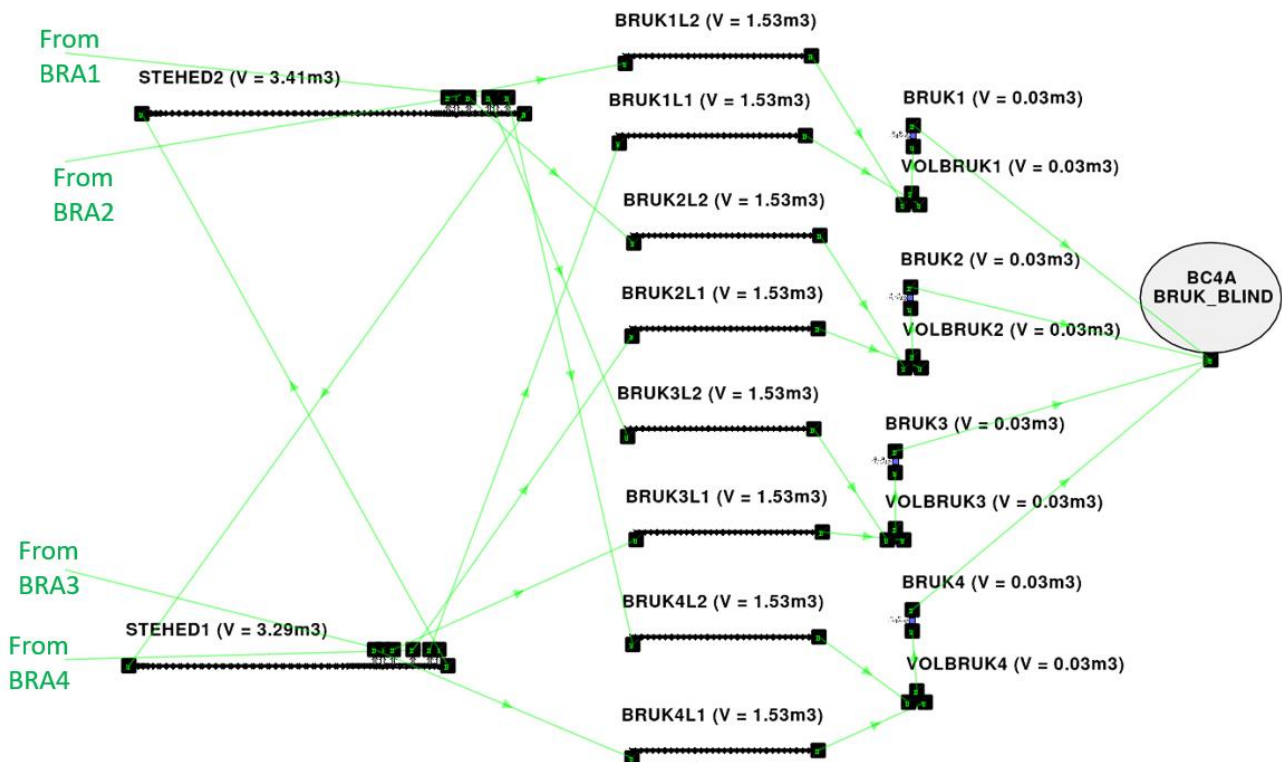


Figure 30: VVER-1000 UNIT 6 Steam headers and BRUKs

3.4.1.4 Main controllers

- Primary pressure controller

The pressurizer heaters maintain the primary pressure high enough. There are five groups of pressurizer heaters with the following parameters:

Group	Power [kW]	Switch on pressure	Switch off pressure
-------	------------	--------------------	---------------------

		[MPa]	[MPa]
1	270	15.95	16.1
2	270	15.95	16.0
3	720	15.7	15.8
4	1260	15.7	15.8

The heaters are switched off for pressurizer level below 4.2 m.

3.4.2 Initial conditions

The initial conditions defined in [1] were used for the analysis of the MSLB transient.

3.4.3 Extension of the plant model for the transient simulation

To model the Main Steam Line Break transient, the following assumptions have been transcribed to the CATHARE3 input deck:

- The MSL4 break is a double-ended break modelled with a RUPTURE element. The break has an inner diameter of 580 mm and opens at 3 ms. The break is located 25 m from the SG4 collector.
- The SCRAM is performed at the first iteration of the transient. The control rods are fully inserted in 4 s with delay of 0.0 s. A turbine trip at the first iteration is also assumed.
- BRU-K pressure control mode is activated: a PI regulation written in the input deck controls the aperture of the BRU-K valves. The secondary pressure setpoint is 62.807 bar at the steam header. The total BRU-K opening/closing time is 15 s. If the pressure exceeds 66.7 bar, the BRU-K valves fully open. If the pressure drops below 57.9 bar, the BRU-K valves fully close.
- MCP-4 trips after 10 s of transient. The coast down time is 55 s.
- Turbine stop valves (MSIV) close 10 s after the reactor scram.
- The feedwater flowrates and temperatures are set manually as defined in the transient boundary conditions.

3.4.4 Description of the core model for APOLLO3®

The present section summarizes the core definition and associated neutronic data needed for the MSLB exercises proposed in Task 7.4, as well as major hypotheses considered for the core modeling with both APOLLO3®/THEDI and the APOLLO3®/CATHARE3 coupling.

It has been decided that for the full core VVER benchmark MSLB case analyzed in Task 7.4, the beginning of cycle 1 instead of cycle 8 as in the previous NEA benchmarks has to be considered. The boundary conditions for the MSLB transient have been defined and updated by INRNE and they are the object of a dedicated update of D3.2.

The interest on moving to a 3D neutronic modelling and more advanced coupling has pushed the partners to choose a configuration that requires small effort on cross-section preparation and may allow to reduce the sources of discrepancies due to burnup models. During the Task 7.4 meeting, it was decided to use the core data of Task 7.3 MCP-Restart benchmark as first demonstrator. This choice is not impacting the interest on this first comparison proposed in the CAMIVVER project.

Here in Task 7.4 the first application of the APOLLO3®/CATHARE3 POC coupling is realized modeling the KNPP full primary and secondary system.

Initially the MSLB accident input configuration for CATHARE3 stand-alone was not yet available and only during the very final months of the project the MSLB configuration has been realized with a point kinetic neutronic model embedded. Anyway, the functionality and the feasibility of such exercise is already available while adopting the existing CATHARE3 deck for the MCP-Restart benchmark.

The simulation of boundary conditions in primary and secondary systems thermal-hydraulics fully representative of the defined MSLB benchmark is completed and first results are under investigation.

Despite all functionalities are there, full coupled 3D neutronics MSLB simulation and comparison among partners may not be possible before the end of the project. Nevertheless, all achievements will enhance activities mainly devoted to the follow up of the project, capitalizing the knowledge, input options, and progresses in MPOs newest version of NEMESI.

In the following subsections a short description of the core loading and operational conditions at steady-state for BOL (cycle1) Kozloduy NPP Unit 6 core, in support to Task 7.4 activities, is presented.

3.4.4.1 Core neutronic model

The core model, used for task 7.4 calculations and provided by APOLLO3 preprocessor, is shown in Figure 31. It is characterized by 163 FA and 48 reflector assemblies. Axially, the reactor core has a total active core height of 355 cm. The upper and lower axial reflectors have a thickness of 23.6 cm. Zero flux boundary conditions are specified on outer reflector surface for both radial and axial reflectors.

Fuel assemblies with different U235 enrichments are present in the core. This is the first cycle for NPP Kozloduy Unit 6 and all assemblies are fresh.

The proposed grouping is shown in Table 6 and the radial core layout is presented in Figure 32.

Two types of CRs are considered:

- Partial length CR (group V): control rods with neutron absorber only in its lower half
- Fully (groups I-IV and VI-X)

The CR are represented as well in Figure 32 and Table 7.

For any further specification and details the information will be provided by Task 7.4.

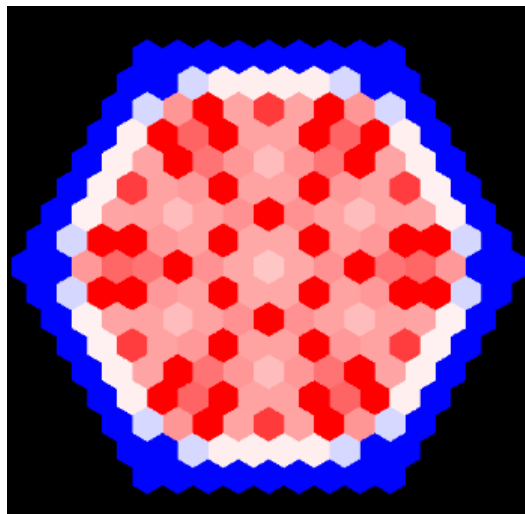


Figure 31: Kozloduy-6 NPP CORE

Table 6: Cycle 1 type of ASSEMBLIES

Assembly type	Enrichment, w/o	Colors in Figure 32
1	2.0	Red
2	3.0	Green
3	3.3	Purple
4	3.3 profiled	Black
5	Reflector	Grey

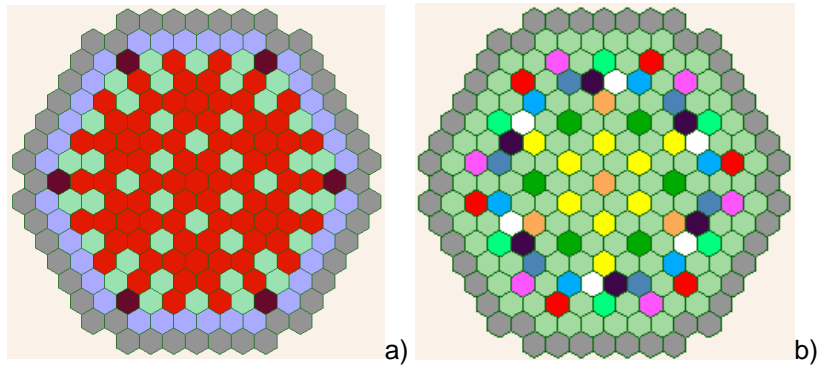


Figure 32: a) CORE LAYOUT CYCLE 1 and b) CR LOCATION

Table 7: Cycle 1 CR POSITION

Assembly type	Purpose	Colors in Figure 32
I	Safety	Black
II	Safety	White
III	Safety	Magenta
IV	Safety	Red
V	Partial-length	Orange
VI	Safety	Yellow
VII	Safety	Grey
VIII	Safety	Blue
IX	Safety	Light Green
X	Regulation	Dark Green

4 SELECTED RESULTS FOR THE STATIONARY FULL POWER CONDITIONS

In this chapter, the main results predicted by the partners for the stationary nominal plant conditions are presented and discussed.

4.1 RELAP5 results for the stationary plant conditions (ENERGORISK)

The plant parameters used for the initialization of the transient calculation are summarized in Table 8

Table 8: Initial parameters

Parameter	Plant Design	RELAP5
Reactor thermal power, MW	3000	3002.5
Primary pressure, MPa	15.7	15.69
Pressurizer Level, m	8.77	8.77
Coolant temperature at reactor inlet, K	560.15	564.0
Coolant temperature at reactor outlet, K	592.05	594.0
Mass flow rate through one loop, kg/s	4400	4400
Reactor mass flow rate, kg/s	17600	17598
Total bypass of reactor core, %	3-5	2.2
Pressure in SG, MPa	6.27	6.28
Feedwater temperature, K	493.15	493.15
Pressure in the main steam header (MSH), MPa	6.08	6.08
Steam mass flow rate through SG steam line, kg/s	408	410
SG Water Levels, m	2.40	2.40
Liquid mass in the SG secondary side, t	From 43 to 56 (from different references)	48

4.2 RELAP5 results for the stationary plant conditions (INRNE)

The plant parameters used for the initialization of the transient calculation are summarized in Table 9

Table 9: Initial parameters

Parameter	Plant Design	RELAP5
Reactor thermal power, MW	3000	3000
Primary pressure, MPa	15.7	15.7
Pressurizer Level, m	8.77	8.77
Coolant temperature at reactor inlet, K	560.15	560,2
Coolant temperature at reactor outlet, K	592.05	590,96
Mass flow rate through one loop, kg/s	4400	4394
Reactor mass flow rate, kg/s	17600	17574
RPV bypass, %	0.1	521

Total bypass of reactor core, %	3-5	2.9
Pressure in SG, MPa	6.27	6.18
Feedwater temperature, K	493.15	493
Pressure in the main steam header (MSH), MPa	6.08	5.92
Steam mass flow rate through SG steam line, kg/s	408	409
SG Water Levels, m	2.40	2.26
Liquid mass in the SG secondary side, t	From 43 to 56 (from different references)	48

4.3 TRACE results for the stationary plant conditions (KIT)

The plant parameters used for the initialization of the transient calculation are summarized in Table 10.

Table 10: Comparison of reference plant data for the nominal conditions compared to the predictions of TRACE/PARCS

Parameter	Plant Design	TRACE/PARCS
Reactor thermal power, MW	3000	3000
Primary pressure, MPa	15.7	15.65
Pressurizer Level, m	8.77	8.76
Coolant temperature at reactor inlet, K	560.15	561,3
Coolant temperature at reactor outlet, K	592.05	590,8
Avg. mass flow rate through loops, kg/s	4400	4340
Reactor mass flow rate, kg/s	17600	17383
RPV bypass, %	0.1	-
Total bypass of reactor core, %	3-5	3.2
Pressure in SG, MPa	6.27	6.09
Feedwater temperature, K	493.15	493
Pressure in the main steam header (MSH), MPa	6.08	5.955
Steam mass flow rate through SG steam line, kg/s	408	407
SG Water Levels, m	2.40	2.26
Liquid mass in the SG secondary side, t	From 43 to 56 (from different references)	49,9

Relative Radial Power Distribution :0.0 s

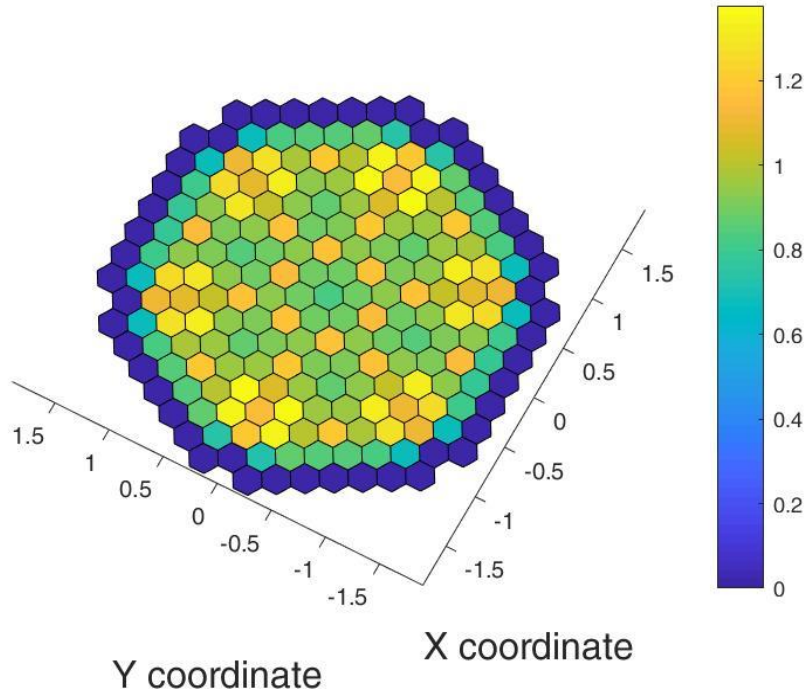


Figure 33: Axially averaged relative radial power distribution of the core as predicted by TRACE/PARCS

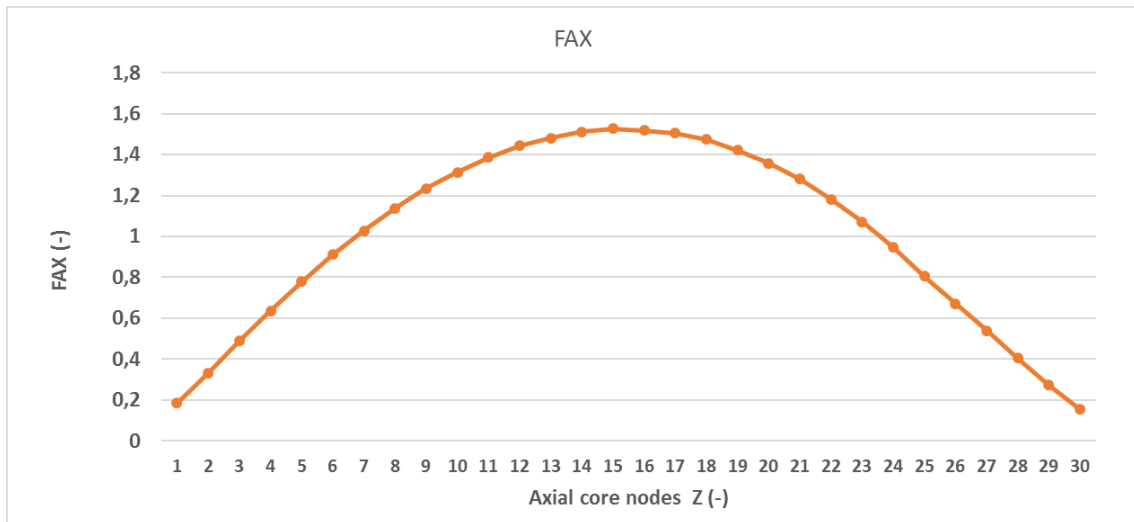


Figure 34: Radially averaged relative axial power distribution of the core as predicted by TRACE/PARCS

4.4 CATHARE3/APOLLO3® results for the steady state plant conditions

4.4.1 Core modeling issues for Kozloduy core

Here important hypothesis to improve the core neutronic core model of Kozloduy-6 Cycle 1 NPP with APOLLO3 and CATHARE3 are presented and discussed.

- **Assemblies and grids models**

The core model is shown in Figure 32. Radially, the core is divided into hexagonal cells with a pitch of 23.6 cm, each corresponding to one fuel assembly (FA), plus a radial reflector (shaded area) of the same size. There are a total of 211 assemblies, 163 FA and 48 reflector assemblies. Axially, the reactor core is divided into 10 layers with a height (starting from the bottom) of 35.5 cm, adding up to a total active core height of 355 cm.

The available gap width is 0.08 mm (distance between pellet surface and inside clad wall). For the neutronic problem, each of the FAs is homogeneous.

Assembly data are available at D4.3.

Grids are not explicitly modeled in a first approach, but their modeling could be considered in order to extend comparisons to experimental data coming for instance from Kozloduy-6 power plant.

- **Reflector modeling**

An average fuel temperature value equal to 600 K is used for the radial reflector cross-section modelling in both the initial steady-state and transient simulations, and the average coolant density for the radial reflector is equal to the inlet coolant density. For the axial reflector regions, the following assumptions are made: for the bottom reflector the fuel temperature is equal to the inlet coolant temperature (per T-H channel or cell) and the coolant density is equal to the inlet coolant density (again per channel); for the top reflector the fuel temperature is equal to the outlet coolant temperature (per channel) and the coolant density is equal to the outlet coolant density (per channel).

For a first guess comparison a major hypothesis shared among partners corresponds to keep for the reflectors (top, bottom and radial) the same compositions as moderator.

An update with heavy reflector may be realized during the follow-up and fixed before the end of the deliverable D5.2, once and if the cross sections currently under development in WP4 will be provided. Otherwise, this activity needs to be pursued with further actions.

4.4.2 Boundary conditions and steady-state conditions before transient

The newly defined hypotheses concerning core and assemblies and reflectors compositions change the core state at the beginning of the transient.

A core model is provided by KIT and FRAMATOME to perform sensitivities oriented to define the steady-state operating conditions before transient.

Some effort was spent to find optimal conditions to reach criticality and some sensitivities have been performed by KIT with Serpent2, confirmed by FRAMATOME with APOLLO3®, to provide a suitable configuration for boron concentration and control rod banks positions.

To fix conditions to be shared before any comparison, a first scenario may have the boron concentration fixed to 1200 ppm, the core operated at hot full power with xenon in equilibrium. Critical state may then be achieved tuning control rod banks IX and X, as previously defined in Table 7.

First sensitivities oriented to define a more realistic as possible pre-accidental condition close to criticality already realized by KIT and FRAMATOME are presented here after.

As final specifications are still ongoing till the very last period of the project they will be integrated to the last revision of documentation.

At the beginning the generation of 2 groups homogenized cross-sections (XSs) to feed the core simulations with APOLLO3® to consolidate first KIT analyses has been realized providing MPOw generated via NEMESI prototype (WP4).

After some comparisons at assembly level (ARO and B4C) see Table 11, comparison between Serpent2 (KIT) and APOLLO3® (FRA) at core level has been realized.

Table 11: Comparisons at assembly level (Kinf at BOL without Xenon) for the 4 KZL6 FAs composing cycle 1

SERPENT2 (KIT)				
	FA2_F	FA3_F	FA3_3_F	FA3_3_G
HFP, NULL XENON, ARO	1.09810	1.22105	1.24675	1.24054
HFP, NULL XENON, ARI	0.82319	0.94299	0.96966	0.96294
NEMESI (FRA)				
HFP, NULL XENON, ARO	1.09832	1.22121	1.24682	1.24061
HFP, NULL XENON, ARI	0.82330	0.94327	0.96987	0.96314
Discrepancy A-S (pcm)				
ARO	18	11	5	5
ARI (=B4C)	15	32	22	21

In addition, several tests have been carried out between KIT and FRAMATOME in order to consolidate practices around core modeling for the Kozloduy-6 NPP, see Table 12.

Table 12: comparisons at core level - KZL6

STATE	BOR ON	SB1-8	SB9	CB10	SERPENT2 KEFF	PARCS KEFF ADF OFF	PARCS KEFF ADF ON	AP3	DIFF AP3/S2, pcm	DIFF SERP/PARCS ADF OFF, pcm	DIFF SERP/PARCS ADF ON, pcm
HFP	1200	A	R	O	1.04800	1.04635	1.04651	1.05306	505	-150	-136
HFP	1200	100%	100%	0	1.04012	1.03751	1.03825	1.04433	421	-242	-173
HFP	1200	100%	0	100%	1.04223	1.04069	1.04104			-142	-110
HFP	1200	100%	0	0	1.03227	1.02955	1.03064	1.03613	385	-256	-153
HFP	1200	A	R	I	0.95481	0.94903	0.95303	0.95655	175	-637	-196

As it could be observed in Table 12, in order to target Keff = 1 the control rod should be drastically moved without proposing too high boron concentration responsible for unacceptable modification in moderator feedbacks, see Table 13 as example.

Table 13: Relationship between Safety banks position and boron concentration

STATE	XE	SP. GRID	BORON (ppm)	Others SB	SB10
HFP	NO	NO	1630.	100%	20%
HFP	NO	NO	1692.	100%	80%

Optimum configuration is still under discussion and will be presented by Task 7.4 adopting tools and models provided in collaboration with WP4 and WP5.

Among contribution to be pursued by WP4 it could be mentioned the improvement enabling the Xenon feedbacks by ad hoc parametrization.

Concerning WP5 contribution, APOLLO3® core loading with rod bank modeling will be continued till the end of the project. An additional contribution will be the development and consolidation of core interfaces enabling the coupling between the core modeled with APOLLO3®/CATHARE3 Multiphysics coupling and the full primary and secondary systems Kozloduy-6 CATHARE3 input deck realized in the framework of the CAMIVVER for the Task 7.3. Its improvement to attain the final boundary conditions enabling a MSLB transient will be continued till the end of the project and pursued in the project follow up.

4.4.3 Comparison of main thermal hydraulic parameters predicted by CATHARE3 with the reference data

The plant parameters used for the initialization of the transient calculation are summarized in Table 14.

Table 14: Initial parameters

Parameter	Plant Design	CATHARE 3
Reactor thermal power, MW	3000.0	3000.0
Primary pressure, MPa	15.7	15.8
Pressurizer Level, m	8.77	8.77
Average coolant temperature at reactor inlet, K	560.15	563.3
Average coolant temperature at reactor outlet, K	592.05	593.6
Mass flow rate through one loop, kg/s	4400.0	4370
Reactor mass flow rate, kg/s	17600.0	17450
RPV bypass, %	0.1	
Total bypass of reactor core, %	3-5	2.8
Pressure in SG, MPa	6.27	6.32
Pressure in the main steam header (MSH), MPa	6.08	6.16
Steam mass flow rate through SG steam line, kg/s	408.0	411
SG Water Levels, m	2.40	2.42
Liquid mass in the SG secondary side, t	From 43.0 to 56.0- from different references.	46

4.4.4 First test with the coupling core 3D neutronics and full system thermal-hydraulics

During the CAMIVVER project it has been possible to take the deck CATHARE3 produced in the framework of the task 7.3 for the Main Coolant start-up test and adapted it in order to couple the full system thermal-hydraulics to the core 3D neutronic solver of APOLLO3®, thanks to the C3PO engine.

First results of such a coupling are presented in Figure 35 below.

Currently, before the end of the project the same exercise is ongoing in order to prepare the CATHARE3 input deck for the MSLB KZLD6 transient and propose a 3D neutronic coupling with APOLLO3 also on this heterogeneous transient. If all components are available for the CAMIVVER project and a first feasibility has already been performed for the MCP start-up test, the fulfillment of the coupling for the MSLB transient will be completed for the project follow-up.

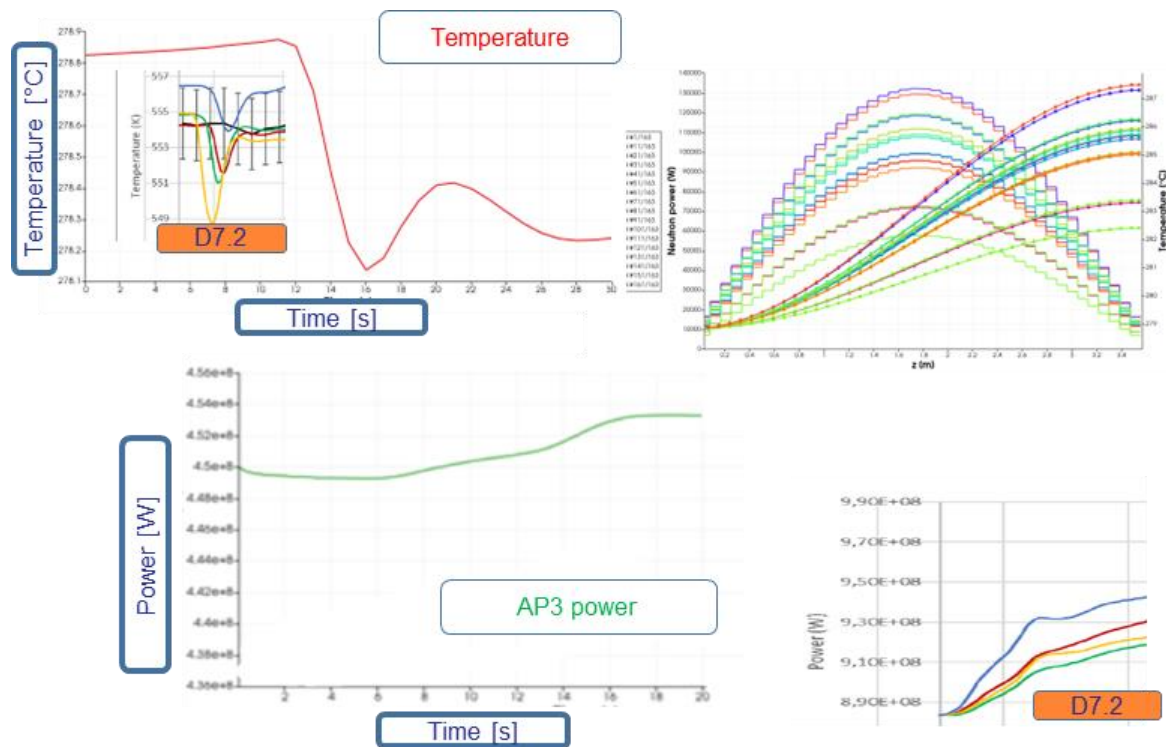


Figure 35: MCP start-up simulation CATHARE3 deck (Task 7.2) core + system thermal hydraulic simulation – Feasibility of the full system plus 3D neutronics coupling

4.4.5 CATHARE3 results for the stationary plant conditions

A stationary calculation is performed to reach the initial state of the transient as described in [1]. The controllers are used to stabilize the primary pressure with the heaters and the secondary level in the SGs with the feed water mass flow. The calculation is run until it stabilizes and reaches the desired state to start the transient.

Below are a few plots of the main parameters that were set during this steady-state calculation. The primary pressure is regulated by the pressurizer heaters which activate sequentially depending on the pressure (displayed on Figure 36). The pressurizer level is not actually controlled with the make-up/let down system (not represented in the model): the level is forced to the nominal value assuming that the primary pressure is also the operating one. For the transient, the level is no longer imposed and evolves freely depending on the other parameters since the make up/let down system is considered isolated in this transient.

The level in the steam generators (see Figure 42) is controlled by adjusting the feed water mass flow. The corresponding mass is also displayed on Figure 43.

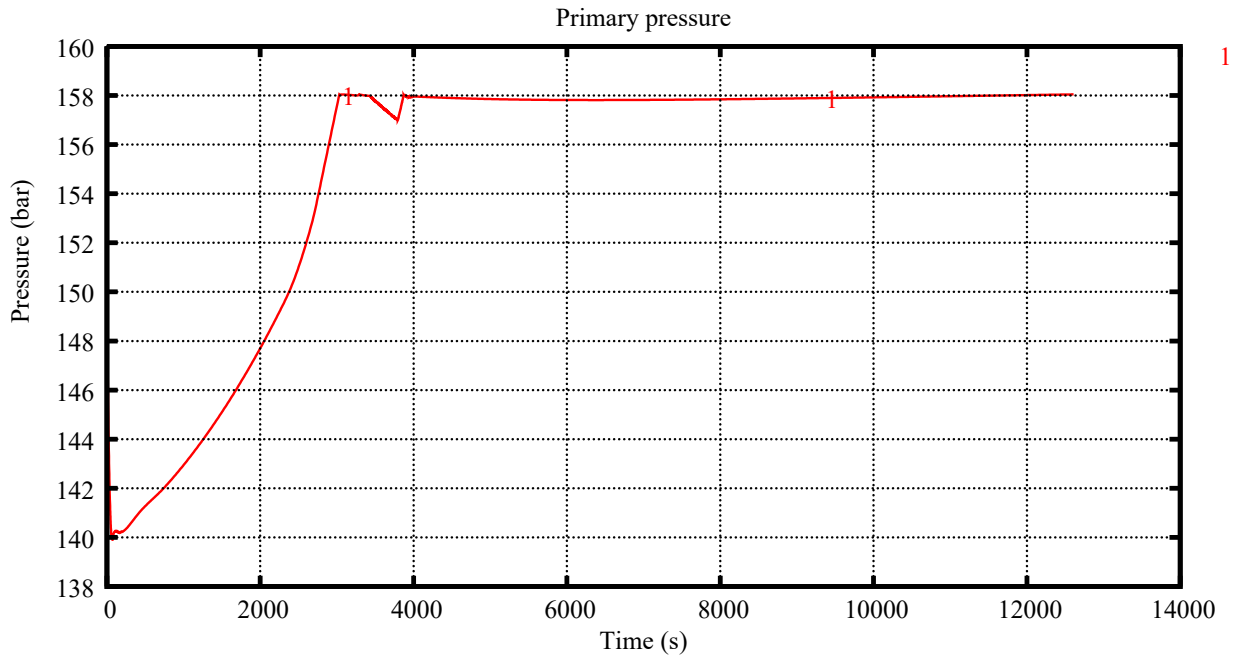


Figure 36: Stationary plant conditions – Primary pressure

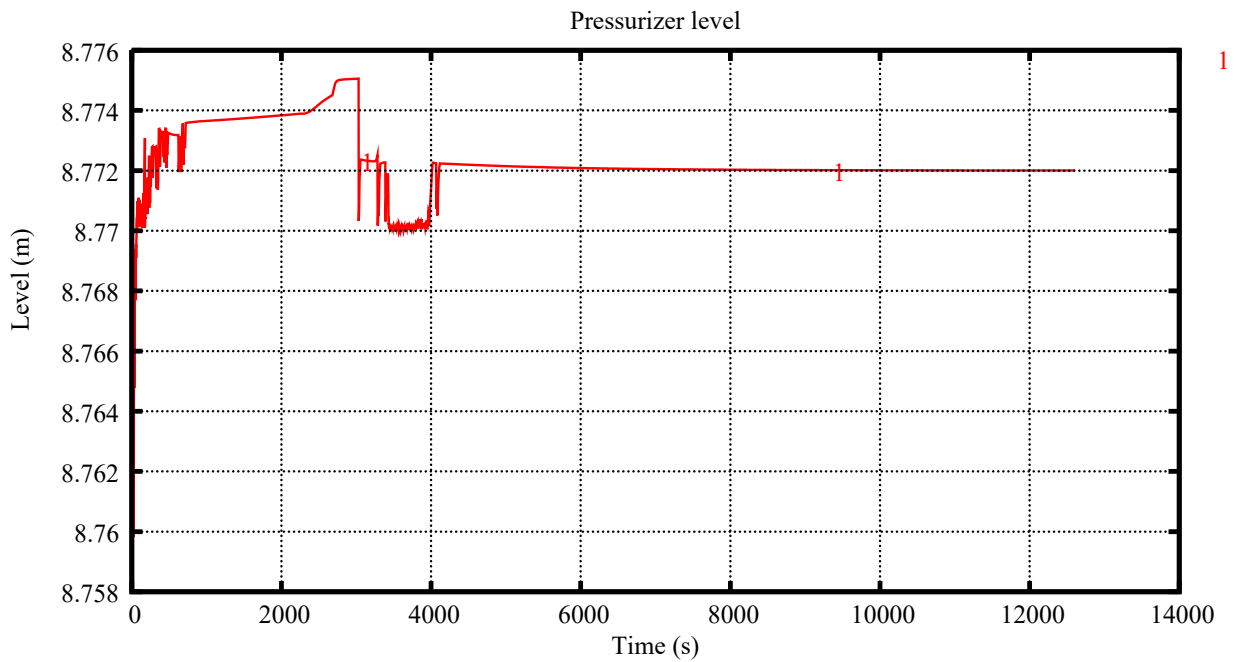


Figure 37: Stationary plant conditions – Pressurizer level

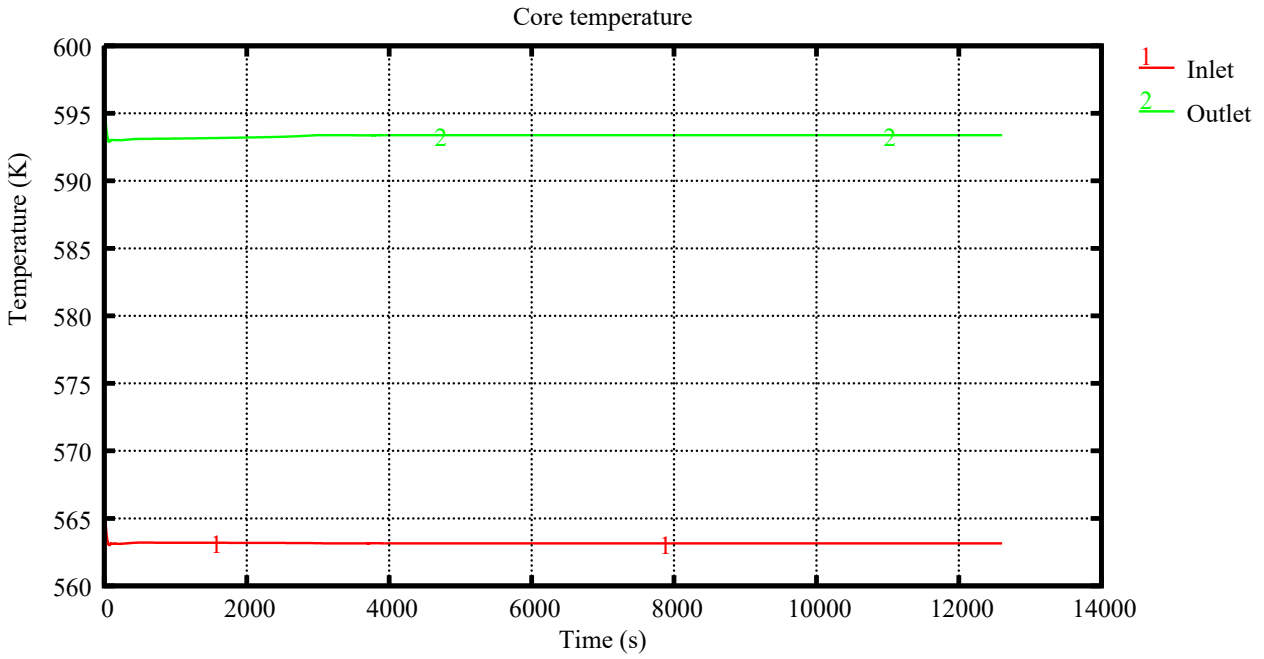


Figure 38: Stationary plant conditions – Core inlet (red) and outlet (green) temperatures

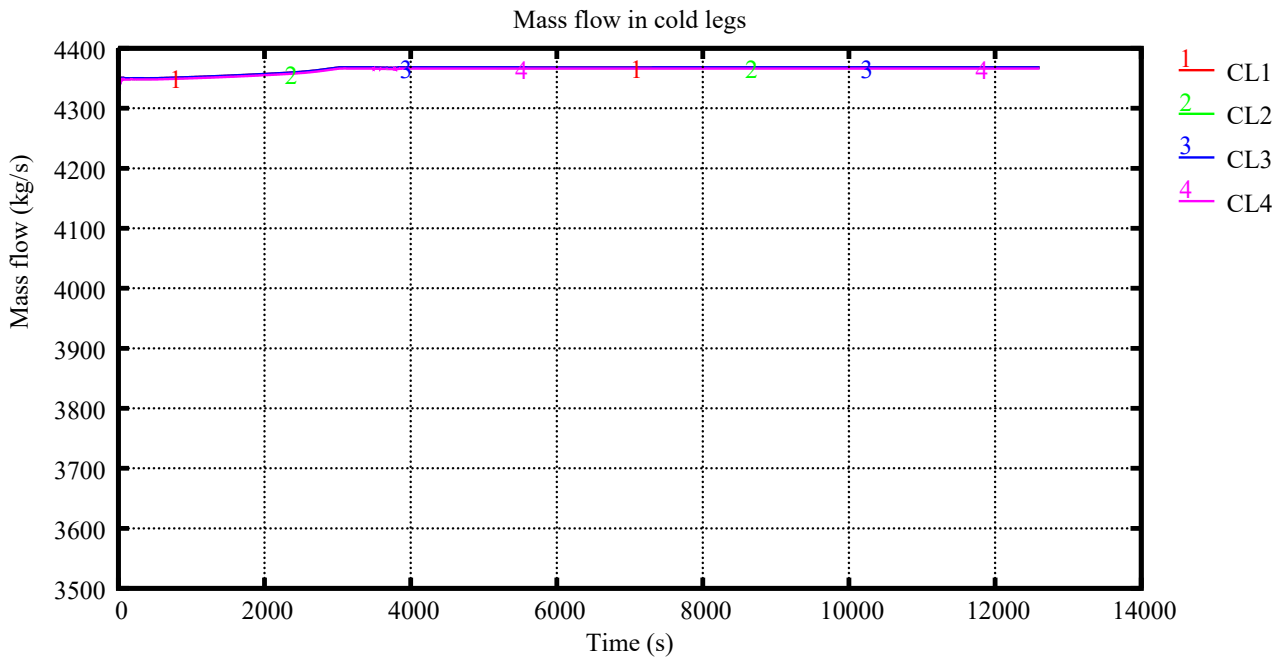


Figure 39: Stationary plant conditions – Mass flow in the cold legs

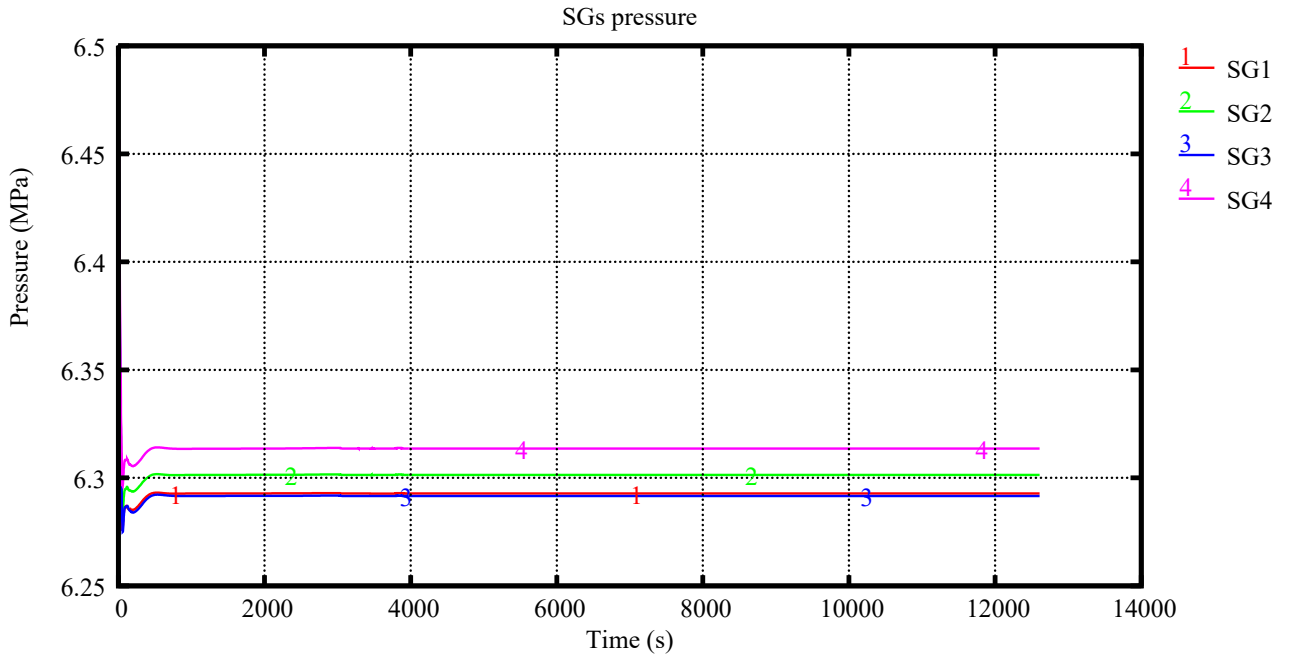


Figure 40: Stationary plant conditions – Pressure in the steam generators

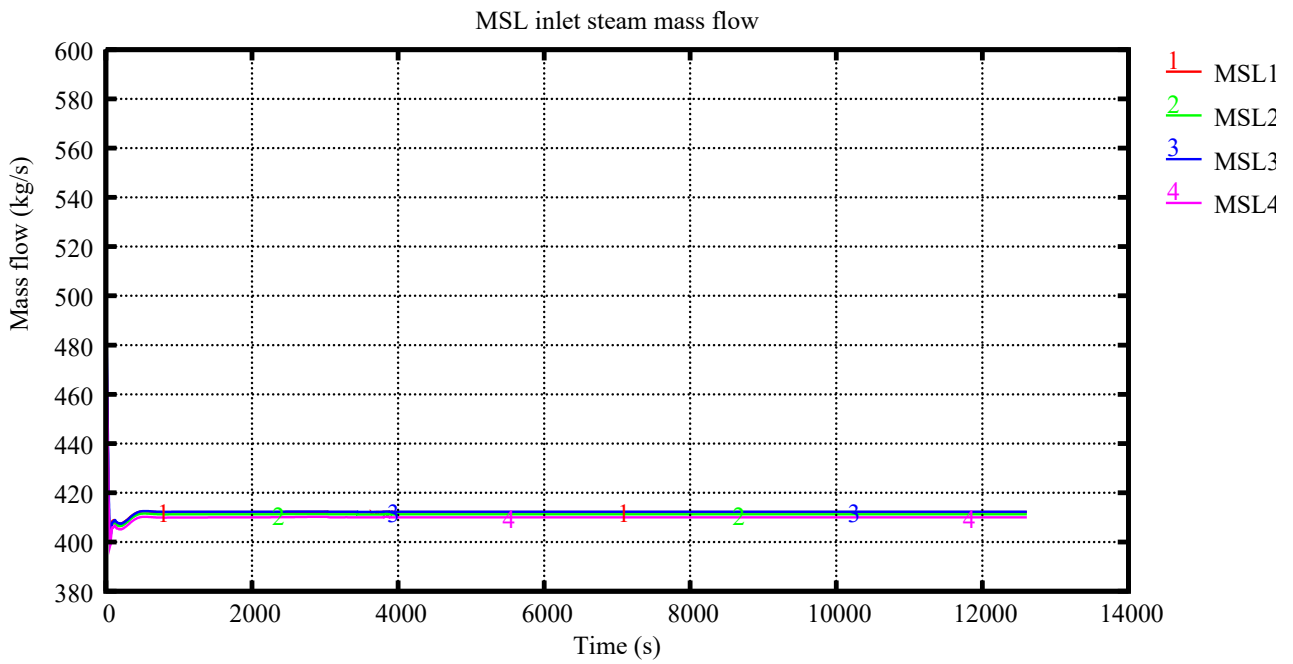


Figure 41: Stationary plant conditions – Inlet mass flow in the Main Steam Lines

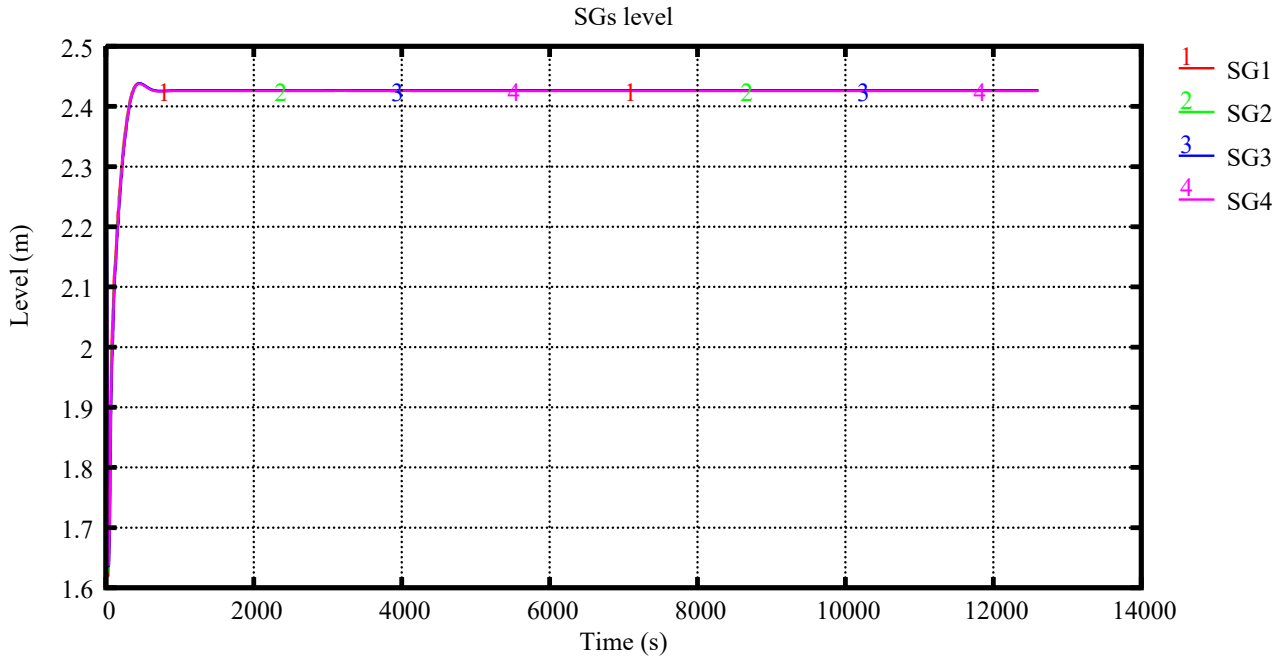


Figure 42: Stationary plant conditions – Water level in the steam generators

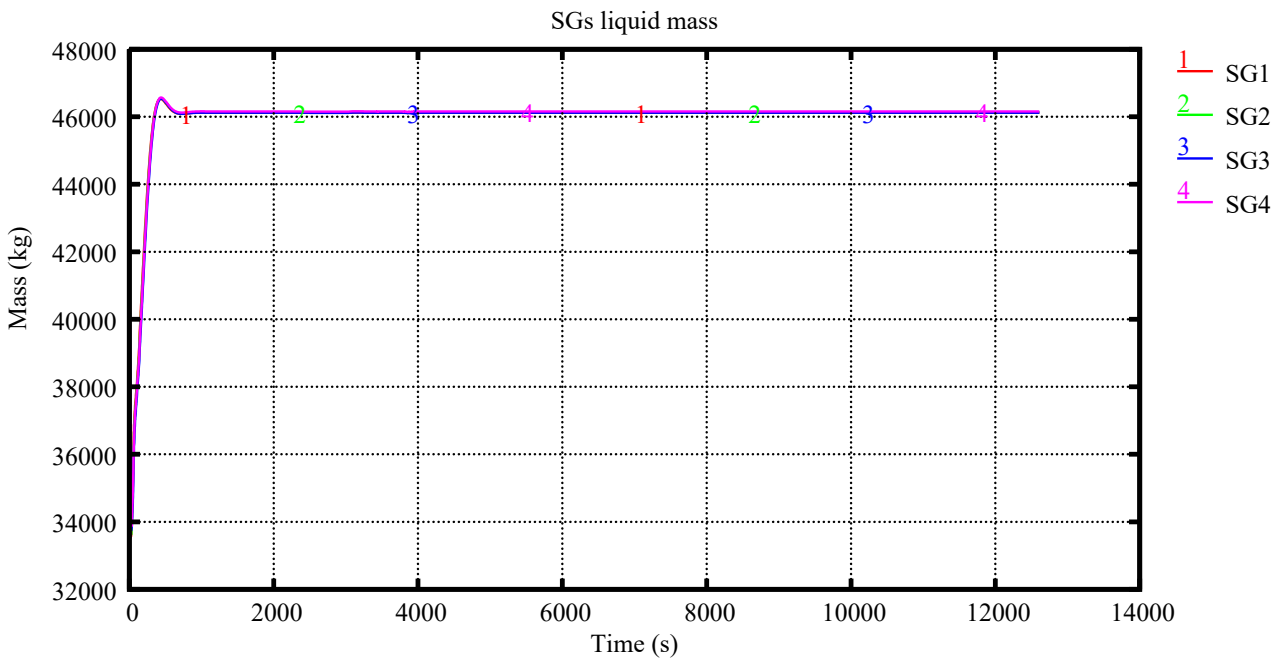


Figure 43: Stationary plant conditions – Water mass in the steam generators

5 Selected results of transient simulations of each partner

5.1 RELAP5 (ENERGORISK)

This section presents the results of the calculation analysis of the “SB LOCA + SG line break” under the initial and boundary conditions described in subsequent subsections. The calculated chronological sequence of events is presented in the Table 15.

Table 15: Chronological sequence of events for the “MSLB”

Event description	Time, s
Break opens	0
MCP trips	1.34
Turbine stop valves close	12
BRU-SN begins to open	-
BRU-K begins to open	13
Pmsh > 6.67MPa	-
BRU-K starts to close	25
PRZ level lower than 4.2 m	48.9
Minimum loop temperature	187
Maximum total power	0
SG-4 empty	-
Transient ends	600

At 0.0 s MSLB (ID=30 mm) occurs on main steam line #1 with internal diameter 580 mm between the steam generator (SG) and the steam isolation valve (SIV), outside the containment.

It is assumed reactor scram simultaneously with a break opening. Following the break and the scram, one of the most reactive peripheral control assemblies remains stuck out of the core and is assumed to be close to the location of maximum overcooling (not necessarily in the faulted loop sector).

The MCP of the faulted loop trips to mitigate the overcooling, with a coast down time of approximately 55s. The main feed water flow to the faulted SG is terminated by closure of the feed water block valve in 52 s.

At 11 s steam isolation valve #4 starts to close and the check valve in the broken line closes to isolate the MSH from the break. Time to fully open/close SIV – 10 s. At 13 s turbine bypass to condenser (BRU-Ks) starts to open and switches to MSH pressure control mode after closing MSIV. Total dryout of PRZ occurs in 48.9 s. The calculation stops at 600 seconds.

The main results of thermos-hydraulic calculation in graphical form are shown below.

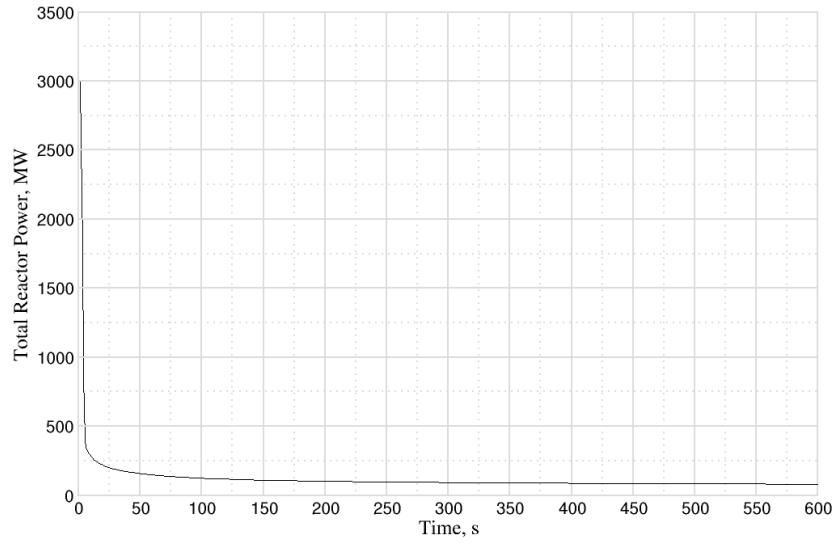


Figure 44: Total Reactor Power

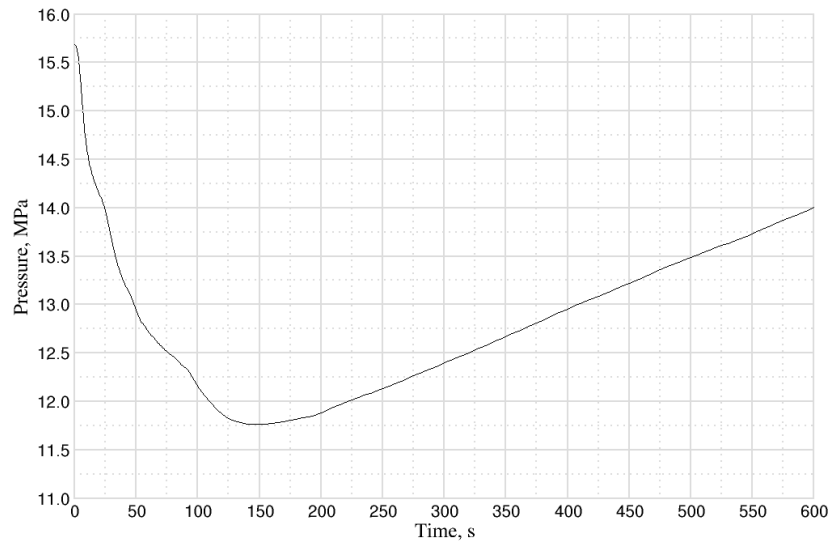


Figure 45: Primary pressure (at core exit)

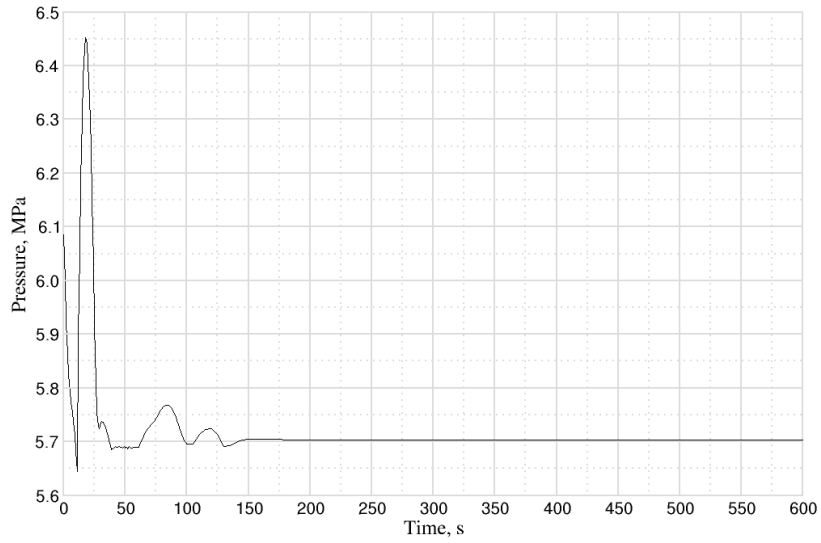


Figure 46: Secondary pressure at MSH

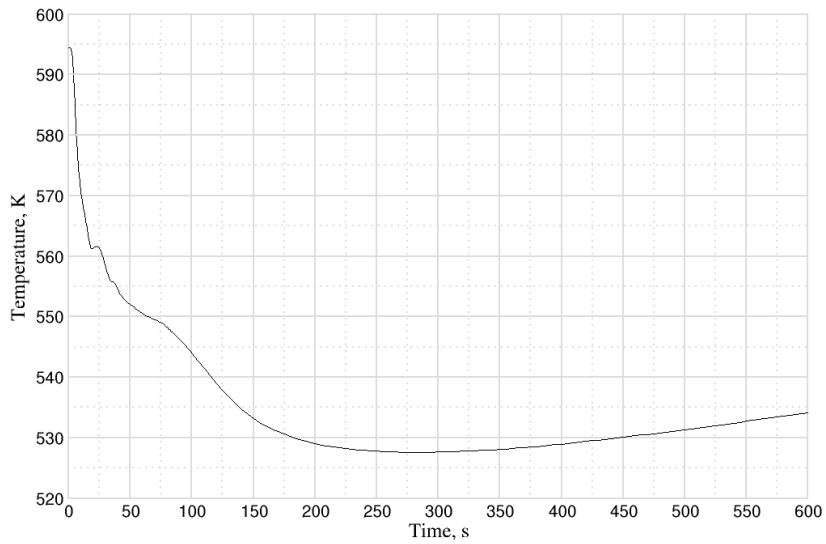


Figure 47: Core exit coolant liquid temperature

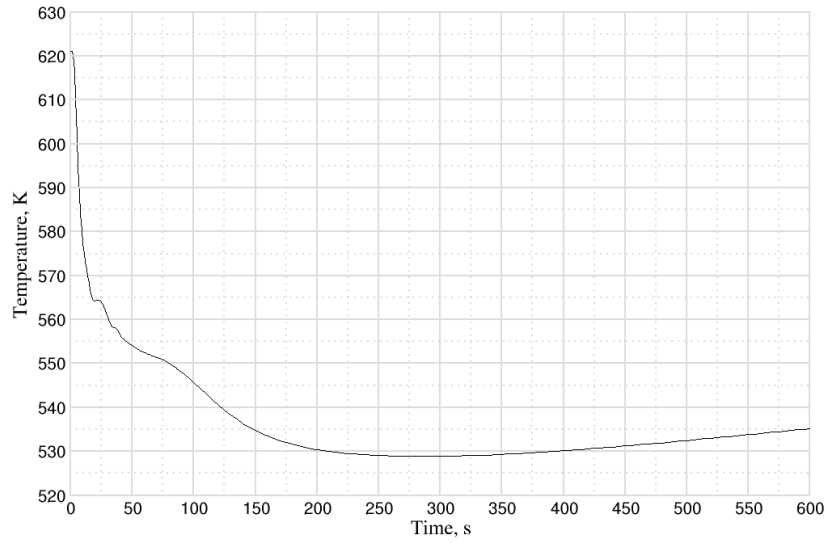


Figure 48: Core exit cladding temperature

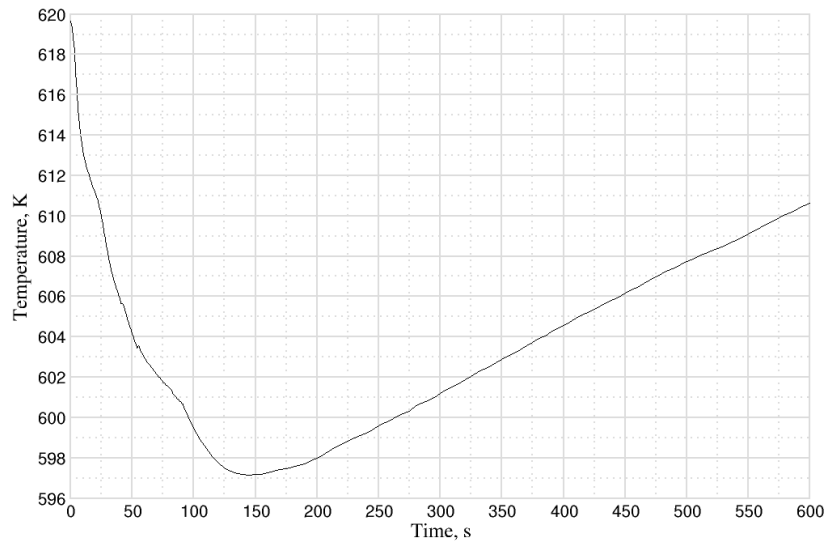


Figure 49: Core exit coolant (gas) temperature

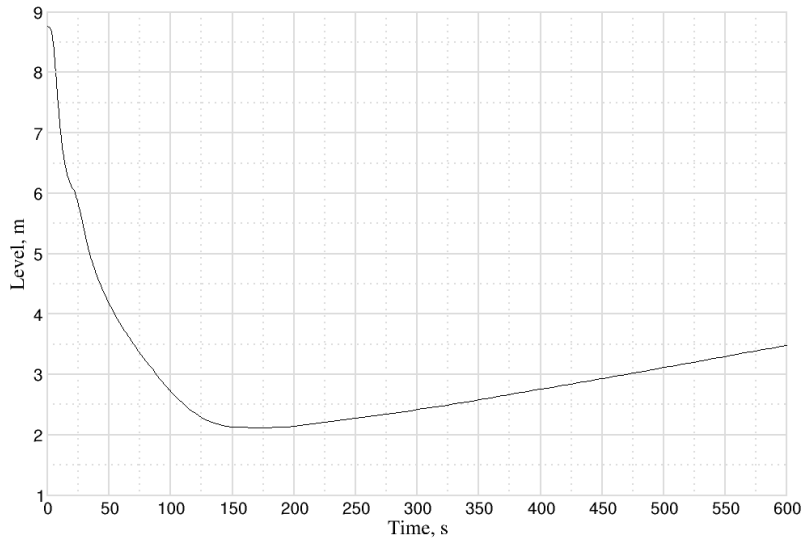


Figure 50: Pressurizer water level

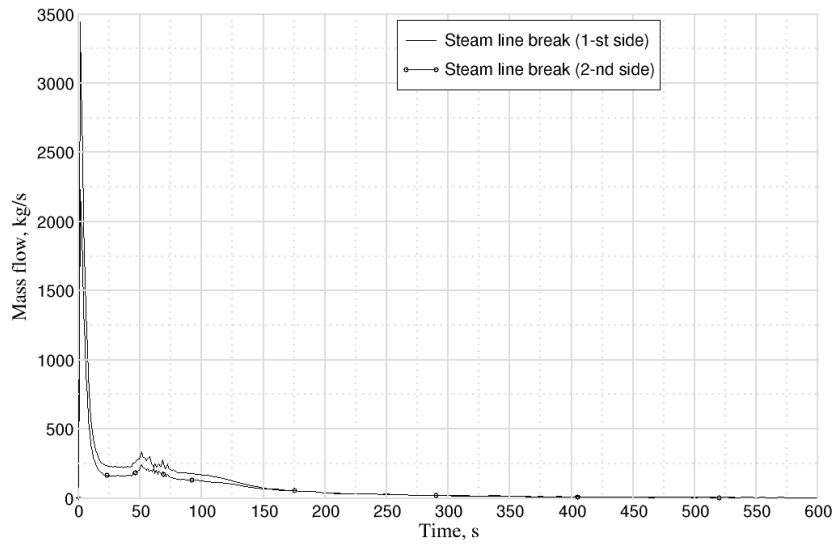


Figure 51: MSLB - differential break flow rate

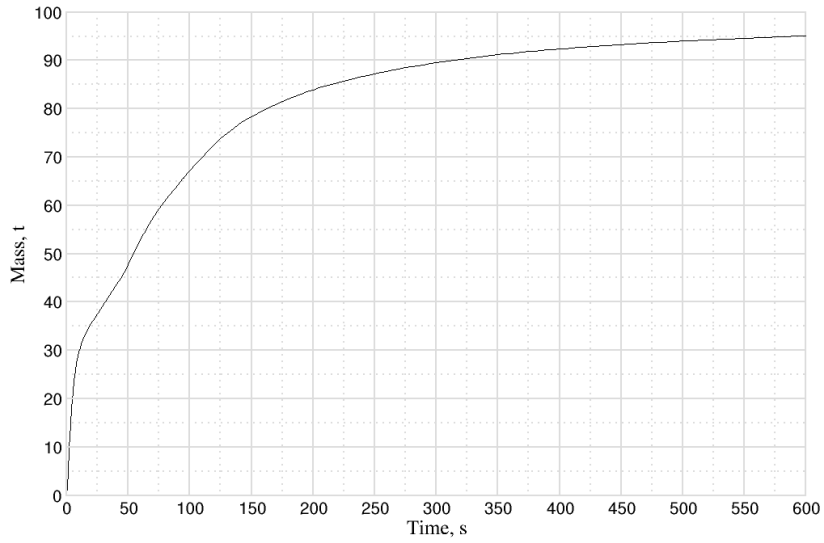


Figure 52: MSLB - differential break flow rate (on both sides)

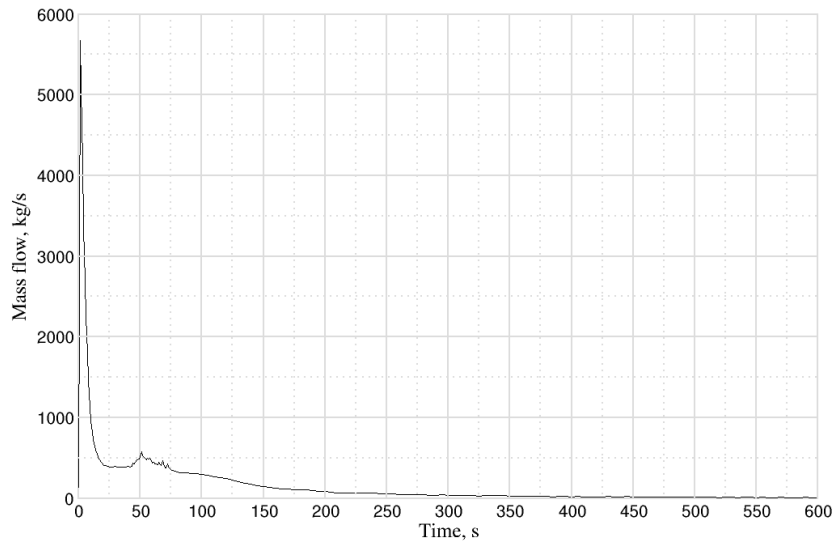


Figure 53: Integral MSLB flow rate from secondary circuit

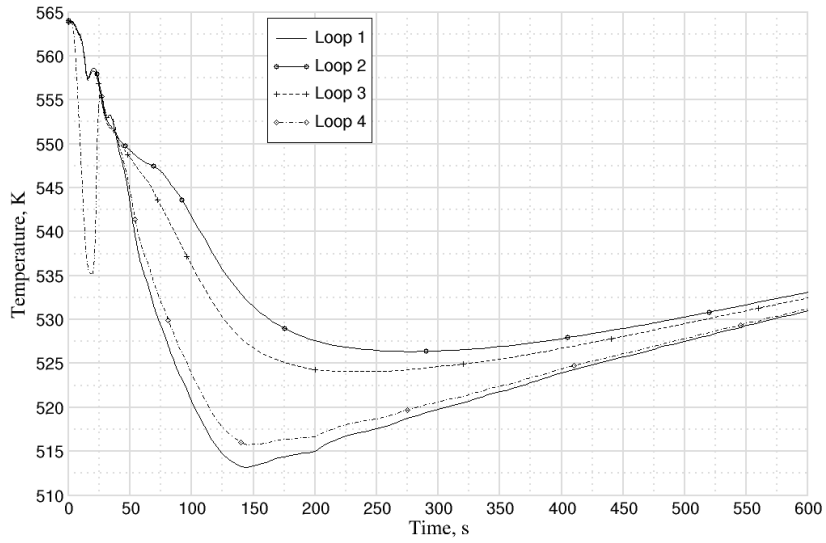


Figure 54: Cold leg liquid temperature

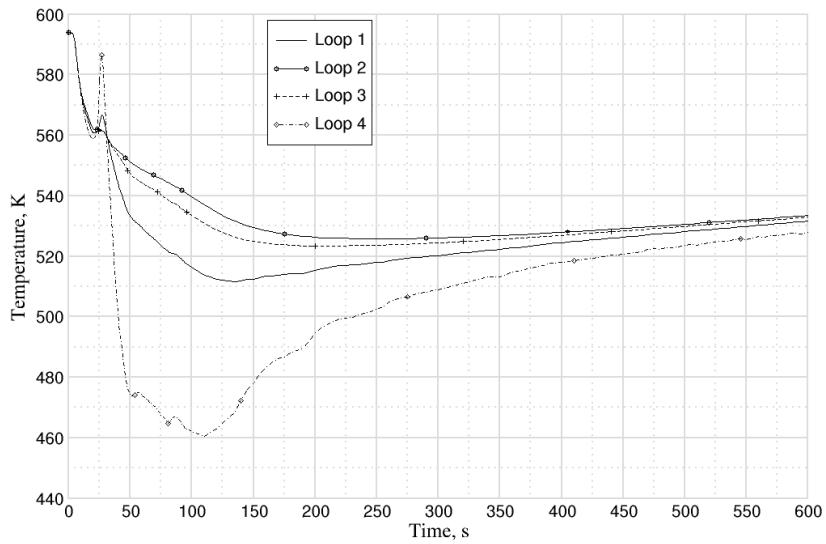


Figure 55: Hot leg liquid temperature

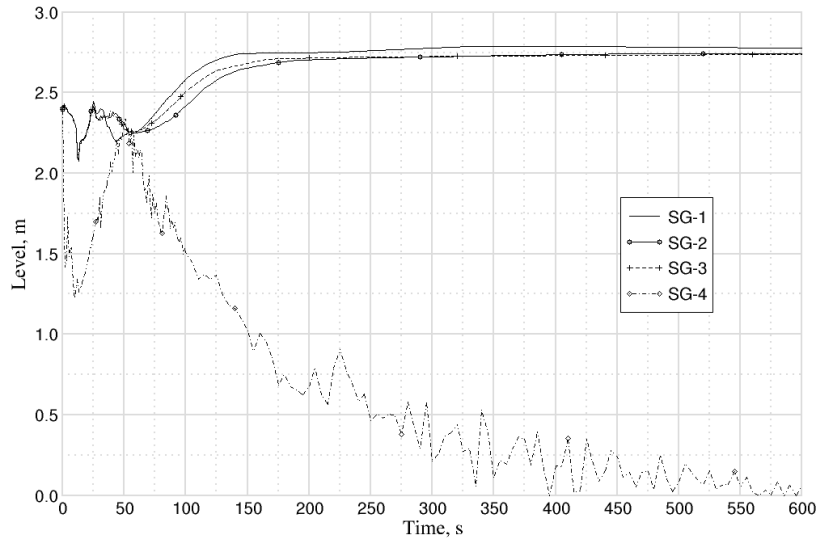


Figure 56: Steam generators water level

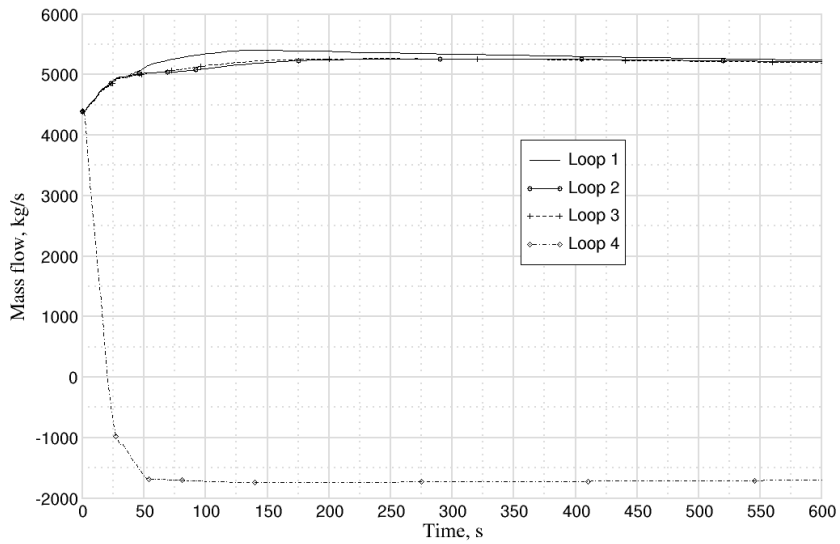


Figure 57: Coolant flow rates in cold legs

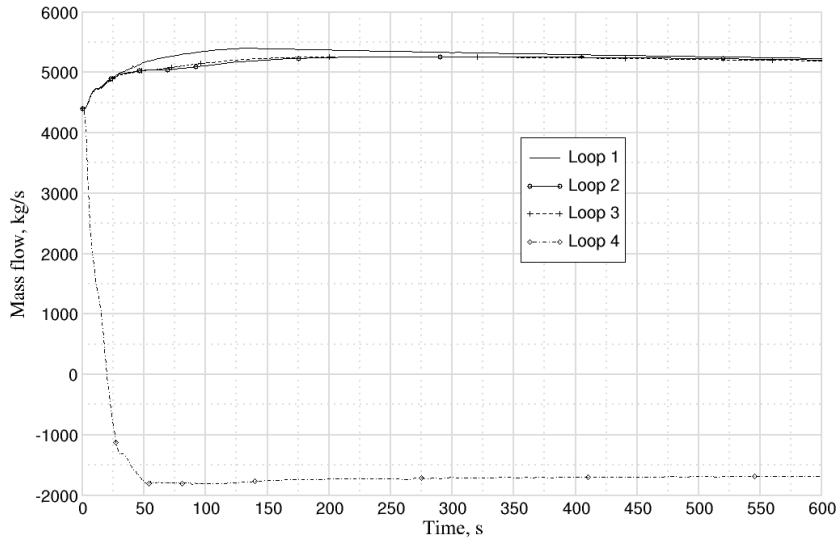


Figure 58: Coolant flow rates in in hot legs

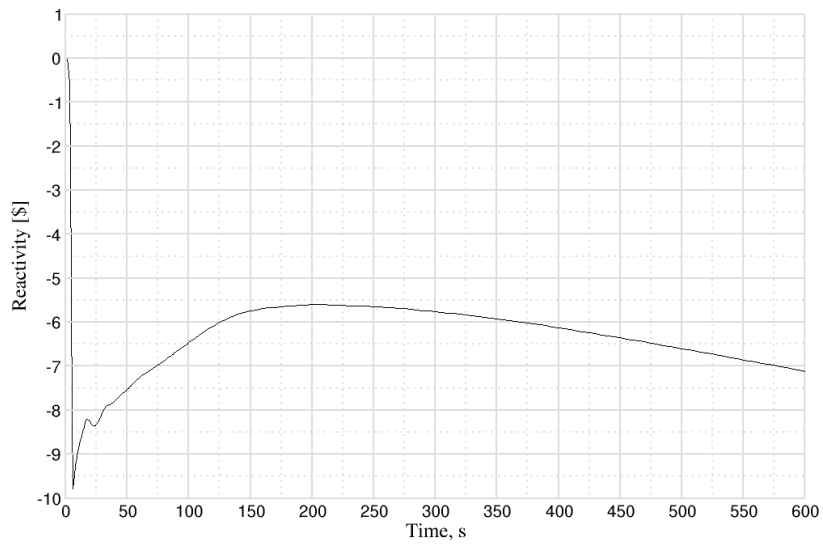


Figure 59: Total reactivity

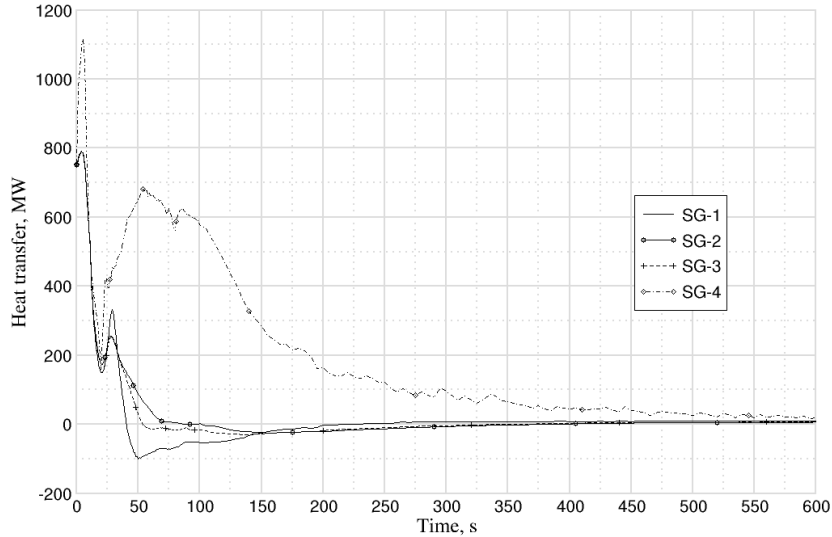


Figure 60: Heat transfer from primary to SGs (initial -750 MWx4)

5.2 RELAP5 (INRNE)

The presented MSLB results are performed using extracted KIT kinetics data considering HFP state with a critical boron concentration 1630 ppm.

The coolant inventory on the SG4 secondary side starts to decrease rapidly after the steam line break initiation, Figure 61. At the break initiation it is observed around 2000 kg/s coolant losses, which is reducing to 0 kg/s after 250 sec due to pressure reducing at SG#4. The observed small fluctuations in the period between 20 sec and 100 sec, are due to the code numerical problems. For break flow modelling it is used Henry-Fauske critical flow model.

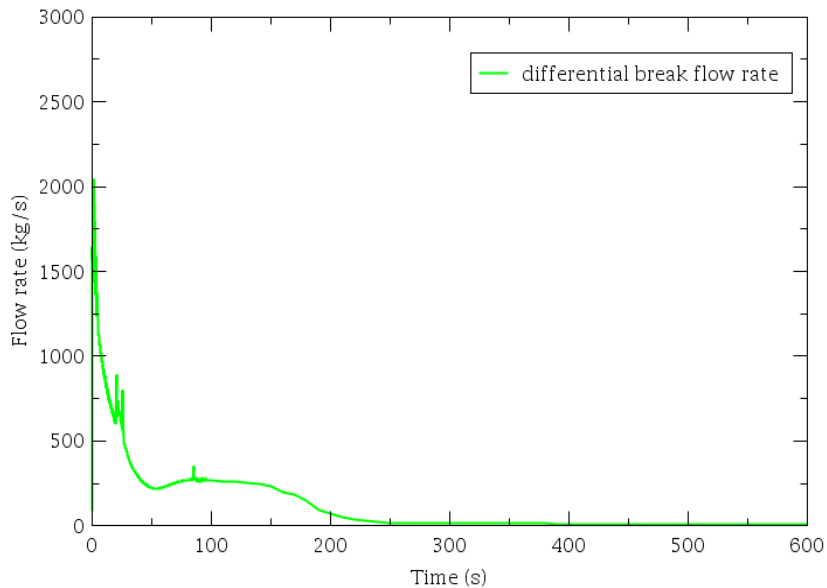


Figure 61: Evolution of the break mass flow rate

The total integrated mass from the break is 71 tons as can be observed in Figure 62.

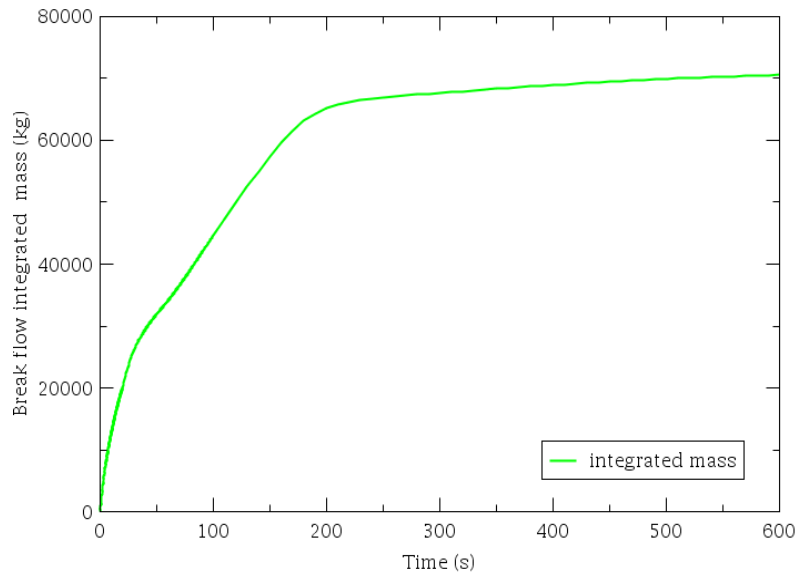


Figure 62: Evolution of the integrated mass of the coolant leaving the break

After the break initiation in loop#4 and activation of reactor SCRAM, the core exit pressure starts to decrease rapidly in first 10 sec, Figure 63. The pressure decreases rapidly due to the coolant shrinkage (after the reactor SCRAM) and overcooling of primary system from the secondary side. At 200 sec, the primary pressure starts to increase slowly after the secondary system isolation, when the following conditions are reached: $P_{SG} < 50 \text{ kgf/cm}^2$, the temperature difference $dT_s(I-II) > 75 \text{ }^\circ\text{C}$ and $T \text{ primary} > 200^\circ\text{C}$.

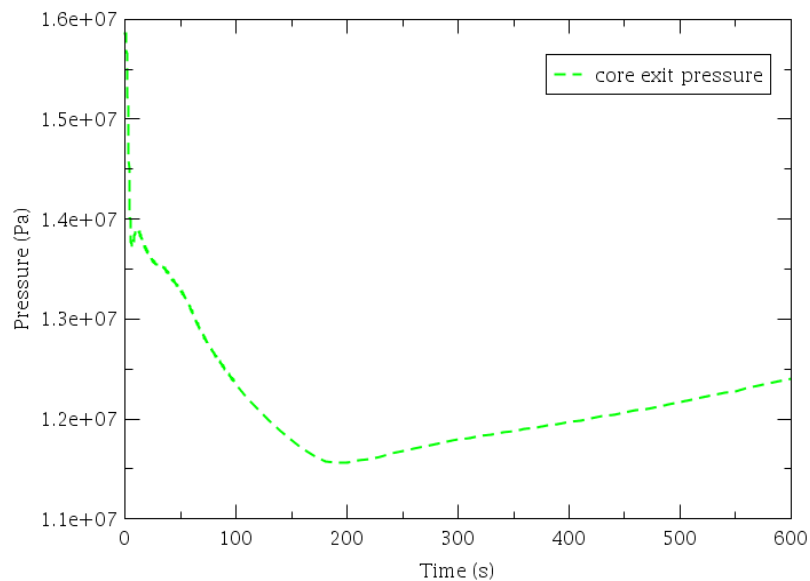


Figure 63: Evolution of the pressure at the core outlet

The core exit temperature starts to decrease rapidly after the initiation of event and activation of SCRAM, Figure 64. The SLB causes significant cooling of primary circuit, also the reactor SCRAM reduces significantly the heating of primary side to the decay power. Due to the uncontrolled increasing of steam flow, the overcooling of primary system is observed, which lead to temperature decrease. After the isolation of affected SG#4, the reactor coolant temperature starts to increase slowly and reach to 525K.

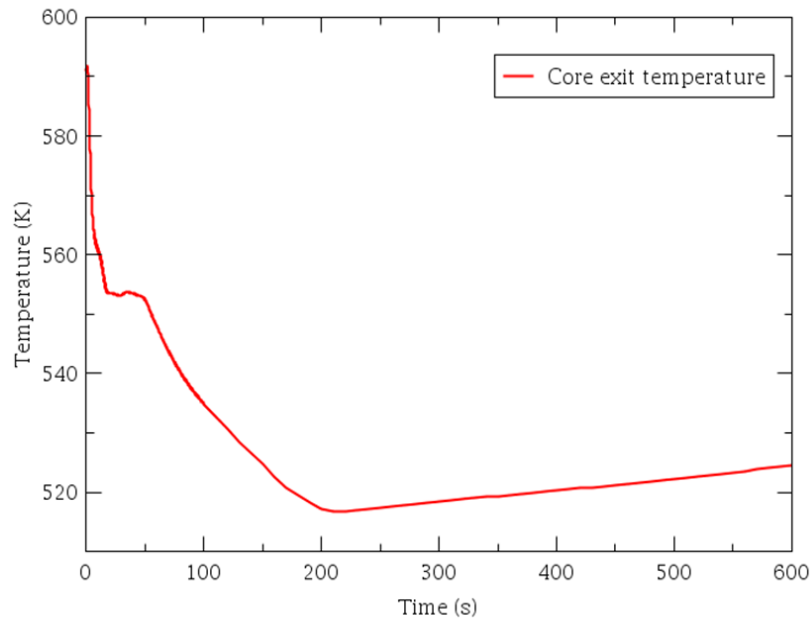


Figure 64: Evolution of the core exit temperature

The PRZ water level starts to decrease after the break initiating, Figure 65. It decreases to 1.8 m at app. 190 sec, after that it starts to increase slowly to 2.2m. The PRZ heaters work in correspondence with their set point. After the break initiation the heaters start to work and to support the primary pressure. The heaters switch off when the PRZ water level drop to 4.2 m.

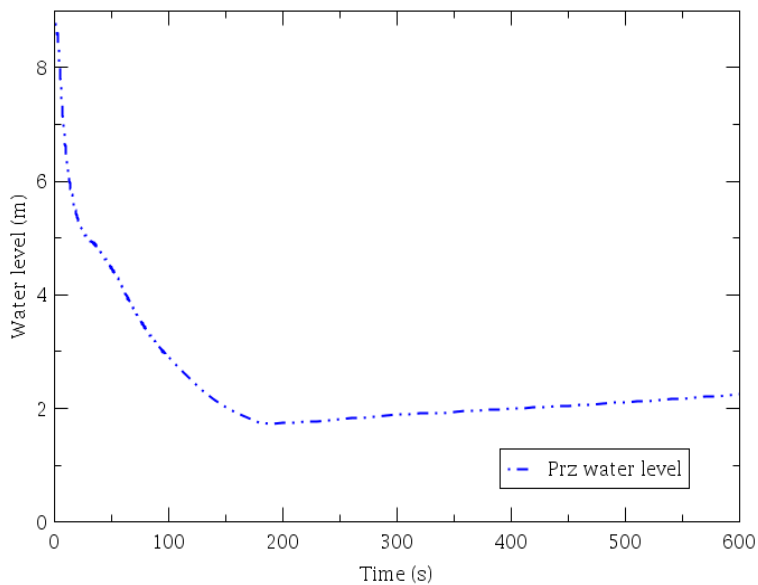


Figure 65: Evolution of the PZR-water level

The primary circuit mass flow rate in Loop#1 starts to increase after the break initiation. The maximum flow rate is 5300 kg/s at app. 200 sec, after that it decreases slowly and reaches 4800 kg/s until the end of transient, Figure 66 . The reason for observed behavior could be explained with changing of coolant due to the cooling.

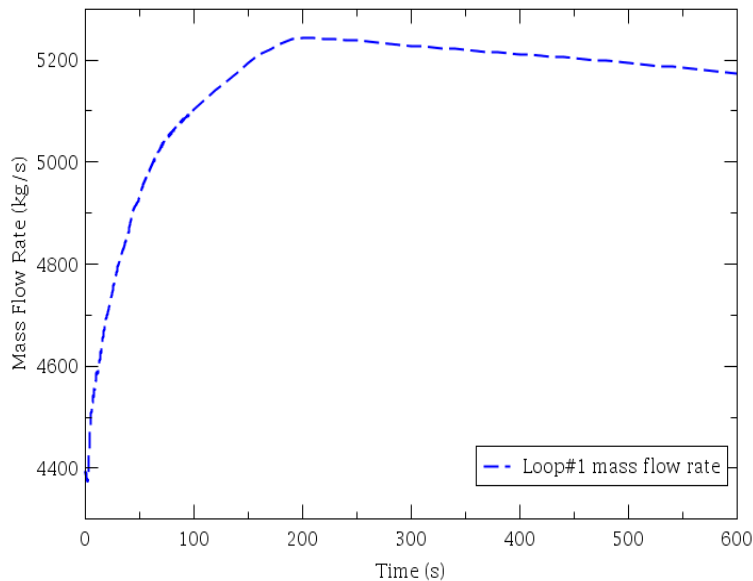


Figure 66: Evolution of the mass flow rate of the intact loop-1

The flow rates in affected Loop#4 start to decrease immediately after the break initiation and decrease the flow to (- 1500) kg/s at 45 sec from the beginning of event Figure 67. In this way it is observed revers flow, due to MCP #4 switching off, while the other 3 MCPs are in operation. The biggest flow rate leads to coolant heat up in affected SG#4 and also to faster primary side cool down.

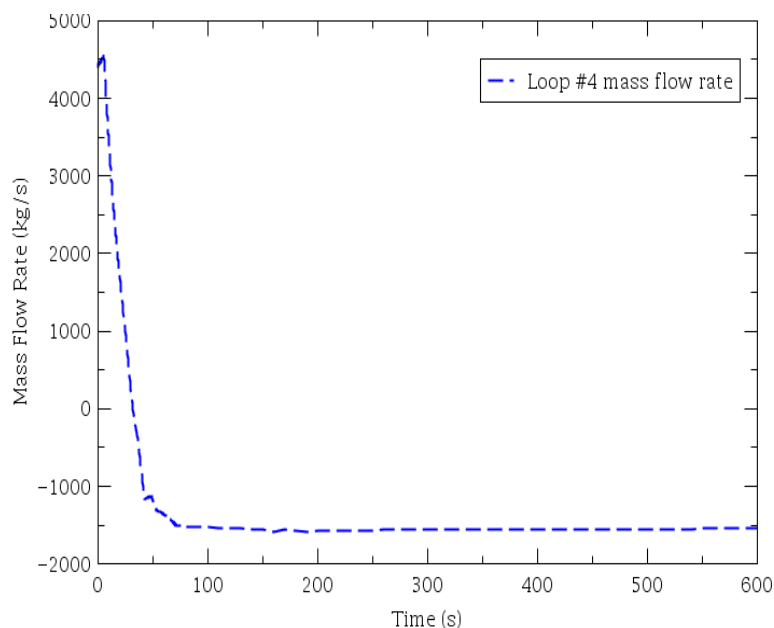


Figure 67: Evolution of the mass flow rate of the Loop-4 primary

The secondary side pressure drops shortly after the start of the transient, then after 10 sec from the start of the accident, it starts to rise, Figure 68. The secondary pressure increases due to the closing of turbine MSIV and isolating of affected SG#4 with SIV (BZOK). This also leads to increase of pressure at the non-affected SGs. After reaching the set points for safety valve BRU-K activation, they open and start to regulate the secondary pressure. The BRU-K opens when the secondary pressure reaches 6.67 MPa, reducing the pressure and controls it to the 6.28 MPa, when the secondary pressure drop to 5.79 MPa the BRU-K closes.

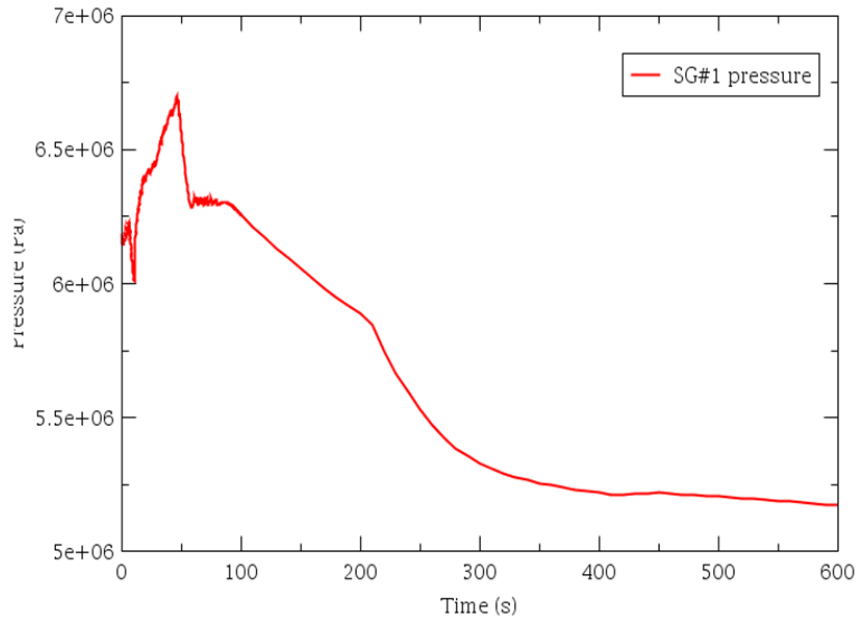


Figure 68: Evolution of the pressure of the intact SG-1

The secondary side pressure in affected SG#4 decreases rapidly after the break initiation and after 100 sec continues to decrease slowly to approximately 250 sec, Figure 69. The decay heat in the first 50 s is removed mainly from SG#4. After depressurization of SG#4 at around 220 s, the decay heat is removing from work of BRU-K.

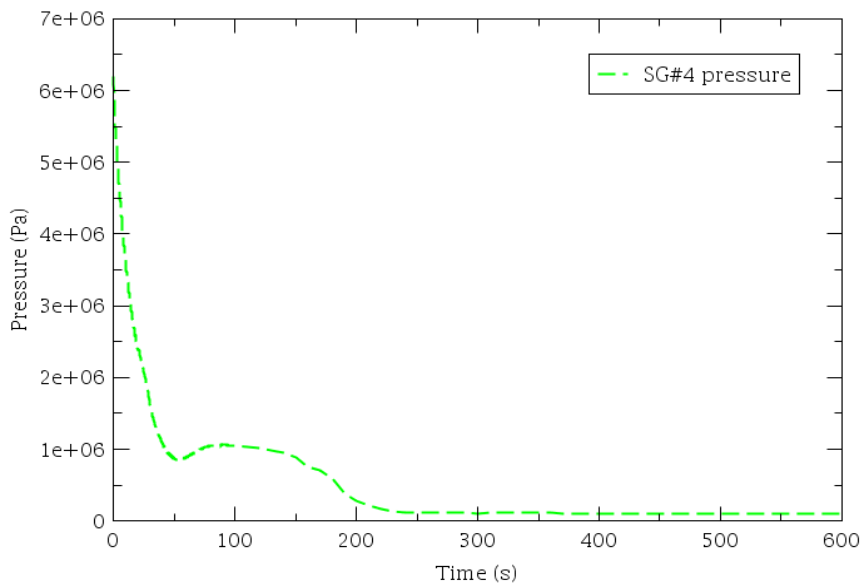


Figure 69: Evolution of the pressure of the broken SG-4 dome

The SG#1 mass inventory starts to increase immediately after the reactor SCRAM and reaches to 75000 kg until the end of transient, Figure 70. The behaviour of SGs water mass depends of boundary conditions provided for the test. The initial mass inventory was stabilized at 48 ton based on the boundary conditions.

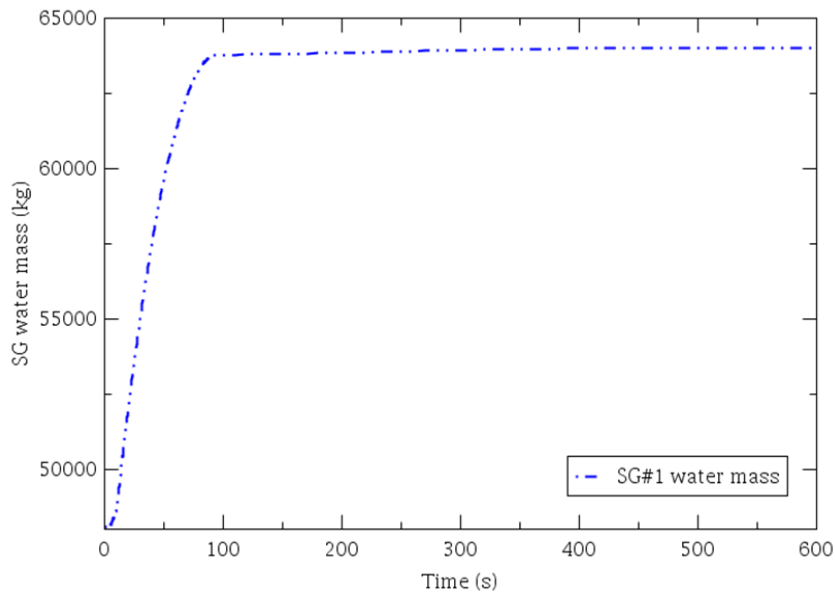


Figure 70: Evolution of the mass inventory of the intact SG-1

The SG #4 water mass decreases rapidly in first 200 sec., after that the SG mass of affected loop#4 reduces slowly to the inventory empty, Figure 71, . The initial mass inventory was stabilized to 48 ton based on the boundary conditions.

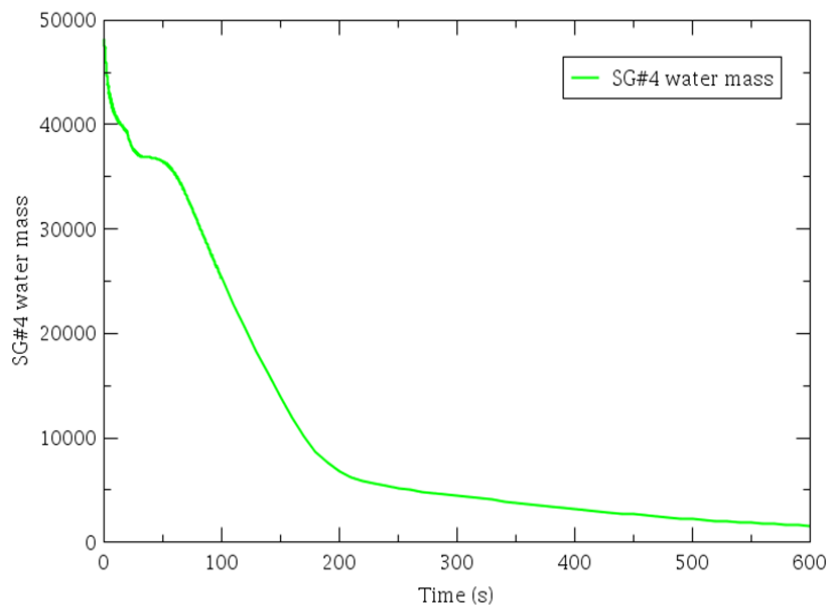


Figure 71: Evolution of the mass inventory in the fault SG-4

After the water inventory from the faulted SG is blowdown through the break, the temperature in the primary system starts to increase slowly, which causes the FB reactivity decrease. The total reactivity is negative and it is -10 \$, Figure 72.

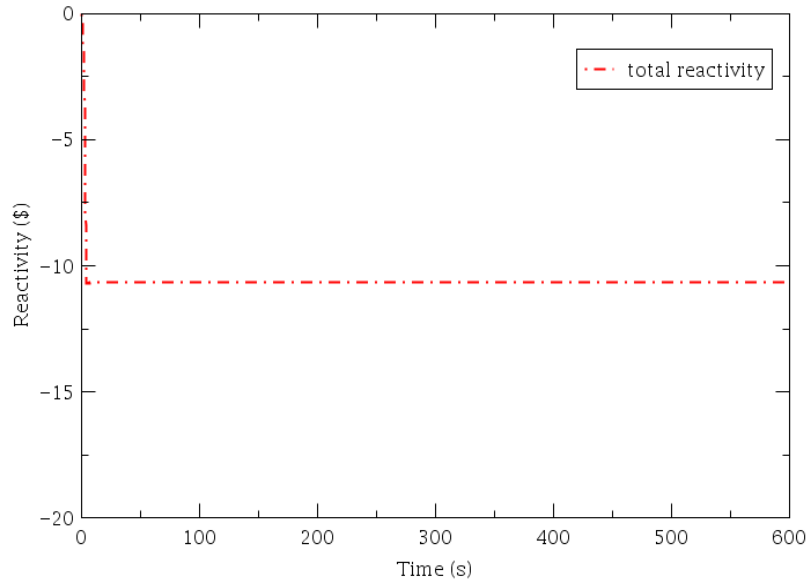


Figure 72: Evolution of the total reactivity predicted by RELAP5

5.3 TRACE/PARCS (KIT)

5.3.1 Core behavior during the transient

Due to undercooling of a sector of the primary coolant associated with the broken loop-4 (break in steam line of SG-4), the coolant temperature of one sector was reduced about 50 K at 36 s after the transient initiation. In Figure 73, both the coolant outlet temperature distribution and the Doppler temperature distribution are shown. There can be observed that a coolant mixing between the sectors associated with the loop-4 and its neighbor sectors too place after the transient start.

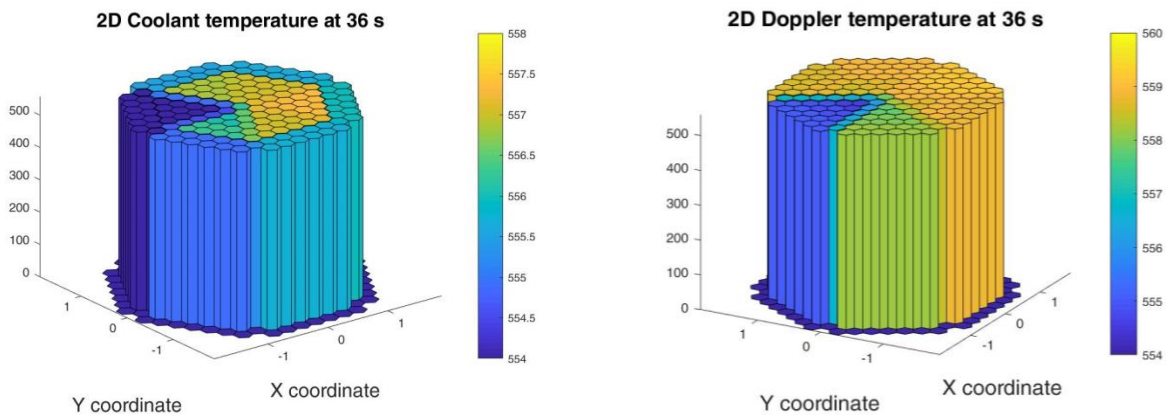


Figure 73: 3D coolant temperature at the fuel assembly outlet at 36 s transient time (lowest value of the coolant temperature at core inlet)

As a consequence of the coolant decrease, the power of these fuel assemblies and specially, of the one located at the stack-rod position, has increased thanks to the higher coolant density and neutron moderation while the power of the fuel assemblies not adjacent to the one of loop-4 remains at lower values.

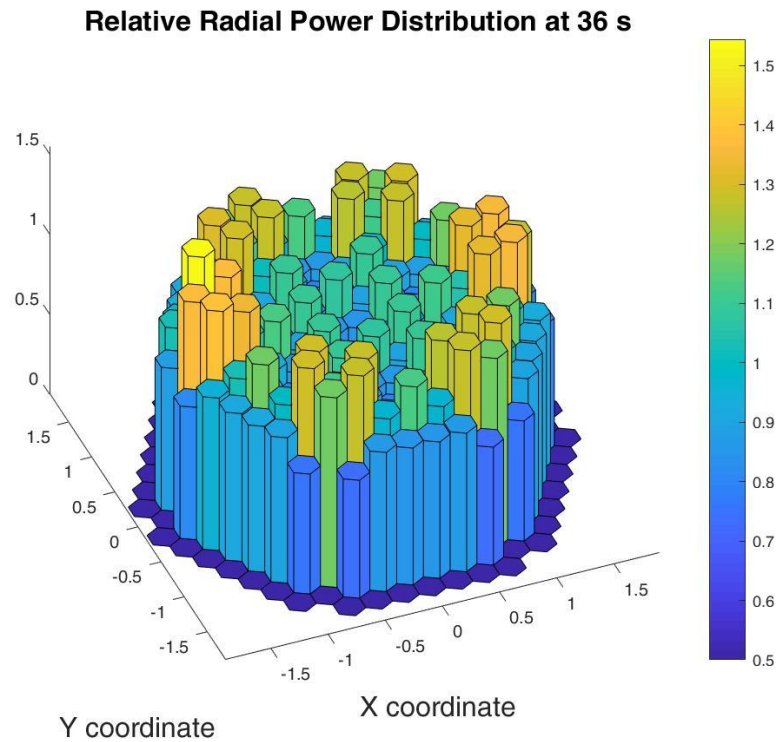


Figure 74: 3D fuel assembly power distribution at 36 s transient time (lowest value of the coolant temperature at core inlet)

In Figure 75, both the coolant outlet temperature distribution and the Doppler temperature distribution at the time of the lowest PZR-level are shown. There can be observed that a coolant mixing between of the affected sector associated with the loop-4 and its neighbor sectors is not negligible.

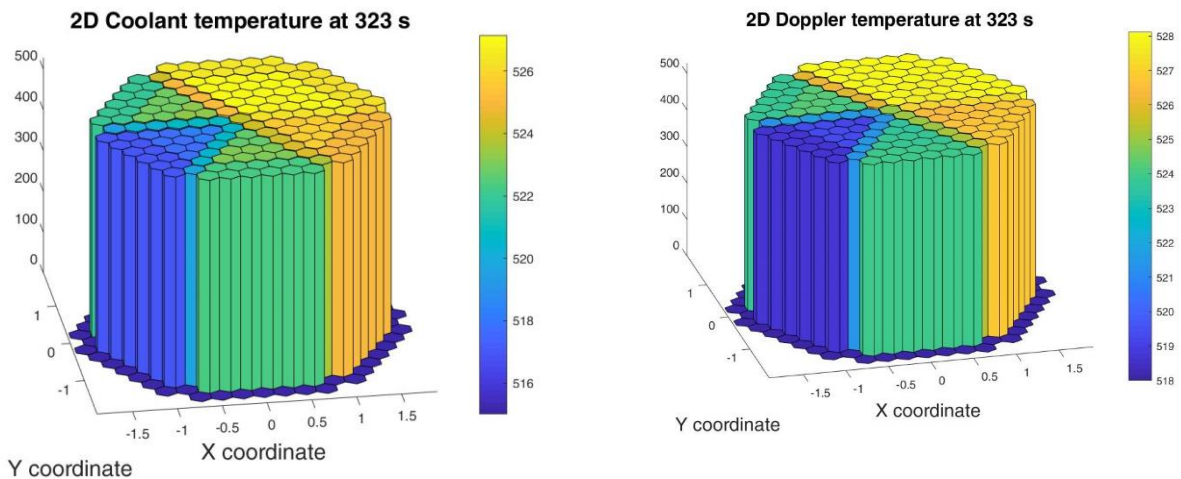


Figure 75: 3D coolant temperature at the fuel assembly outlet at 323 s transient time (lowest value of the coolant temperature at core inlet)

The corresponding power distribution of the fuel assemblies shown in Figure 76 changed compared to the one shown in Figure 74. Consider that at that time the decay heat has reduced considerably.

Relative Radial Power Distribution at 323 s

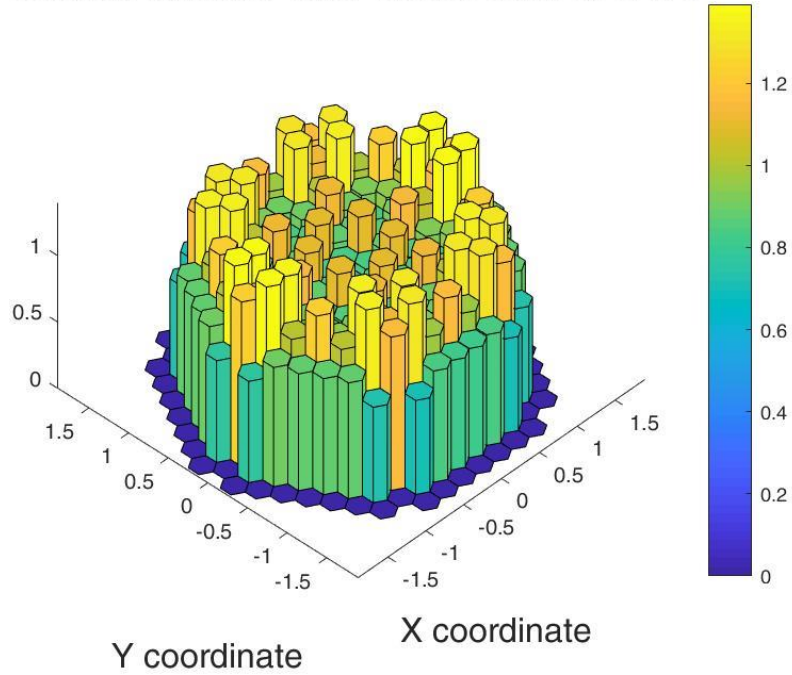


Figure 76: 3D fuel assembly power distribution at 323 s transient time (lowest value PZR water level)

5.3.2 Plant behavior during the transient

Selected results obtained with the coupled version of TRACE/PARCS for the MSLB transient at BOC conditions (academic case) will be presented and discussed below. In Figure 77 the change mass flow rate after the break opening at time 0s in the steam line of the SG4 is shown. High values are predicted at just after the break opening driven by the large pressure difference of the SG4-secondary side with respect to the environment.

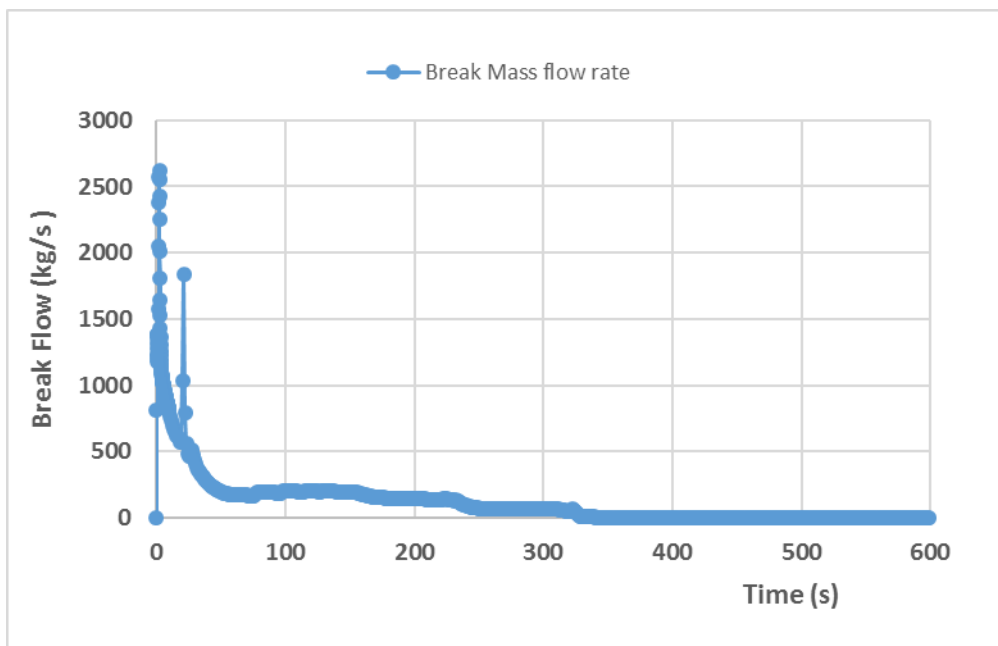


Figure 77: Evolution of the break-outflow as predicted by TRACE/PARCS

The pressure of the broken steam line (Pn-406 Dome) and the one of the loop-1 (Pn-106-Dome) are shown in Figure 78 as predicted by the coupled code. There you can see the fast pressure decrease leading to strong flushing and evaporation of the coolant inventory on the SG4-secondary side.

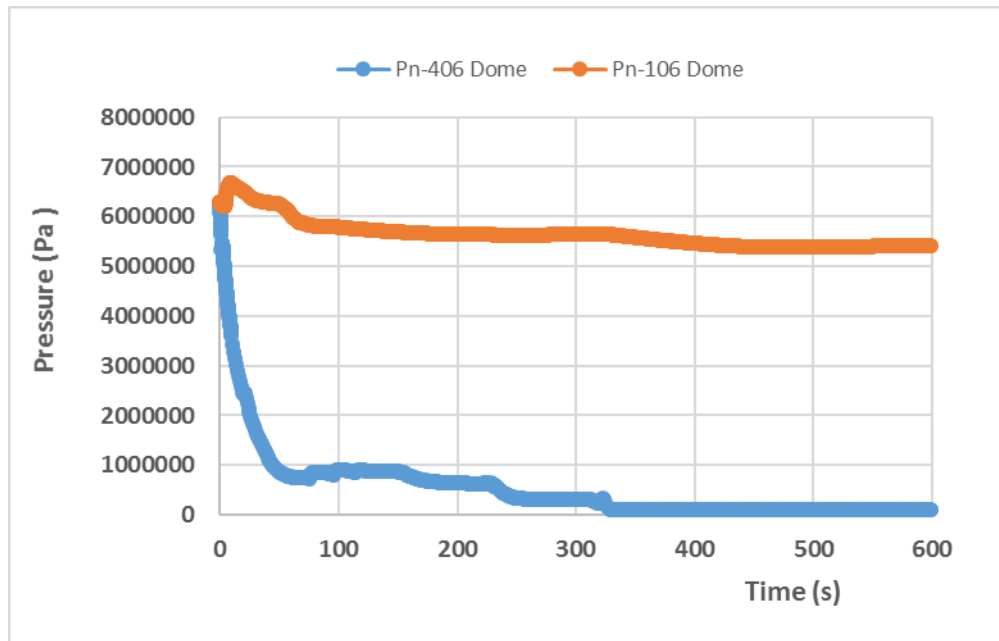


Figure 78: Evolution of the pressure in the SG-dome part of loop-4 (broken Steam line) and the adjacent loop-1 as predicted by the coupled code

This process leads to an increase heat transfer from the primary to the secondary side of the broken steam generator of loop-4 (SG-4), which as consequence cool-down the coolant of the primary side i.e. of the corresponding cold-leg 4 as you can observe in Figure 79. The temperature decreases amounts around 50 K. There, it can be also observed that the primary coolant of the adjacent loop-1 is also experiencing a cooling down caused by the mixing process going on in the upper plenum, downcomer and lower plenum.

The cool-down of the primary circuit coolant stops at round 250s when the feedwater inventory of the secondary side of the broken SG-4 is almost empty. Later on, the heat transfer from the primary to the secondary side is no more sufficient and hence the respective loop-4 and –loop-1 temperature on the primary side starts to increase slowly.

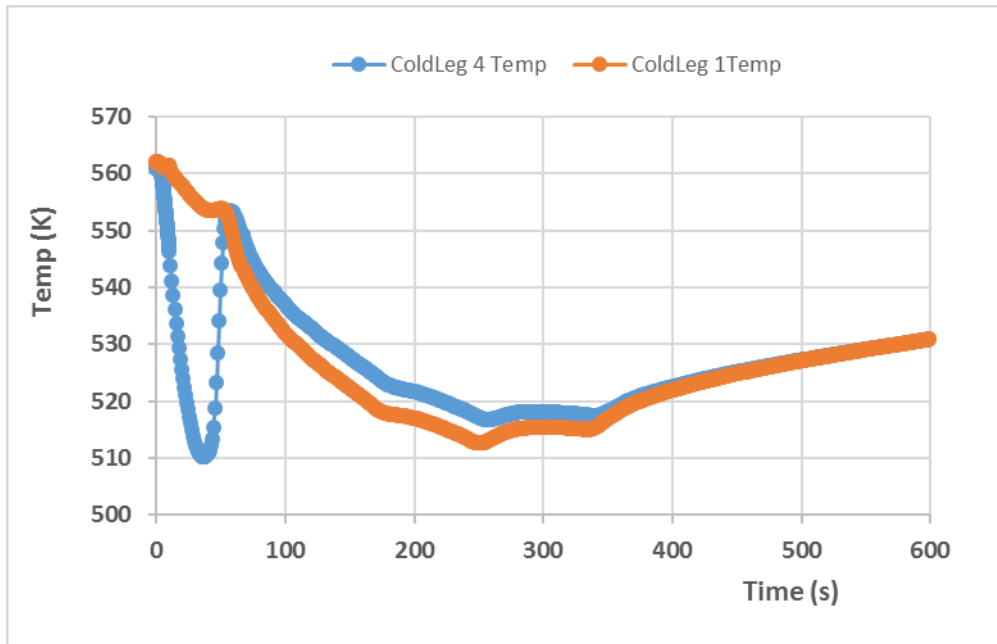


Figure 79: Coolant temperature evolution of the cold leg 1 and 4 during the transient progression as predicted by TRACE/PARCS

As a consequence of the cool-down of the primary water sector corresponding to the SG-4, a positive reactivity insertion is introduced into the core, which will lead to an increase of the total reactivity and total power.

It is worth to mention, that in the MSLB-scenario, it was assumed that the reactor will be shut-down immediately after the break is opening (not as in the realistic case, when one of three conditions are fulfilled). Hence, in Figure 80, it can be seen the sharp total reactivity decreased caused by the insertion of the shutdown rods (except the most reactive one) which amounts for ca. -10 \$. Afterwards, the total reactivity starts to increase mainly driven by the Doppler and coolant reactivity coefficients according to the evolution of the core averaged fuel temperature and the one of the coolant.

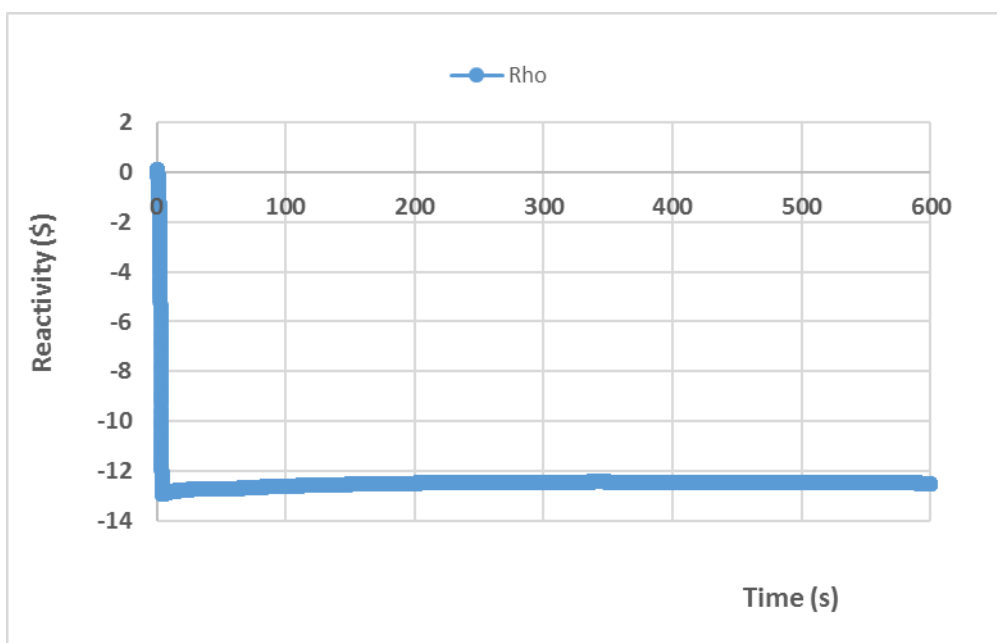


Figure 80: Evolution of the total reactivity after the SCRAM as predicted by TRACE/PARCS

In Figure 81, the resulting total power increase is plotted, where the decay heat is dominating. No return-to-power is observed for this core as can be observed in a two loop plant e.g. the TMI 1 plant.

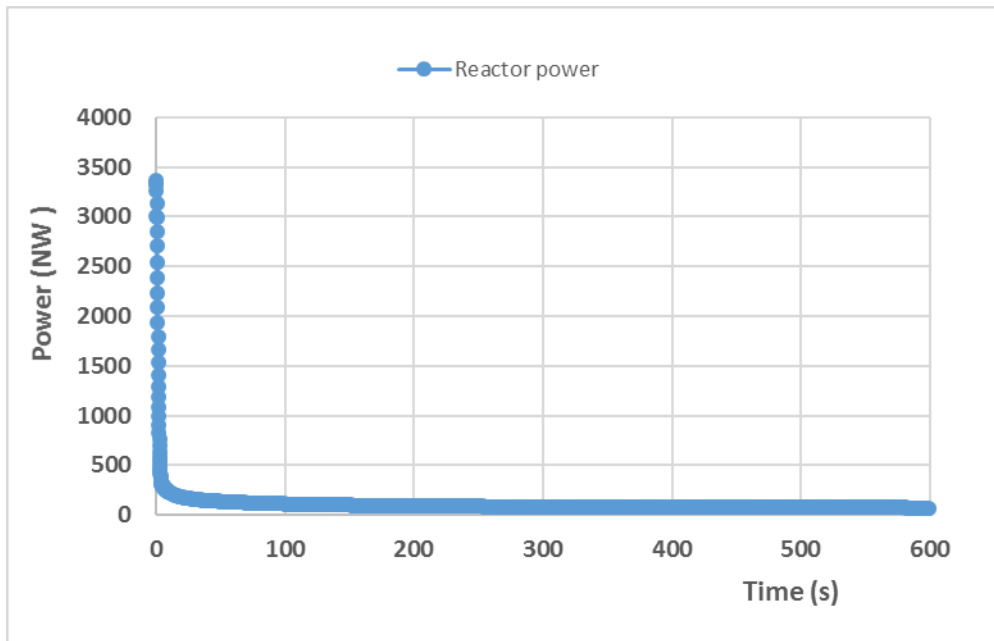


Figure 81: Evolution of the total power after the SCRAM as predicted by TRACE/PARCS

Regarding the second concern of a MSLB-transient, in the case of this VVER-core at BOC-conditions, there is no risk for re-criticality since total reactivity is far below the zero value.

5.4 CATHARE3/APOLLO3® (FRAMATOME)

The transient calculation is not perfectly operational yet. At this point, some parameters are still set to arbitrary values, mainly because the calculation is difficult to run for a long time and ends unexpectedly due to errors happening in the secondary circuit. These errors are being analyzed at the time this document is written and need further investigation in order to set-up the model properly

For instance, the pressure at the outlet of the BRU-K is set at 55 bar instead of 1 bar (atmospheric pressure) and the opening/closing of the BRU-K happens instantly depending on the pressure and not over the course of 15 s. These parameters are used for now because they make the calculation run longer, which in turn gives more data to analyze and help understanding the phenomena at hand.

Mesh refinements are being performed near the check valves in the steam lines, since it seems the problems encountered might start in this area.

However, a calculation has been run for 461 s instead of 600 s with these biased parameters. Some outputs are displayed on the figures below.

The core power decreases due to the SCRAM at the very beginning of the transient. For this activity associated to the optimization of the CATHARE3 MSLB input deck, the core has been modeled with the integrated point kinetic module. The mass flow in the cold leg n°4 also drops rapidly when the main coolant pump is stopped.

The opening of the break on the steam line n°4 causes the associated SG to empty rapidly and the pressure inside to decrease. This also leads to a higher steam mass flow towards the main steam header.

An increase in temperature and pressure happens in the primary circuit at 250 s when the feed water mass flow stops in the SGs and the n°4 dries up.

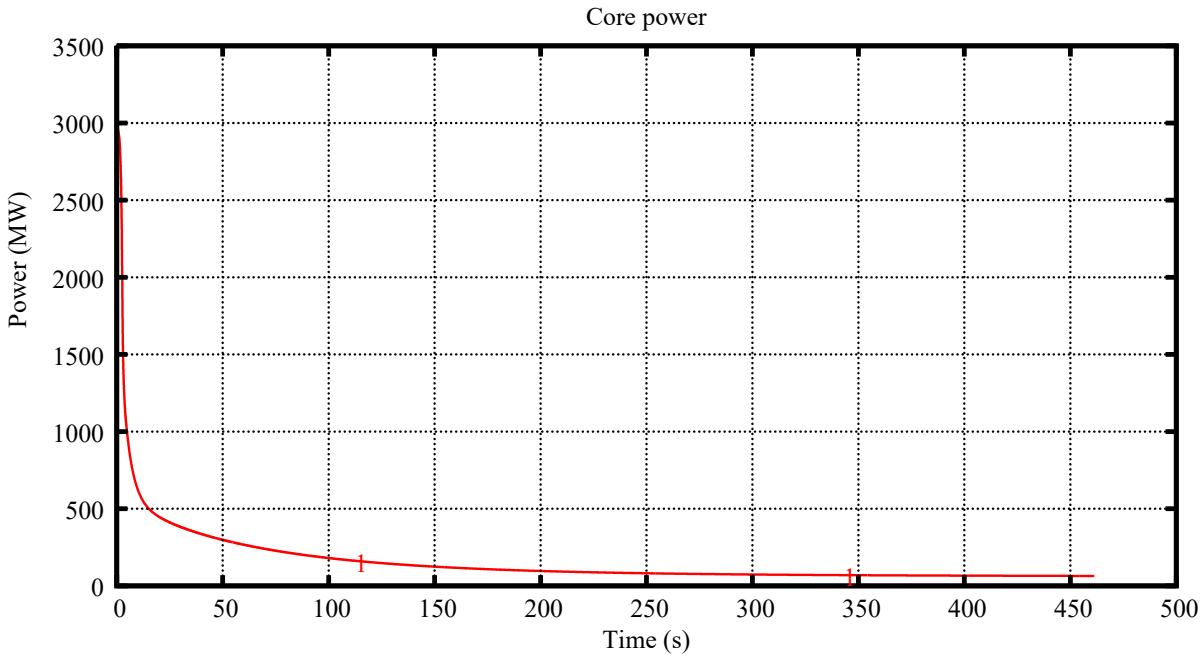


Figure 82: CATHARE3 transient – Core power

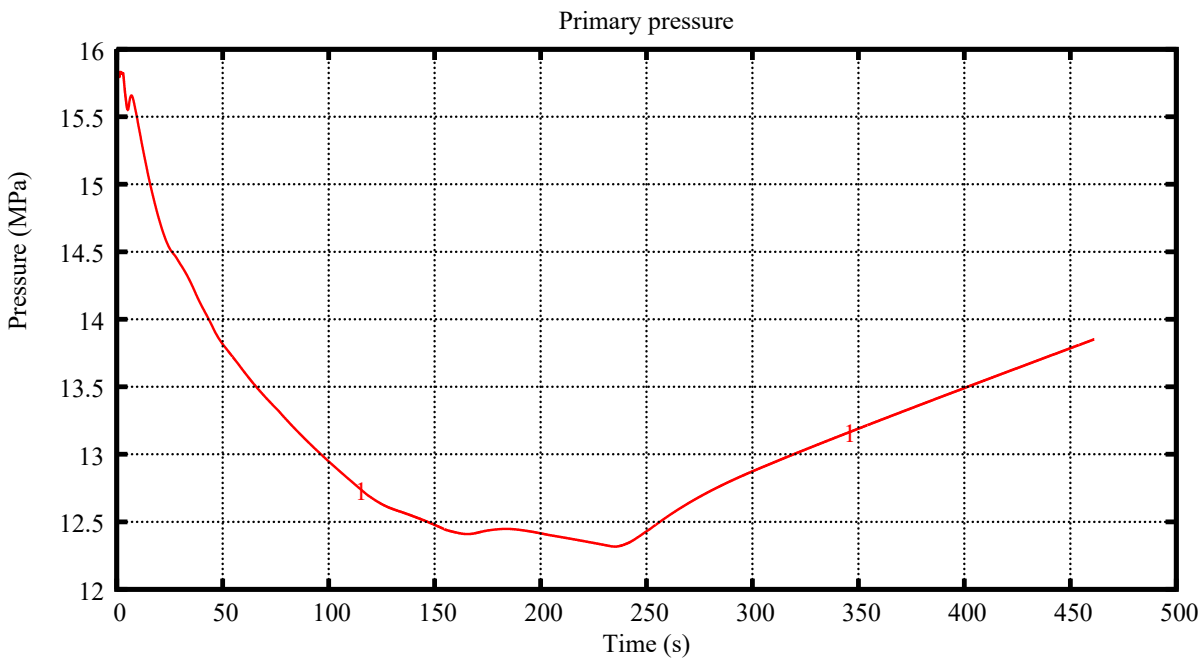


Figure 83: CATHARE3 transient – Pressure in the pressurizer

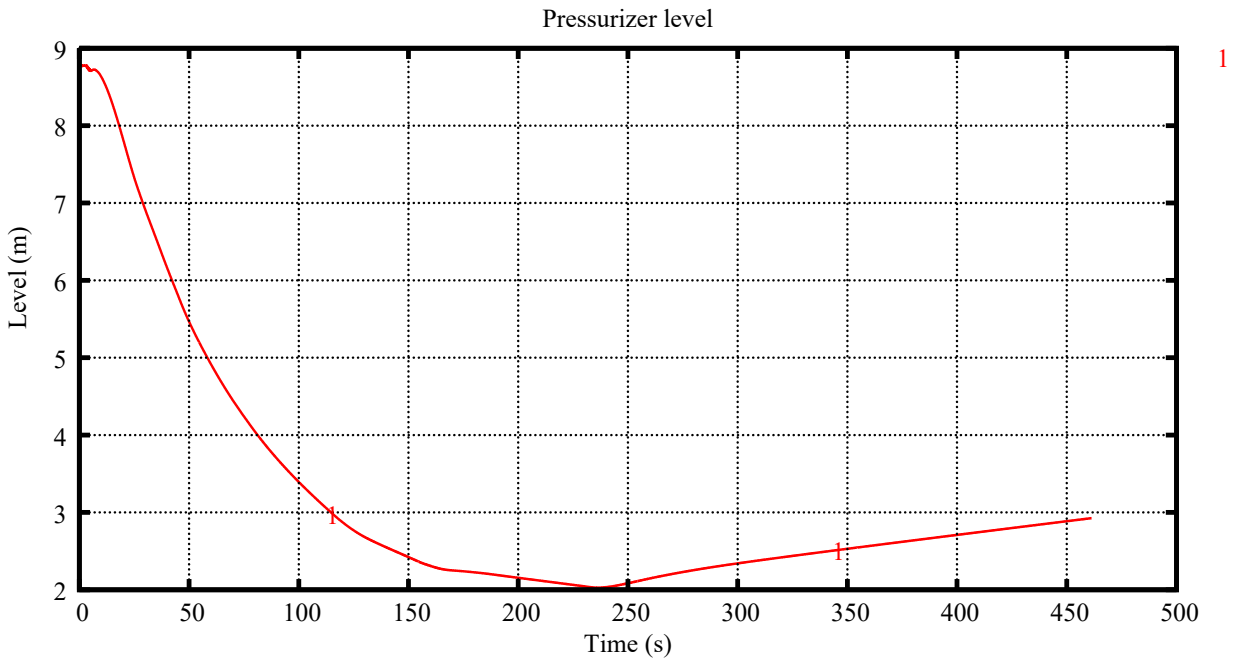


Figure 84: CATHARE3 transient – Level in the pressurizer

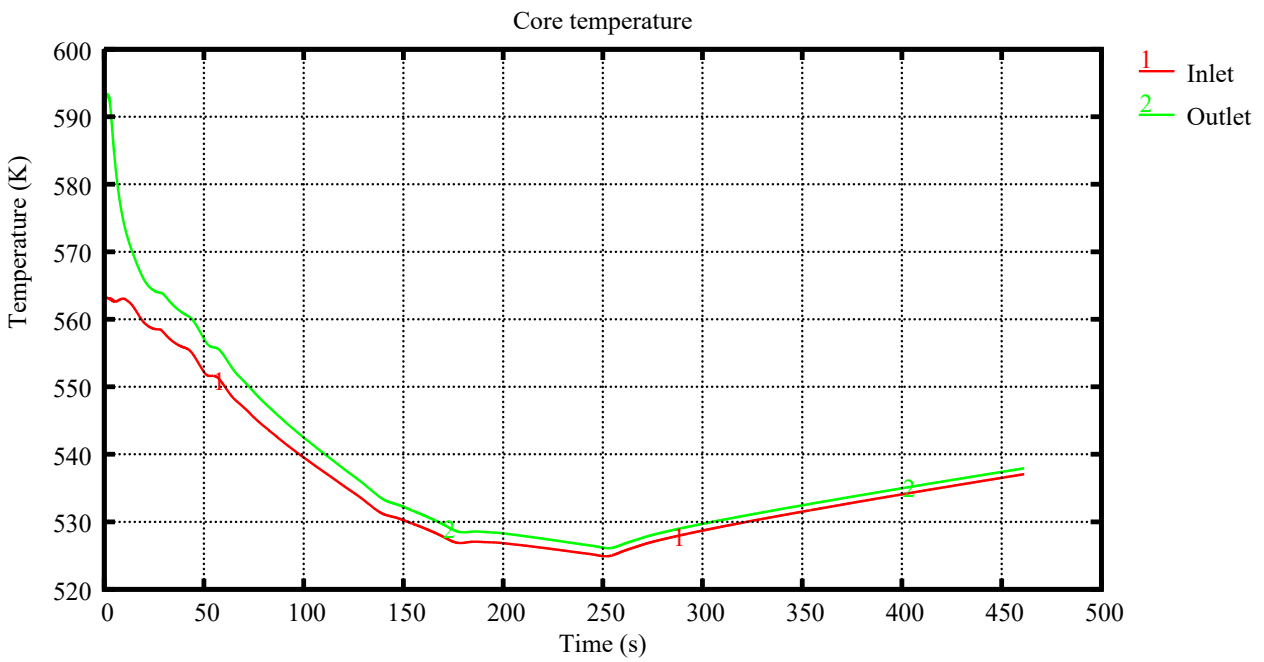


Figure 85: CATHARE3 transient – Core temperature

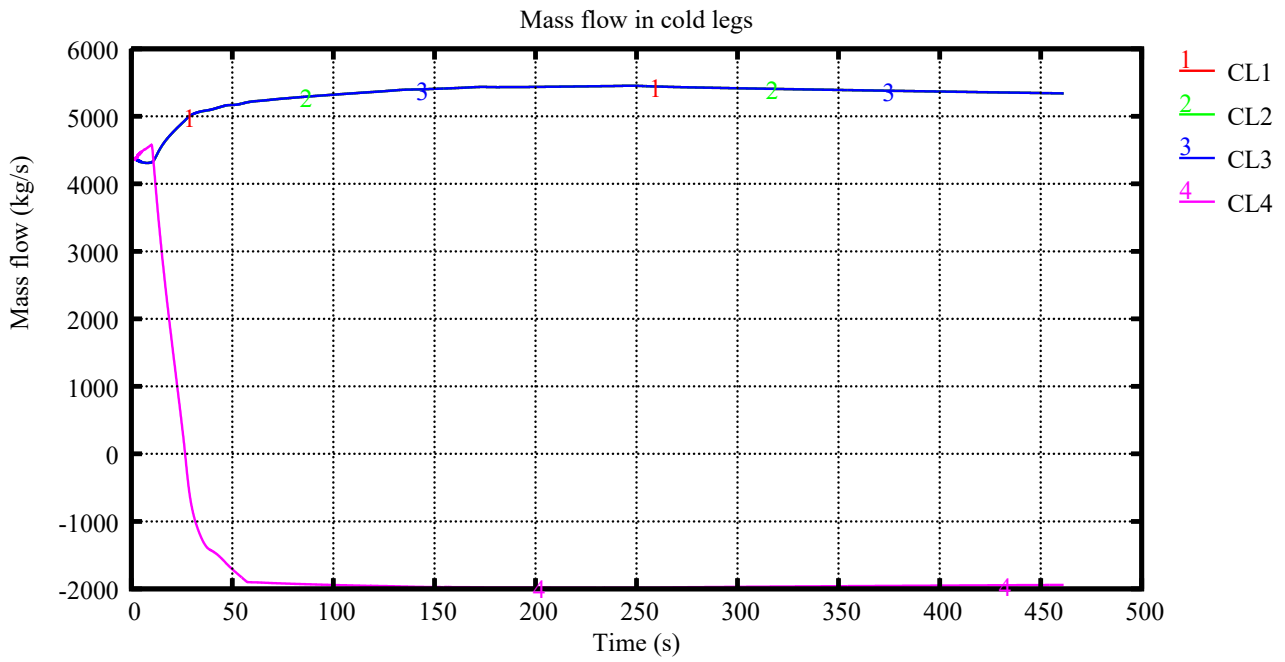


Figure 86: CATHARE3 transient – Cold legs mass flow

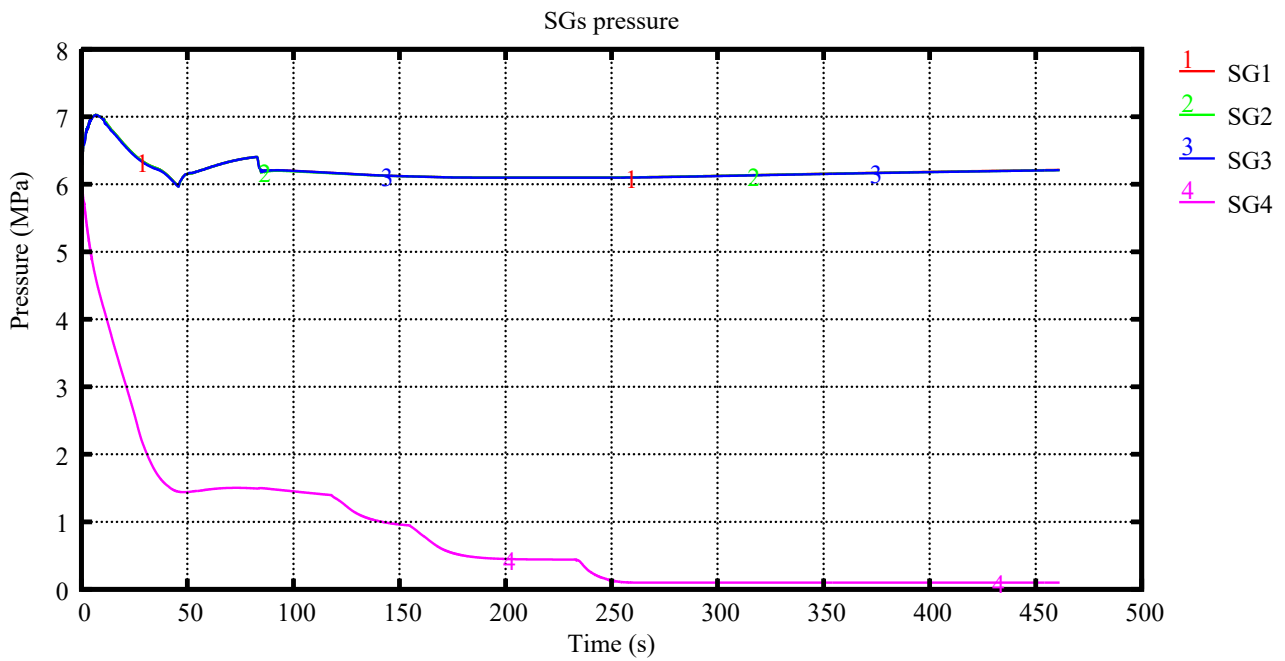


Figure 87: CATHARE3 transient – Pressure in the steam generators

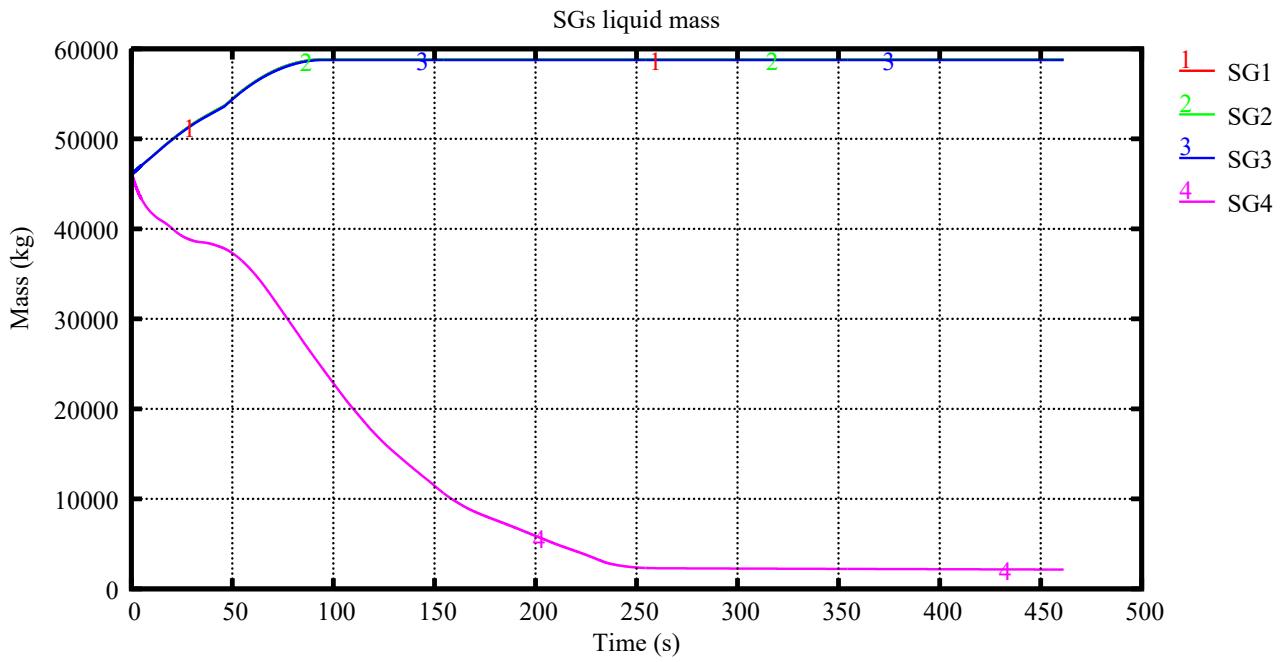


Figure 88: CATHARE3 transient – Water mass in the steam generators

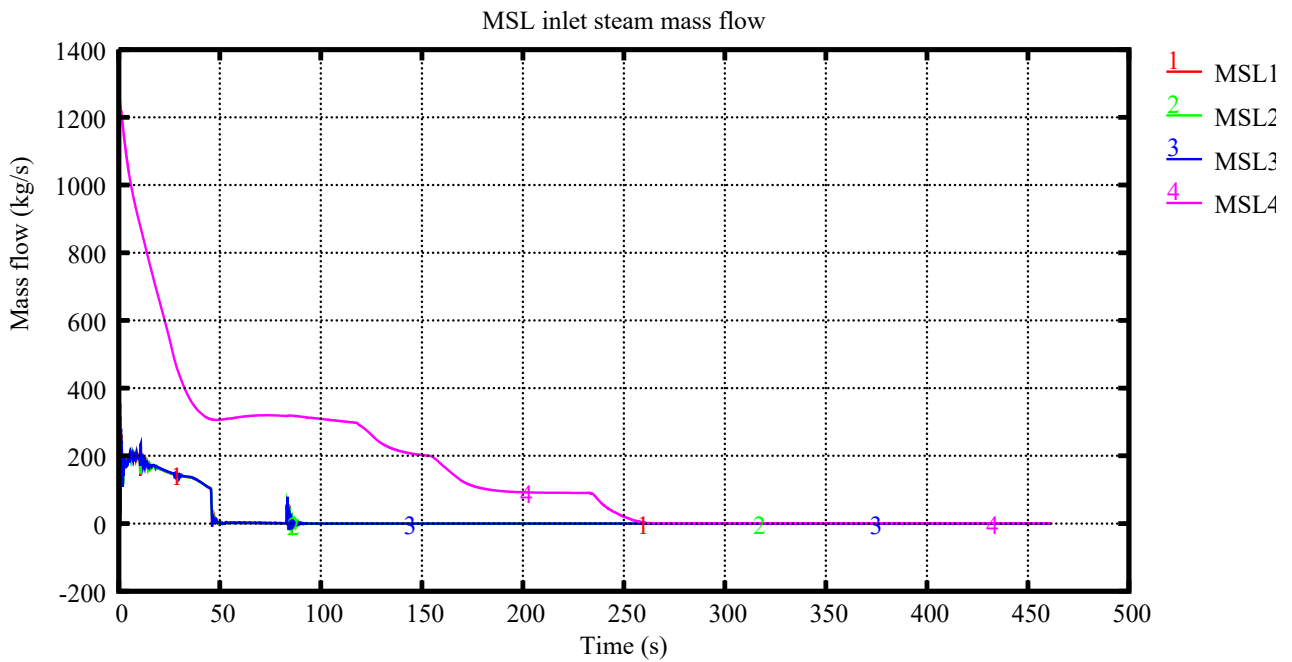


Figure 89: CATHARE3 transient – Steam mass flow in the main steam line

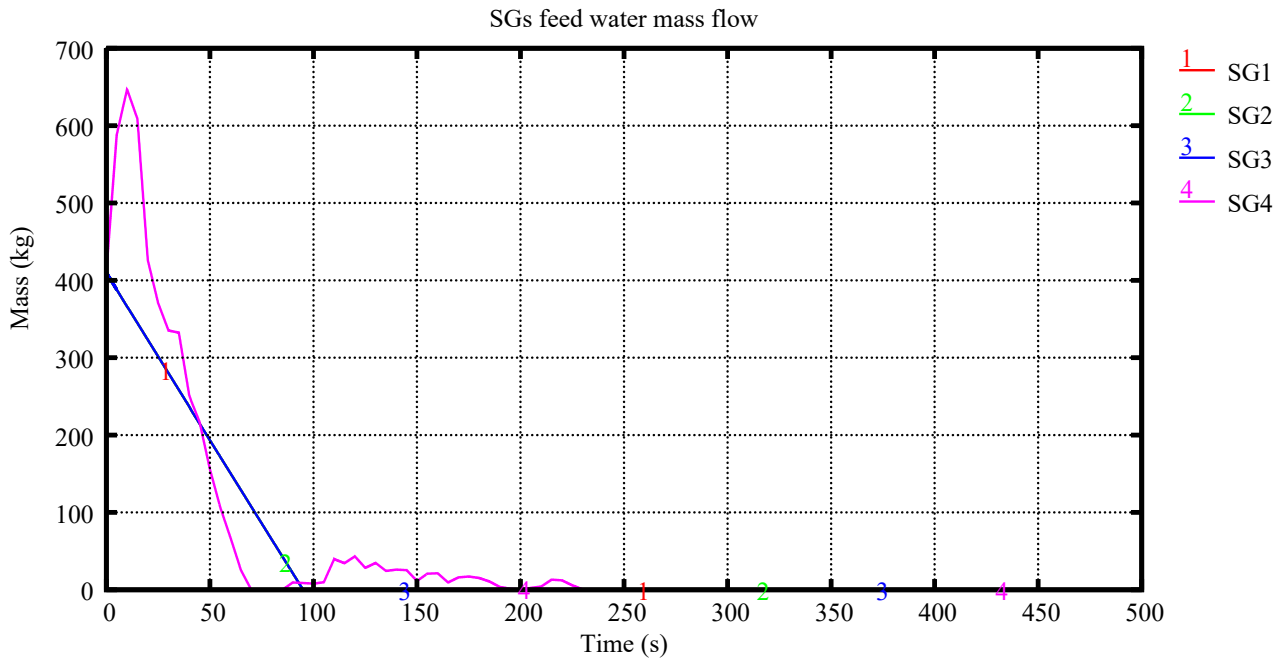


Figure 90: CATHARE3 transient – Feed water mass flow

6 COMPARATIVE ANALYSIS

A comparative analysis of the main results obtained by the different partners was conducted and will be discussed here.

6.1 Thermal hydraulic parameters

Here both thermal hydraulic parameters and core parameters predicted by the 3D solvers will be compared. In Table 16, a comparison of thermal hydraulic parameters of the Kozloduy VVER-1000 reactor at nominal conditions as predicted by the different partners is given. The predicted parameters show a good agreement with the reference design data; merely for few parameters small deviations exist.

Table 16: Comparison of selected thermal hydraulic parameters for the nominal plant conditions just before the MSLB transient

Parameter	Plant Design	KIT	FRAM	INRNE	ENERGORISK
Reactor thermal power, MW	3000	3000	3000.0	3000	3002.5
Primary pressure, MPa	15.7	15.65	15.8	15.7	15.69
Pressurizer Level, m	8.77	8.76	8.77	8.77	8.77
Coolant temperature at reactor inlet, K	560.15	561,3	563.3	560,2	564.0
Coolant temperature at reactor outlet, K	592.05	590,8	593.6	590,96	594.0
Avg. mass flow rate through loops, kg/s	4400	4340	4370	4394	4400
Reactor mass flow rate, kg/s	17600	17383	17450	17574	17598
Total bypass of reactor core, %	3-5	3.2	2.8	2.9	2.2
Pressure in SG, MPa	6.27	6.09	6.32	6.18	6.28
Feedwater temperature, K	493.15	493	493	493	493.15
Pressure in the main steam header (MSH), MPa	6.08	5.955	6.16	5.92	6.08
Steam mass flow rate through SG steam line, kg/s	408	407	411	409	410
SG Water Levels, m	2.40	2.26	2.42	2.26	2.40
Liquid mass in the SG secondary side, t	From 43 to 56 (from different references)	49,9	46	48	48

6.2 Transient phase

Here, selected results of the transient phase of the MSLB-transient will be presented and discussed.

6.2.1 Sequence of main events

In Table 17, a comparison of the sequence of main MSLB-events as predicted by the partners is shown. The differences can be explained by the fact the thermal hydraulic plant models are not similar (user effect) e.g. the break model, the water levels in the SG-secondary side are not exactly the same, the control of the valves on the secondary side is also not fully implemented by all partners as specified.

Table 17: Comparison of sequence of main events predicted by partners

Time, s	KIT	INRNE	ENERGO
Break opening, s	0.0		0.0
SCRAM start, s	0.66	0.66	0.66
SCRAM end, s	4.66	4.66	4.66
Closure of Turbine stop valve, s	4.4		1.34
BRU-K opens, s	79	48	-
BRU-K closes, s	92	58	-
Lowest reactivity at, s / value, \$	4.66s / -12.95 \$	5s / -10.7\$	6s / -11.9 \$
Coolant temperature of loop-4 reached its lowest value at, s / value, K	36.2s / 510.16K	33s / 509.24K	170s / 515K
PZR-level below 4.2 m, s	73.8	58	48.9
PZR-level reached lowest value at, s/ value, m	323 s / 1.645 m	202 s / 1.735 m	175 s/ 2.067 m
SG-4 water almost empty at, s / value, m	323s / 0.106m	494s/ 0.109m	400s/0.10m
Re-criticality achieved, s	No	no	no
Return-to-power peak, s / value, MW	No	no	no
Transient end, s	600	600	600

6.2.2 Selected global thermal hydraulic parameters (all partners)

In this subchapter, a comparative analysis of selected thermal hydraulic parameters predicted by the partners except FRAMAOTME with different simulation tools are presented and discussed. The reason of not including the FRAMATOME results of the MSLB-transient phase is the preliminary character of the results as major effort was put in consolidating the primary and secondary system modelling.

Figure 91 shows the break outflow in the steam line 4 after the break opening during the 600 s and during the first 50 s transient time. The KIT and INRNE calculations show similar trends in general. The reason that the INRNE-predictions does not show a sharp increase at the beginning by be that the plot frequency in RELAP5 is not high enough so that some values are missing. The break outflow predicted by ENERGORISK using RELAP5 is much larger than the one of INRNE and KIT. The reason may be the break modelling. ENERGORISK considered two breaks (Double End Break) while the other partners modelled the break by

only one break model. Hence, after the liquid collected in the steam line 4 upstream of the break is gone, the break outflow of ENERGORISK is similar to the one of the other partners.

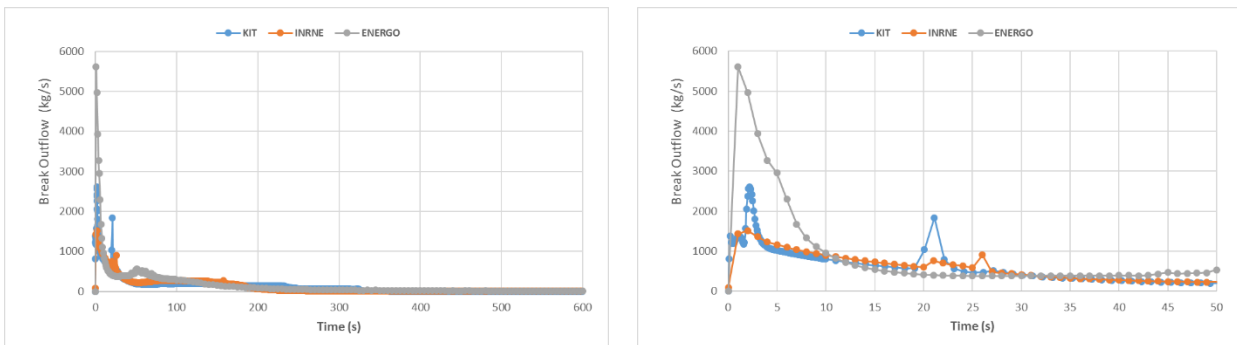


Figure 91: Evolution of the break-outflow as predicted by the partners (right: zoom of the first 50 s)

Figure 92 shows the evolution of the pressure in the mean steam header (left side) and of the core outlet (right side) after the break opening. All three participants predicts a sharp pressure increase leading to the opening of the BRU-Ks for short period of time. The secondary pressure increases after the closure of the MSIV and due to the isolation of the SG4 by closing the SIV, which also impacts the pressure in the intact secondary loops. On the right side, the primary pressure at the core outlet of three simulations is presented. Again, all three predicted pressure trends are similar until around 250 s. Later on, they predictions deviates do to a different heat transfer from the primary to the secondary side, especially over the defect SG4 driven also due to the different pressure trends predicted at the MSH on the secondary side.

While in the simulations of KIT and INRNE, the BRU-Ks valves opens for a short time, in the ENERGORISK simulation they remain opens since the pressure there seems to be kept constant (regulated) while in the two other simulations the MSH-pressure is going down slowly.

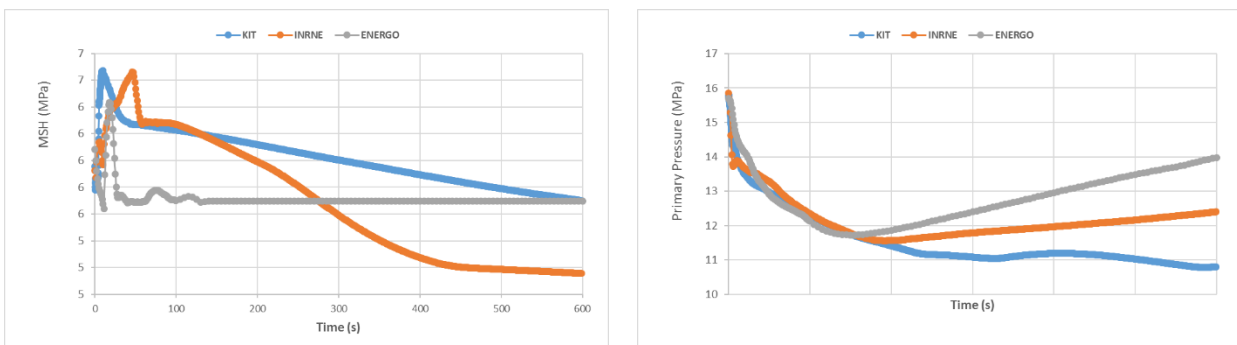


Figure 92: Evolution of the pressure at the main steam header of the secondary side and of the pressure at the core outlet as predicted by the partners

Figure 93 presents the evolution of the coolant temperature of the cold legs number 4 (affected SG4) and number 1 (neighbour). The first cool-down phase is fast, where the coolant temperature of the Cold Leg 4 is reduced by around 50 K for INRNE and KIT but much less –around 35 K- for ENERGORISK. The coolant temperature in loop-4 starts to increase when the reverse flow in this loop begins (KIT: 36s, INRNE: 32s, ENERGORISK: 21s). Later on, the evaporation of the secondary side of the SG4 is continues going on and leading to the reduction of the SG-4 secondary side water level (Figure 97). Consequently, the primary coolant temperature of the loop 4 continues decreasing until the SG-4 inventory is almost empty. The coolant temperature of the Loop-1 which is close to the Loop-4 is also decreasing due to the coolant mixing taking place in the RPV downcomer and lower plenum.

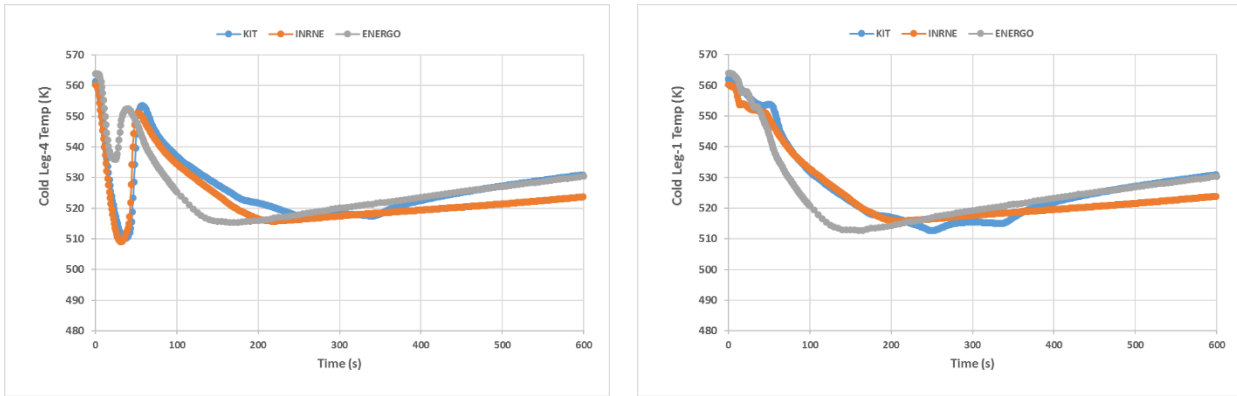


Figure 93: Evolution of the break-outflow as predicted by the partners

Figure 94 shows the total power reduction after the SCRAM as predicted by the 3 partners with RELAP5 using the point kinetics (INRNE, ENERGORISK) models and by TRACE/PARCS using a 3D core neutronic model. The trends are similar. Moreover, in the zoom of the first 50 s, it can be observed that the reduction of the decay power is slightly time-delayed compared to the other two solutions. It may be that in this case, the SCRAM time (0.36s), the delay time for SCRAM (0.3 s) and the time for full control rod insertion (4s) was not used by ENERGORISK.

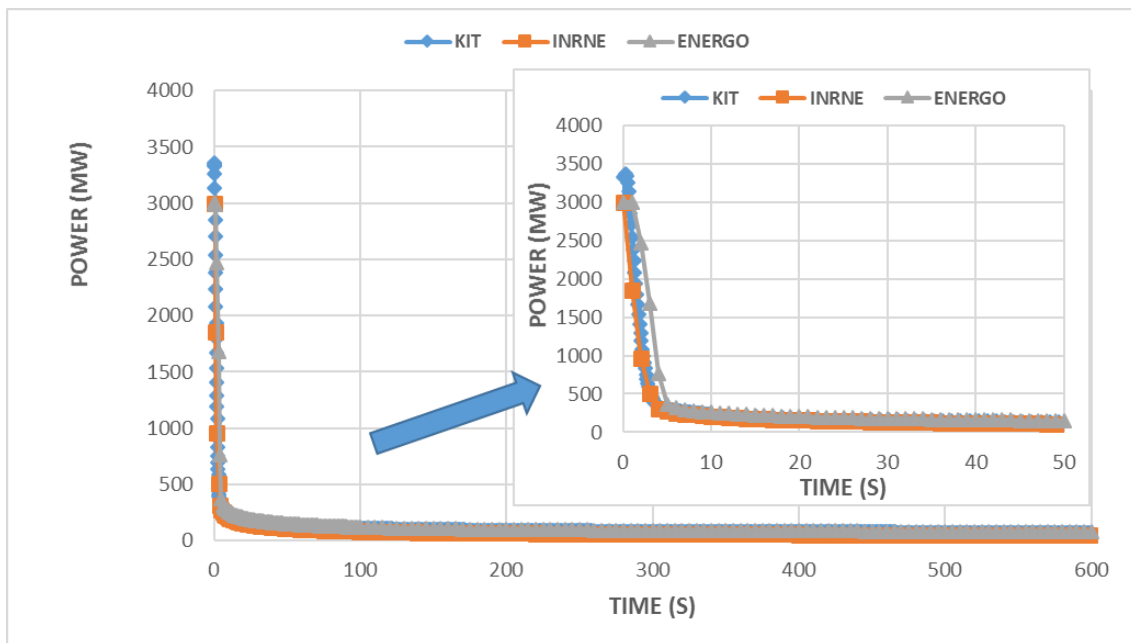


Figure 94: Evolution of the total power as predicted by the different codes (right: zoom of 50 s)

The respective total reactivity evolution during the MSLB calculated by the partners is shown in Figure 95, where it can be observed that the trends of KIT and INRNE are similar except the highest reactivity inserted after the SCRAM. It is worth to note that INRNE is using the Point Kinetics model of RELAP5 with the kinetic parameters and reactivity coefficients predicted using PARCS with the homogenized and condensed cross sections generated with SERPENT2 for the fresh core of the Kozloduy plant. In case of ENERGORISK, it seems that the reactivity coefficients used are not the same used by INRNE. In addition, it must be noted that the core thermal hydraulic parameters predicted by INRNE and ENERGORISK are not the same and they differ from each other. This may also influence the evolution of the total reactivity coefficient. Interesting

to note is that the highest negative reactivity predicted by ENERGORISK is larger than the one of INRNE and smaller than the one predicted by KIT.

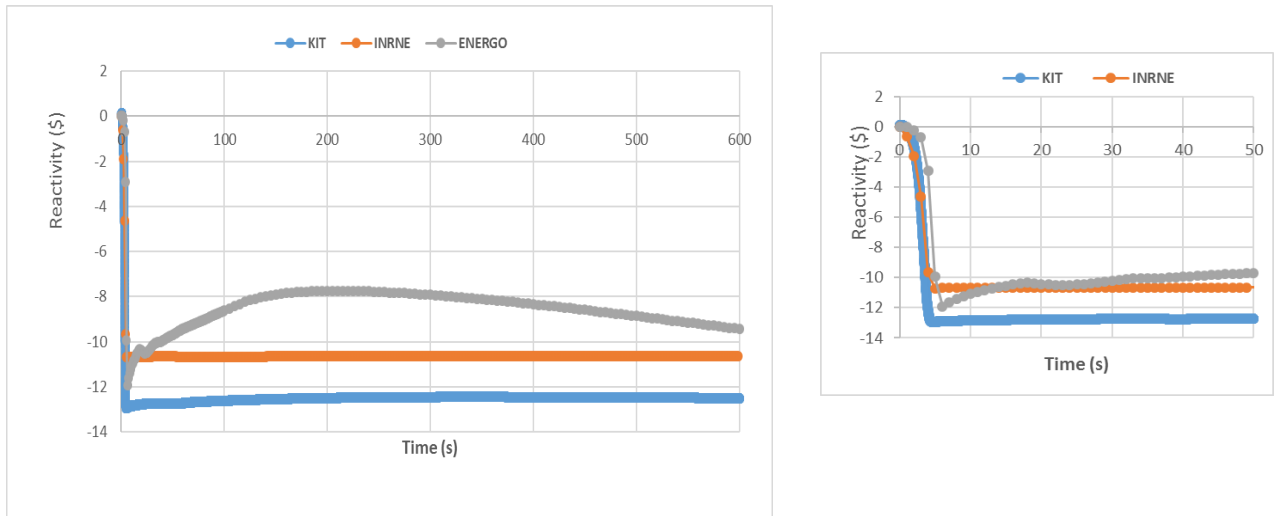


Figure 95: Evolution of the total reactivity as predicted by the different codes (right: zoom of first 50 s)

Figure 96 describes the reduction of the PZR-water level during the transient as predicted by the partners, where the global trends are similar. Moreover, it can be observed that the first 25s, all three solutions have a similar gradient, then when the reverse flow in loop-4 starts, the calculated water levels deviate from each other. From that time until ca. 150s, the INRNE and ENERGORISK trends are quite similar while TRACE/PARCS predicts a slower reduction. Hence, the lowest water level was reached at different times as it is indicated in Table 15.

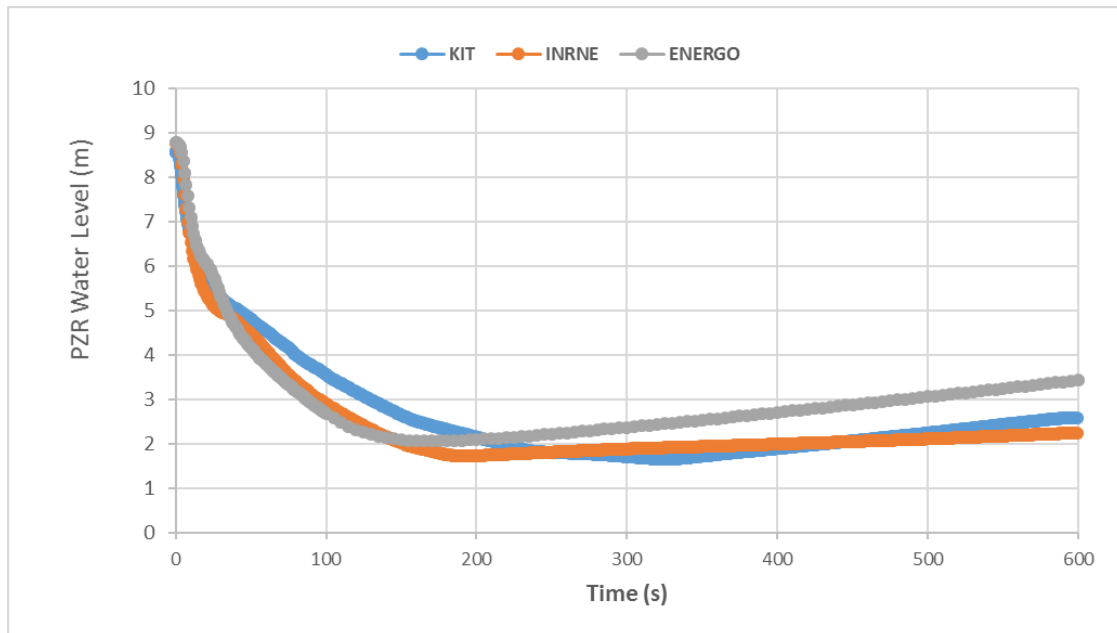


Figure 96: Evolution of the water level in the pressurizer

Finally, Figure 97 exhibits the water level evolution on the secondary side of the affected SG4 (left) and the intact SG1 (right) as predicted by the partners. A water level below 0.1m is achieved at 323s, 494s, and 400s by KIT, INRNE and ENERGORISK, respectively. The evolution of the water level in the intact SG-1 predicted by ENERGORISK differs from the one predicted by KIT and INRNE.

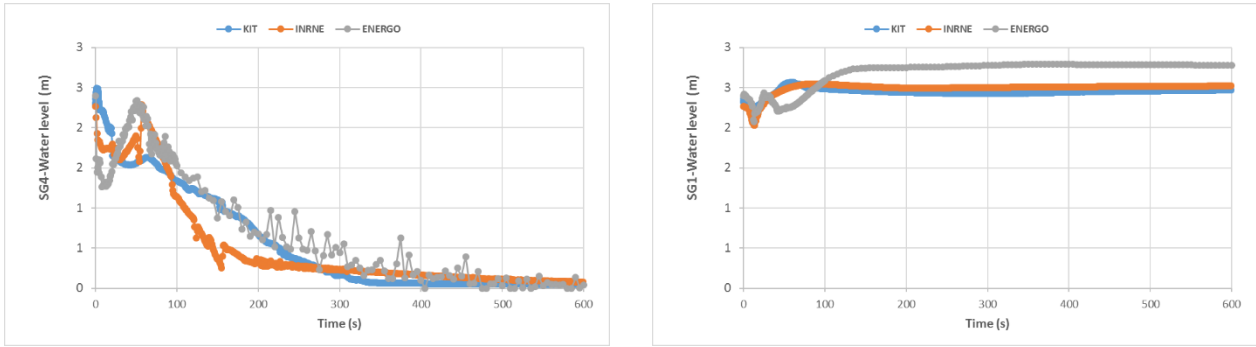


Figure 97: Evolution of the water level of the SG4 (left) and SG-1 (right) during the MSLB

7 CONCLUSIONS AND RECOMMENDATIONS

Based on the results of the participants explained in the former Chapters and on the comparative analysis provided in Chapter 6, the following conclusions can be drawn:

- The integral models of the Kozloduy VVER-1000 plant developed for CATHARE, TRACE and RELAP5 by four institutions are appropriate for the prediction of the steady-state nominal plant conditions as starting point for the transient case.
- The comparison of selected thermal hydraulic parameters taken from four simulations of the stationary plant conditions are in good agreement with the reference plant data.
- The comparison of selected thermal hydraulic parameters predicted by partners for the MSLB-transient have shown that in general the RELAP5 and TRACE/PARCS codes are able to describe the key-physical phenomena taking place during the MSLB-transient e.g. the strong coupling of the thermal hydraulic parameters with the core neutronics. In addition, the fast evaporation and critical flow through the broken steam line 4 are predicted well by the codes and they agreement is reasonable. Addition work may be necessary to reduce the differences of the integral plant models developed for TRACE, CATHARE3 and RELAP5 that will lead to lower the discrepancies of the predicted nominal parameters as well as the discrepancies among the trends of selected parameters calculated by the different tools.
- The 3D thermal hydraulic model e.g. in TRACE was able to catch the coolant mixing in the downcomer, upper and lower plenum inside the RPV due to the overcooling of one of the four sectors in which the core and RPV were discretised in addition to the radial and axial discretization.
- A comparison among the solutions of the RELAP5 code used by INRNE and ENERGORISK have shown that some parameters have a similar trend but others not. It seems to be caused by the different point kinetics parameters and the time for the start of SCRAM, delay time for SCRAM, etc. Hence, the total reactivity of both solutions after the SCRAM are not the same.
- The different treatment of the coolant mixing in the upper/lower plenum, and downcomer between the RELAP5 models (INRNE, ENERGORISK) and the one of TRACE/PARCS (KIT) may be responsible for the deviations between the cold and hot leg temperatures on the primary side.
- The FRAMATOME simulations are of preliminary nature still because of major effort to be provided in full system and MSLB transient input options. Hence, they are not considered in the comparative analysis. Moreover, the authors have identified the issues to be tackled in order to be able to perform a MSLB-transient simulation.
- The simulations performed with TRACE/PARCS have shown that the couple code is able to predict the power increase in the sector attached to the sector of the loop-4, where the increased heat transfer to the secondary side took place during the MSLB.
- Finally, the coupled simulations indicates that the Point kinetics models tend to over-predicts the impact of the overcooling of the coolant due to the use of global reactivity coefficients and a fixed axial power profile over the full transient time. Hence, the total reactivity predicted by TRACE/PARCS is lower than the ones calculated by the two RELAP5 simulations.

Following recommendations are to be made based on the performed analysis of the MSLB for BOC-conditions (academic case):

- For a truly comparative analysis of a MSLB-transient analysis it has to be sure that all partners are considering the same geometry, dimensions, initial and boundary conditions.
- The comparison of the code predictions for the steady state plant conditions should have small discrepancies compared to the reference data i.e. the power must be the same, the water levels at the SGs secondary side, too.

- In addition, the initial and boundary conditions of the input decks to be compared to each other must be the same, which is sometimes not too easy to make it sure.
- In addition, for the proper prediction of the Doppler temperature as an important feedback to the neutronics, it should be assured that all partners are using the same thermos-physical properties of the fuel and cladding as well as the gap heat transfer coefficient.
- It must be assured that the Point Kinetics models in RELAP5 are implemented in the same manner and the reactor kinetics parameters are the same in the simulations with system TH codes.
- A more detailed comparison of the core conditions at nominal parameters predicted by two different 3D core solvers is needed to make sure that there is no biases in the reading of the nodal cross section sets developed by two different approaches e.g. at KIT (based on Serpent2) and at FRAMATOME (based on APOLLO3®)

8 References

- [1] A. Stefanova, N. Zaharieva, P. Vryashkova and P. Groudev,, "The CAMIVVER Definition report with the specifications of rht NPP with VVER_1000 reactor with respect to selected transients," CAMIVVER, Paris, 2020.
- [2] N. Kolev, N. Petrov, J. Donovan, D. Angelova, S. Aniel, . E. Royer, K. Ivanov, E. Lukanov, Y. Dinkov, D. Popov and S. Nikonov, " VVER-1000 Coolant Transient Benchmark – Phase 2 (V1000CT-2). Vol. II: MSLB Problem – Final Specifications.," NEA/NSC/DOC(2006)6, April, 2006.
- [3] RELAP5, "RELAP5/MOD3.3 CODE MANUAL, VOLUME I: CODE STRUCTURE,SYSTEM MODELS, AND SOLUTION METHODS,," INEL, NUREG/CR-5535/Rev P5-Vol I, , Maryland, Idaho Falls, Idaho, 2016.
- [4] Nuclear Safety Analysis Division 2001, RELAP5/Mod3.3 code manual Volume I: Code Structure, System Models, and Solution Methods., vol. 1..
- [5] "U. NRC, TRACE V5.1051 Theory Manual, Washington, DC: Division of Safety Analysis Office of Nuclear Regulatory Research, U. S. Nuclear Regulatory Commission," 2016.
- [6] K. Zhang, "The multiscale thermal-hydraulic simulation for nuclear reactors: A classification of the coupling approaches and a review of the coupled codes," *International Journal of Energy Research*, 2019.
- [7] "MEDCoupling Developer's Guide," SALOME-platform, [Online],Available: <http://docs.salome-platform.org/latest/dev/MEDCoupling/developer/index.html>. [Accessed 04 02 2019]..
- [8] T. Downar, A. Ward, Y. Xu and V. Seker, "PARCS, Volume II: User's Guide. NRC - v3.3.0 Release," 2018.
- [9] P. Mosca, L. Bourhrara, A. Calloo, A. Gammicchia and F. Goubioud, "APOLLO3®: Overview of the new code capabilities for reactor physics analysis," *Proceeding International Conference M&C2023, Niagara Falls, Ontario, Canada, August 13-17, 2023*.
- [10] CEA, "CATHARE-3 V2.1: The new industrial version of the CATHARE code," [Online]. Available: <https://hal-cea.archives-ouvertes.fr/cea-04087378/>.
- [11] C. Patricot, "C3PO Open Source Access," [Online]. Available: <https://sourceforge.net/projects/cea-c3po>.
- [12] ENERGO, "Project of in-depth safety analysis of power unit № 5 of Zaporizhia NPP. Data base on the YPPU of unit № 5 of the ZNPP," Final report. 10044DL12R. ZAES, Kiev, 2000.
- [13] CAMIVVER, " Description of thermal-hydraulics models. Results of steady-state benchmark (D7.1)," Paris, 2021.
- [14] V. Sanchez-Espinoza and M. Bottcher, "Investigations of the VVER-1000 coolant

transient benchmark phase with the coupled system code RELAP5/PARCS," *Progress in Nuclear Energy*, vol. 48, 2006.

- [15] KNPP, "Data Base for VVER1000: Safety Analysis Capability Improvement of KNPP (SACI of KNPP) in the field of Thermal Hydraulic Analysis," INRNE, Sofia, 2015.
- [16] NRC, "TRACE V5.840, User's Manual: Input Specification," 2017.
- [17] B. Calgaro and G. Huaccho, "Description of the core reference test cases - Part 1 + Part 2," CAMIVVER Deliverable 5.2, 2023.

9 APPENDIX I: Reactivity coefficients & kinetic parameters

9.1 Reactivity coefficients

Reactivity coefficients are provided for system codes that use point kinetic models. The level of boron concentration level has a significant impact on the values of reactivity coefficients, particularly the one associated with the coolant density. At critical boron concentration (1630 ppm) a negative value was obtained for this reactivity coefficient, while a positive value was obtained for the reference boron concentration (1200 ppm), as presented in Table 18.

Table 18. Reactivity coefficients for nominal and critical boron concentration.

State, boron	$\beta/\Delta\text{Coolant density}$	$\beta/\Delta\text{Boron in coolant}$	$\beta/\Delta\text{Fuel temperature}$	$\beta/\Delta\text{Coolant temperature}$
	$\$/\text{kgm}^{-3}$	$\$/\text{ppm}$	$\$/\text{K}$	$\$/\text{K}$
HFP, 1200 ppm	2.23E-03	-1.53E-02	-3.37E-03	-1.03E-03
HFP, 1630 ppm	-4.54E-03	-1.43E-02	-3.36E-03	-3.40E-03

This difference in the sign can be explained by analysing how kinf changes with the coolant density at different boron concentration levels as illustrated in Figure 98 and Figure 99. In the absence of boron (1 ppm) a positive slope for $\Delta\text{kinf}/\Delta\text{density}$ is always obtained. However, as the boron concentration is increased, there is a certain point in density where the slope changes in sign.

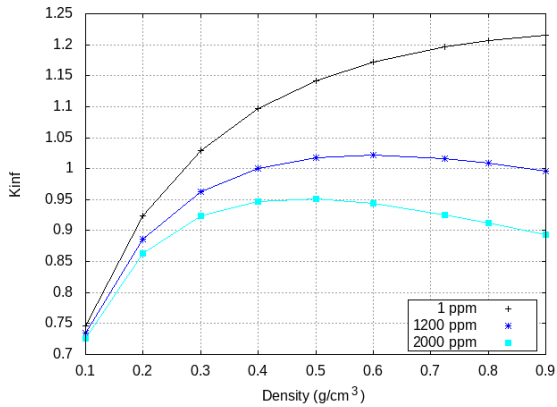


Figure 98. kinf as a function of DC for different boron concentration in FA type 1.

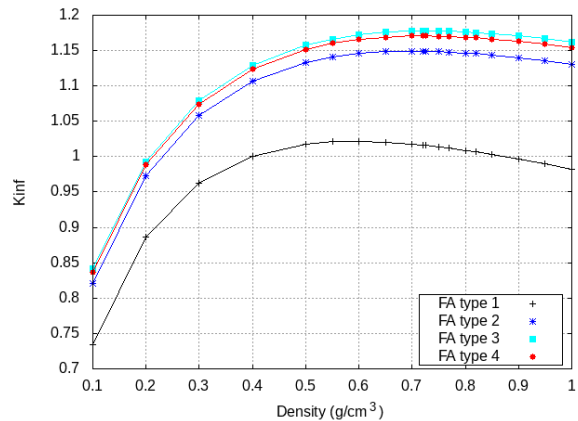


Figure 99. kinf as a function of DC for the different FA types, with fixed 1200 ppm boron concentration.

9.2 Kinetic parameters

The following kinetic parameters were extracted from PARCS considering a HFP state with a critical boron concentration of 1630 ppm. Additionally, the SCRAM control rod worth is provided in Table 21 using PARCS stand-alone.

Table 19. Kinetic data

Parameter	Value
Total beta effective (pcm)	705
Neutron generation time (μ s)	25.7
Group of precursors	8

Table 20. Delayed neutron fraction and decay constant data.

Group	Beta fraction	Lambda (1/s)
1	2.085E-04	1.2467E-02
2	1.023E-03	2.8292E-02
3	5.940E-04	4.2524E-02
4	1.334E-03	1.3304E-01
5	2.264E-03	2.9247E-01
6	7.558E-04	6.6649E-01
7	6.261E-04	1.6348E+00
8	2.474E-04	3.5546E+00

Table 21. SCRAM worth with stuck control rod.

Keff SB 1-9 @ 100% extracted RB 10 @ 80% extracted	1.00114
Keff SB 1-9 totally inserted (except stuck control rod) RB 10 totally inserted	0.929727
Control rod worth	7672 pcm
Control rod worth (considering $\beta_{eff} = 705 \text{ pcm}$)	10.9 \$